SCUOLA DI DOTTORATO
UNIVERSITÀ DEGLI STUDI DI MILANO-BICOCCA

Department of Statistics and Quantitative Methods (DISMEQ)

PhD in Statistics and Mathematical Finance Cycle: XXXII

Curriculum in Mathematical Finance

Moment based approximations for arithmetic averages with applications in derivatives pricing, credit risk and Monte Carlo simulation

Candidate: Brignone Riccardo

Registration number: 741254

Tutor: Prof. Gianluca Fusai

Supervisors: Dr. Ioannis Kyriakou, Prof. Gianluca Fusai

Coordinator: Prof. Giorgio Vittadini

ACADEMIC YEAR: 2018/2019

Abstract

In this thesis we consider three different financial applications that involve arithmetic averages of a stochastic process, whose distribution is unknown, therefore the related problems preclude explicit true solutions. We propose moment-based approximations and study problems in exotic derivatives pricing, credit risk and random number sampling and show that this kind of solution can efficiently reduce the computational cost of already existing methodologies in the literature. The first chapter of the thesis presents moment-based approximations as well as some relevant technical details, including some facts about the so-called *moment problem*, common approximations techniques, a literature review linked to the use of moments in finance and numerical illustrations. In the second chapter, we propose accurate moment-based closed-form expressions for the price of Asian options when the underlying asset price is represented by a mean-reverting stochastic process with jumps. In the third chapter, we introduce an efficient methodology, based on moment matching, for the calibration of the default intensity, which is modelled by an exponential Ornstein-Uhlenbeck process and apply this result to the calculation of Credit Value Adjustment (CVA) in presence of wrong way risk for interest rate derivatives. In the fourth chapter, we consider the problem of simulating stochastic volatility models. Exact simulation schemes have been proposed in the literature for various models, but these are not computationally efficient due to the need to simulate the time-integral of the variance process, whose distribution function is not explicitly known. In this case, we show how to compute the moments of this and develop a new simulation methodology which achieves an exceptional runtime-accuracy balance compared to some exact simulation scheme. Within the spirit of the first chapter, we revisit in the final chapter the pricing problem of Asian options for a double exponential jump diffusion model where the jump intensity is a stochastic process of Hawkes type. This dynamics has been introduced in the literature to model the jump clustering phenomenon, which is widely observed in financial and commodity markets. We derive the characteristic function of the integral of log-returns and focus on the evaluation of geometric Asian options.

Contents

List of Figures

List of Tables

Introduction

It often happens in quantitative finance that certain key quantities do not admit explicit expressions that can be computed exactly, therefore one must resort to numerical methods. Nevertheless, the use of numerical methods usually can be quite cumbersome so there is a need to develop suitable speed ups while remaining accurate, i.e., we need to take care of the speed-accuracy tradeoff. In this thesis, we consider three such problems in finance, including the pricing of Asian option, credit risk modelling and stochastic volatility models simulation; all three involve an arithmetic average, that is, our key quantity, with an unknown distribution law and we propose solutions based on approximating distributions based on the moments of the arithmetic average. We start by providing, in Chapter 1, some theoretical background about the use of moments to approximate unknown distributions, emphasizing the so-called *moment problem* and approximation techniques, including also several practical examples. In Chapter 2, we tackle the problem of Asian options' pricing when the underlying dynamics are represented by an exponential Lévy driven Ornstein-Uhlenbeck process. In that case, the unknown distribution of the arithmetic average is required, so first we derive formulas for its moments and then employ them to approximate its distribution and produce pricing formulas. In Chapter 3, we consider the problem of computing CVA (Credit Value Adjustment) for interest rate derivatives. CVA is the correction to the value of a derivative instrument that accounts for the probability of default of the counterparty. We compute this under the assumption that the probability of default of the counterparty and the credit exposure are correlated, i.e., in the presence of wrong (or right) way risk. We show that, under the specified model, the problem is expressed in terms of a partial differential equation (PDE) that depends on the arithmetic average of the default intensity process, whose distribution is unknown. We propose a methodology based on the moments of this average to perform parameter calibration to real data. Our results are accurate and are obtained considerably faster than using other methods based on Monte Carlo simulation. In Chapter 4, we propose an efficient methodology for the simulation of stochastic volatility models. In this case, the key quantity is the arithmetic average of the variance process, whose distribution is again not known. We propose an efficient algorithm to compute its moments and draw random numbers from such distribution. This allows us to derive an efficient simulation scheme for stochastic volatility models, which turns out to be much faster than bench-

mark competitors for a similar level of accuracy. In the final Chapter 5, we derive the characteristic function of the arithmetic average of the log-returns when the underlying is given by a jump diffusion process with a stochastic jump intensity of Hawkes-type. This theoretical result enables us to evaluate geometric Asian options under the specified model. The use of moments in this chapter is only marginal, in particular, we show how to compute the moments of some key quantities involved in the pricing procedure to make the numerical inversion algorithms employed for option valuation more accurate. More detailed introductions, including literature reviews, research questions and motivations are given in the first section of each chapter. Chapters 2-4 are joint works with Gianluca Fusai and Ioannis Kyriakou, whereas Chapter 5 is a joint work with Carlo Sgarra and has been accepted for publication in *Annals of Finance* (Brignone and Sgarra, Forthcoming).

Chapter 1

Approximating densities using moments

In this chapter we explore the problem of approximating unknown distributions by exploiting knowledge of their moments. We start by illustrating in Section 1.1 the moment problem, i.e. the problem of determining if a distribution is the only one with a given moments sequence. This is important as moment based approximations are more accurate in such cases. Then, we discuss, in Section 1.2, moment matching and orthogonal polynomials expansion techniques for distributions approximation. A particular focus will be given to moment matching through two particular systems of distributions, i.e. the Johnson's and Pearson's families, which we will use extensively throughout the thesis. After that, we illustrate in Section 1.3 two theoretical results on the error committed when approximating an unknown distribution with a known one sharing the same first $2n$ integer moments. In Section 1.4 we provide a (non-exhaustive) literature review on the usage of moments in finance, with emphasis on applications in option pricing, model calibration, portfolio management and forecasting. In Section 1.5 we put moment based approximations in practise, considering a well known problem in finance, i.e. the pricing of Asian options in the Black-Scholes model. We explore several techniques and highlight their weaknesses and strengths with the support of some numerical results. The scope of this example is also to highlight the poor performances of some particular moment based approximations, which, consequently, are not used within the thesis. Finally, we illustrate, in Section 1.6, a further numerical experiment on moment problem. We consider an option pricing problem in which the true density is known but is replaced by another one, which is totally different, but presents exactly the same sequence of moments. Curiously, numerical results show that option prices are not so different as one would expect looking at the densities.

1.1 Moment problem

Let $\{\mu_n\}_{n=0}^{\infty}$ a sequence of real numbers with $\mu_0 = 1$ and $\mathcal{D} \subset \mathbb{R}$ a fixed interval. Suppose that there is at least one density $f(x)$, $x \in \mathcal{D}$ such that:

$$\mu_n = \int_{\mathcal{D}} x^n f(x) dx \tag{1.1}$$

If $f(x)$ is uniquely specified by $\{\mu_n\}_{n=0}^{\infty}$ we say that the moment problem is determinate, i.e. the distribution is uniquely determined by its moments, otherwise the moment problem is indeterminate. In other words, the moment problem consists in establishing whether or not $f(x)$ is the only density with moment sequence given by $\{\mu_n\}_{n=0}^{\infty}$. In the case $\mathcal{D} = [0, +\infty)$ the moment problem is called the Stieltjes moment problem, while in the case $\mathcal{D} = (-\infty, +\infty)$ we speak of the Hamburger moment problem. In Stoyanov (1997) we can find several sufficient conditions for the moment problem to be determinate or indeterminate.

Criterion 1 (**moment generating function condition**). *If a random variable X has a moment generating function, i.e., $\mathrm{E}[e^{uX}] < \infty \ \forall u \in (-c, c)$, where $c > 0$ is a constant, then the moment problem is determinate.*

Criterion 2 (**Carleman condition**). *If*

$$\sum_{n=1}^{\infty} \mu_{2n}^{-\frac{1}{2n}} = +\infty \quad \textit{(Hamburger moment problem)}$$

or

$$\sum_{n=1}^{\infty} \mu_{n}^{-\frac{1}{2n}} = +\infty \quad \textit{(Stieltjes moment problem)}$$

then the moment problem is determinate.

Criterion 3 (**Krein condition**). *If*

$$\int_{-\infty}^{\infty} -\frac{\ln f(x)}{1+x^2} dx < \infty \quad \textit{(Hamburger moment problem)}$$

or

$$\int_{0}^{\infty} -\frac{\ln f(x)}{1+x^2} dx < \infty \quad \textit{(Stieltjes moment problem)}$$

then the moment problem is indeterminate.

There are two main problems in using above criteria: *i*) they require the knowledge of the moment generating function or of the probability density function, *ii*) they give

sufficient conditions only, so that if they are not satisfied nothing about the determinacy problem can be said. The consequence is that in general it results to be very difficult to prove the determinacy of the moment problem using algebraic moment. Additional necessary and sufficient conditions exist in literature (see, for example, Akhiezer, 1965 and Shohat and Tamarkin, 1943), but these conditions are not easy to check in general. Some other checkable conditions can be found in Lin (2017).

The classical example where the moment problem is determinate (respectively, indeterminate) is the normal (log-normal) distribution. Indeed, in the case of the normal random variable, the first two moments completely characterize the distribution, while in the case of the log-normal it is possible to show that there exist infinitely many distributions with exactly the same sequence of moments, some examples are provided in Stoyanov (1997, pag. 102-104) or Devroye (1986, pag. 693). These facts are well known and can also be easily checked by Criteria 1, 2 and 3. Other interesting examples of different distributions sharing the same moments are given in Godwin (1964), Kendall and Stuart (1977), Widder (1941, pag. 125–126), Lukacs (1970, pag. 20).

1.2 Distribution approximation techniques

In this subsection we show how to approximate unknown distributions given moments. Fusai and Tagliani (2002, pag. 148) identify some desirable conditions when using approximations based on moments:

a) the true density is uniquely determined by the infinite sequence of moments;

b) for a given number of moments, the approximated distribution should be positive;

c) for a given number of moments, a bound to the error made is provided;

d) increasing the number of moments considered, the sequence of approximants is converging to the true distribution in some norm.

The point *a*) depends on the specific problem one faces while *b*), *c*) and *d*) depend on the approximation method. Even if conditions *a*), *b*), *c*) and *d*) typically does not hold simultaneously, there is some initial reason to think that matching moments will give a good approximation. For example, Lindsay and Roeder (1997) show that if two distributions have the same first n moments, then they must cross each other at least n times. Moreover, Akhiezer (1965, pag. 66) shows that the possible error can be bounded, and establishes the relevant relationships of the difference between two distributions that share the same $2n$ moments (this is studied in Section 1.3). Moreover, even in the cases where the moment problem is indeterminate, i.e. there are possibly infinite distributions sharing the same moments, is still possible to get good approximations by fitting moments

introducing some additional constraints based on partial information about the unknown distribution. For example, in many practical cases one knows if the unknown distribution is discrete or continuous, unimodal or multimodal. This partial information can be used to reduce the set of distributions sharing the same sequence of moments limiting the risk to approximate the wrong distribution.

In the course of this section we examine two different approximation techniques: moment matching and polynomial expansions. These will find wide application within this thesis. Alternative methods are also explored in Section 1.5.

1.2.1 Moment matching

Moment matching is the most popular (and simple) approach for approximating unknown distributions using moments. Suppose that X is an unknown distribution whose sequence of moments $\mu_n = \mathrm{E}[X^n]$ is known. The idea is to approximate X through an arbitrary parametric random variable Y sharing the same moments of X. More formally, the unknown density of X is approximated by the known density $f_Y(y;\underline{\theta})$ where $\underline{\theta} \in \Theta \subset \mathbb{R}^n$ is such that $\mathrm{E}[X^j] = \mathrm{E}[Y^j]$, $\forall j \in \{1, n\}$ and Θ is the parameter space. We provide here an example on implementation of moment matching by fitting the first two integer moments, it has not only illustrative scope, but also finds application in Chapter 3.

Example 1 (**Moment matching with gamma distribution**). *Suppose to approximate the density of X by $f_Y(y;\underline{\theta}) = \frac{1}{\Gamma(k)\theta^k} y^{k-1} e^{-\frac{y}{\theta}}$, where $\Gamma(\cdot)$ denotes the gamma function, i.e. the density of a gamma distribution. The parameter vector $\underline{\theta} = [\theta, k]$ can be estimated by solving the following system of moments:*

$$\begin{cases} \mathrm{E}[X] = k\theta \\ \mathrm{Var}[X] = k\theta^2 \end{cases} \Rightarrow \begin{cases} \theta = \frac{\mathrm{Var}[X]}{\mathrm{E}[X]} \\ k = \frac{\mathrm{E}[X]}{\theta} \end{cases}$$

where $\mathrm{Var}[X] = \mathrm{E}[X^2] - \mathrm{E}[X]^2$ is the variance of X.

The choice of the approximating distribution is somewhat arbitrary and depends on many factors, on one hand the higher the number of moments considered the higher the expected accuracy. On the other hand, including too many moments may decrease the analytical tractability of the problem (with the result that time consuming numerical techniques may be required for the solution of the system) and increase the possibility to obtain an unsolvable system of moments. Another constraint to the choice of the number of moments occurs when higher order moments are difficult to compute (an example of this is given in Chapter 2, where computation of higher order moments turns out to be very computationally intensive). The result is that typically moment matching is implemented by fitting only the first few integer moments. When the first four integer moments are

known, two very good ways to fit them is through the Johnson's and Pearson's systems of densities.

Johnson's system

Consider a continuous random variable X with an unknown distribution. In order to approximate it, Johnson (1949) derived a system of curves with the flexibility to cover a wide variety of shapes, under the form of a set of "normalizing" translations. These translations transform the continuous random variable X into a standard normal variable Z according to:

$$Z = a + b \cdot g\left(\frac{X - c}{d}\right),$$

where a and b are shape parameters, c is a location parameter, d is a scale parameter and $g(\cdot)$ is a function defining the four families of distributions of the Johnson's system:

$$g(u) = \begin{cases} \ln(u), & \text{log-normal family} \\ \ln(u + \sqrt{u^2 + 1}), & \text{unbounded family} \\ \ln\left(\frac{u}{1-u}\right), & \text{bounded family} \\ u, & \text{normal family} \end{cases}. \tag{1.2}$$

Such system has the flexibility to match any feasible set of values for the first four integer moments. Skewness and kurtosis also uniquely identify the appropriate form of $g(\cdot)$. As a result, the problem of using the Johnson system to approximate an unknown distribution is reduced to that of finding the values of a, b, c and d that will match the moments of the unknown target distribution with those of the appropriate family from the Johnson system. Hill *et al.* (1976) provide an algorithm that finds, given the first four integer moments of an unknown distribution, the appropriate family, i.e. the form of $g(\cdot)$, and find the values of the parameters required to approximate the unknown distribution. This algorithm is not very intuitive or easy to summarize[1], but is very efficient and typically takes a fraction of a second to compute the required quantities for a single set of moments. Unfortunately, this algorithm does not ensure convergence, moreover, the Johnson's system is better suited for quantile matching than for moment matching (see Devroye, 1986, pag. 685). Alternative approaches for parameter estimation given quantiles can be found in Wheeler (1980) and Tuenter (2001). With the parameters determined as above, the Johnson's system can be expressed as the inverse of normalizing

[1] A Matlab® code due to Jones (2014) can be found at the following link: `https://it.mathworks.com/matlabcentral/fileexchange/46123-johnson-curve-toolbox`.

translation given in formula (1.2):

$$X = c + d \cdot g^{-1}\left(\frac{Z-a}{b}\right) \tag{1.3}$$

where

$$g^{-1}(u) = \begin{cases} e^u, & \text{log-normal family} \\ \frac{e^u - e^{-u}}{2}, & \text{unbounded family} \\ \frac{1}{1+e^{-u}}, & \text{bounded family} \\ u, & \text{normal family} \end{cases}. \tag{1.4}$$

Pearson's system

Pearson (1895) designed a flexible system of seven distributions whereby for every member the probability density function $f(x)$ satisfies the following differential equation:

$$\frac{1}{f(x)}\frac{\partial f(x)}{\partial x} = -\frac{a+x}{c_0 + c_1 x + c_2 x^2}. \tag{1.5}$$

The shape of the distribution depends on the values of the parameters a, c_0, c_1 and c_2. For example, the case where $c_1 = c_2 = 0$ corresponds to the limit case where X is normally distributed, indeed we can rewrite (1.5) as:

$$\frac{1}{f(x)}\frac{\partial f(x)}{\partial x} = -\frac{a+x}{c_0} \Rightarrow f(x) = Ce^{-\frac{ax+\frac{x^2}{2}}{c_0}},$$

where C denotes the integration constant which is chosen to make $\int_{-\infty}^{\infty} f(x)dx = 1$, in this case $C = \frac{e^{-\frac{a^2}{2c_0}}}{\sqrt{2\pi c_0}}$ ensures that $f(x)$ is the density of a normal distribution with mean $-a$ and standard deviation c_0. Before showing how moments can be used to identify a, c_0, c_1, c_2, we start by classifying the various shapes into a number of types[2]. It is evident that the form of the solution of (1.5) depends on the nature of the roots of:

$$c_0 + c_1 x + c_2 x^2 = 0 \tag{1.6}$$

and the various types correspond to these different forms of solution. We denote with a_1 and a_2 the two roots of such equation.

- **Type I, Four-parameters beta:** corresponds to the case where $a_1 < 0 < a_2$, we

[2]We follow Johnson *et al.* (1994a, Chapter 4).

have

$$c_0 + c_1 x + c_2 x^2 = -c_2(x - a_1)(a_2 - x),$$

putting into (1.5) one gets:

$$\frac{1}{f(x)}\frac{\partial f(x)}{\partial x} = -\frac{a + x}{c_2(x - a_1)(a_2 - x)} \Rightarrow f(x) = C(x - a_1)^{m_1}(a_2 - x)^{m_2},$$

where $m_1 = \frac{a+a_1}{c_2(a_2-a_1)}$ and $m_2 = \frac{a+a_2}{c_2(a_1-a_2)}$. Selecting $C = \frac{1}{B(m_1+1,m_2+1)(a_2-a_1)^{m_1+m_2+1}}$, where $B(\cdot,\cdot)$ denotes the beta function, one gets the density of a generalized beta distribution with location parameter a_1, scale parameter a_2 and shape parameters $m_1 + 1$ and $m_2 + 1$ (cfr. Johnson *et al.*, 1994b, Chapter 25):

$$f(x; a_1, a_2, m_1 + 1, m_2 + 1) = \frac{(x - a_1)^{m_1}(a_2 - x)^{m_2}}{B(m_1 + 1, m_2 + 1)(a_2 - a_1)^{m_1+m_2+1}}, \quad a_1 \leq x \leq a_2.$$

- **Type II, Symmetric four-parameter beta:** Corresponds to a special case of Type I, where the distribution is symmetric ($m_1 = m_2$).

- **Type III, Shifted gamma:** Corresponds to the special case where $c_2 = 0$ and $c_1 \neq 0$. In this case (1.5) becomes:

$$\frac{1}{f(x)}\frac{\partial f(x)}{\partial x} = -\frac{a + x}{c_0 + C_1 x} \Rightarrow f(x) = Ce^{-\frac{x}{c_1}}(c_0 + c_1 x)^m$$

where $m = -\frac{ac_1-c_0}{c_1^2}$. Setting $\gamma = -\frac{c_0}{c_1}$ and $C = \frac{e^{\frac{\gamma}{c_1}}}{c_1^{2m}\Gamma(m+1)}$ one gets the density of the generalized gamma distribution with location parameter γ, shape parameter $m+1$ and scale parameter c_1 (cfr. Johnson *et al.*, 1994a, Chapter 17):

$$f(x; \gamma, m + 1, c_1) = \frac{e^{-\frac{(x-\gamma)}{c_1}}(x - \gamma)^m}{\Gamma(m + 1)c_1^{m+1}}.$$

- **Type IV:** Corresponds to the case where equation (1.6) does not have real roots. The following identity is used to write the density function:

$$c_0 + c_1 x + c_2 x^2 = C_0 + c_2(x + C_1)^2,$$

where $C_0 = c_0 - \frac{c_1^2}{4c_2}$ and $C_1 = \frac{c_1}{2c_2}$. Then, we write:

$$\frac{1}{f(x)}\frac{\partial f(x)}{\partial x} = -\frac{-(x+C_0)-(a-C_1)}{C_0+c_2(x+C_1)^2} \Rightarrow$$

$$f(x) = C\left(C_0+c_2(x+C_1)^2\right)^{-(2c_2)^{-1}} e^{-\frac{a-C_1}{\sqrt{c_2C_0}}\tan^{-1}\left(\frac{x+C_1}{\sqrt{\frac{C_0}{c_2}}}\right)}.$$

No common statistical distributions are known with this density, moreover the cumulative distribution function can not be computed analytically. Pearson and Hartley (1972) provide quantiles (percentiles) of Pearson system distributions to four decimal places for different levels of skewness and kurtosis. By interpolation these tables can provide approximate values of the cumulative distribution function, without the need to evaluate C (for which numerical integration would be required).

- **Type V, Inverse gamma location-scale:** Corresponds to the case where $c_1^2 = 4c_0c_2$. Equation (1.5) can be rewritten as:

$$\frac{1}{f(x)}\frac{\partial f(x)}{\partial x} = -\frac{a+x}{c_2(x+C_1)} \Rightarrow f(x) = C(x+C_1)^{-\frac{1}{c_2}} e^{\frac{a-C_1}{c_2(x+C_1)}}$$

setting $C = \frac{\left(\frac{a-C_1}{c_2}\right)^{\frac{1}{c_2}}}{\Gamma(\frac{1}{c_2}-1)}$ we recognize that $f(x)$ is the density of a shifted reciprocal Gamma with location parameter $-C_1$, shape parameter $\frac{1}{c_2}-1$ and scale parameter $\frac{a-C_1}{c_2}$.

- **Type VI, F location-scale:** Corresponds to the case where (1.6) has two real roots with the same sign. Solving (1.5) one gets

$$f(x) = C(x-a_1)^{m_1}(x-a_2)^{m_2}$$

with $m_1 = (a_1+c_1)/(c_2(a_2-a_1))$ and $m_2 = -(a_2+c_1)/(c_2(a_2-a_1))$. If $a_1 < a_2 < 0$ then is possible to write the probability density function as

$$f(x) = \frac{\nu_2}{\nu_1(a_2-a_1)} f_F(x;\nu_1,\nu_2)$$

where $\nu_1 = 2(m_2+1)$ and $\nu_2 = -2(m_1+m_2+1)$, else if $a_1 > a_2 > 0$ then

$$f(x) = \frac{(a_1-a_2)\nu_2}{\nu_1} f_F(x;\nu_1,\nu_2)$$

where $\nu_1 = 2(m_1+1)$, $\nu_2 = -2(m_1+m_2+1)$ and $f_F(x;\nu_1,\nu_2)$ is the probability density function of a Snedecor-F distribution with numerator degrees of freedom ν_1 and denominator degrees of freedom ν_2.

- **Type VII, Student's t location-scale:** Corresponds to the case where $c_1 = a = 0$, $c_0 > 0$, and $c_2 > 0$. In this case the solution of (1.5) becomes

$$f(x) = C(c_0 + c_2 x^2)^{-(2c_2)^{-1}}.$$

Noting similarity with the Student's t distribution we get the following expression for the density

$$f(x) = \frac{1}{\sqrt{c_0/(1-c_2)}} f_T(x;\nu)$$

where $\nu = 1/c_2 - 1$ and $f_T(x;\nu)$ is the probability density function of a Student's t distribution.

We conclude this paragraph by showing how to compute a, c_0, c_1 and c_2 given only the first four integer moments of the distribution $\{\mu_n\}_{n=1}^4$. First, note that given the first four integer moments skewness and kurtosis can be easily computed according to:

$$\begin{aligned}
\text{Skew}[X] &= \frac{\text{E}[X^3] - 3\text{E}[X]\text{Var}[X] - \text{E}[X]^3}{\text{Var}[X]^{\frac{3}{2}}} \\
\text{Kurt}[X] &= \frac{\text{E}[X^4] - 4\text{E}[X]\text{E}[X^3] + 6\text{E}[X]^2\text{E}[X^2] - 3\text{E}[X]^4}{\text{Var}[X]^2}
\end{aligned}$$

Posing $\beta_1 = \text{Skew}[X]^2$ and $\beta_2 = \text{Kurt}[X]$, the formulas for a, c_0, c_1 and c_2 are (see Johnson *et al.*, 1994a, pag. 22):

$$c_0 = (4\beta_2 - 3\beta_1)(10\beta_2 - 12\beta_1 - 18)^{-1}\mu_2 \tag{1.7}$$

$$a = c_1 = \sqrt{\beta_1}(\beta_2 + 3)(10\beta_2 - 12\beta_1 - 18)^{-1}\sqrt{\mu_2} \tag{1.8}$$

$$c_2 = (2\beta_2 - 3\beta_1 - 6)(10\beta_2 - 12\beta_1 - 18)^{-1} \tag{1.9}$$

Given the numerical values of the above quantities and setting $k = \frac{\beta_1(\beta_2+3)^2}{4(4\beta_2-3\beta_1)(2\beta_2-3\beta_1-6)}$, is possible to select the appropriate distribution of the family using the following rules

- **Type I:** $k < 0$
- **Type II:** $\beta_1 = 0$ and $\beta_2 < 3$
- **Type III:** $2\beta_2 - 3\beta_1 - 6 = 0$
- **Type IV:** $0 < k < 1$
- **Type V:** $k = 1$
- **Type VI:** $k > 1$

- **Type VII:** $\beta = 0$, $\beta_2 > 3$.

Note that μ_1 serves to compute variance, skewness and kurtosis but does not appear in the matching procedure. Is standard practise, indeed, to assume that the expected value of the approximating distribution is 0 and then shift the distribution by μ_1 in order to match also the first moment.

1.2.2 Polynomial expansions

Polynomials expansions provide attractive alternatives when it comes to probability density function estimation. They combine the simplicity of fitting a two-parameter density with the flexibility of correcting for higher order moments, often resulting in fast and accurate approximations. This approach allows to approximate the unknown density of X given only the knowledge of its domain and its moments[3]. Polynomial expansion technique can be summarized as follows:

1) select an appropriate density $p(x)$ defined on the same domain $\mathcal{D}$ of the unknown density $f(x)$;

2) identify a set of orthogonal (or orthonormal) polynomials, denoted with $\{P_i(x)\}_{i=0}^{\infty}$, with respect to $p(x)$;

3) perform polynomial expansion based on the moments of X and the orthogonal polynomials.

Performing an expansion around $p(x)$ is possible to express the density of X in terms of the following series (see, for example, Corrado and Su, 1996):

$$f(x) = p(x) \left(\sum_{i=0}^{\infty} \frac{\mathrm{E}[P_i(x)]}{\langle P_i, P_i \rangle} P_i(x) \right), \tag{1.10}$$

with $\langle P_i, P_i \rangle$ denoting the norm of the polynomial $P_i(x)$. Of course, for computational reasons, infinite summation in (1.10) must be truncated, giving the following approximation for the true density:

$$f(x) \approx f_N(x) = p(x) \left(\sum_{i=0}^{N} \frac{\mathrm{E}[P_i(x)]}{\langle P_i, P_i \rangle} P_i(x) \right).$$

Hence, some natural questions arise: does $f_N(x)$ become increasingly accurate and converge when adding more terms? If yes, under which condition? Does $f_n(x)$ integrate to

[3] A similar technique is the Edgeworth series expansion, but, due to its poor practical performances, it is not used throughout this work. Hence, we don't describe here its theoretical properties but simply briefly recall it in Section 1.5

1? These problems have been tackled in Filipović *et al.* (2013) which prove first that $\int_{\mathcal{D}} f_n(x) = 1 \ \forall n \in \mathbb{N}^+$ and then the following

Theorem 1.1. *If $f(x)$ is weighted square integrable, i.e.:*

$$\int_{\mathcal{D}} \frac{f(x)^2}{p(x)} dx < \infty, \tag{1.11}$$

then

$$\lim_{n\to\infty} \int_{\mathcal{D}} \frac{(f(x) - f_n(x))^2}{p(x)} dx = 0. \tag{1.12}$$

This result can be interpreted as: if (1.11) holds true then $f_n(x)$ becomes increasingly accurate when adding more terms (which is equivalent to adding more moments).
For sake of clarity, we summarize here three different polynomial expansion techniques based on three different densities, the first two have been used in literature for the case where the true distribution is defined on $\mathbb{R}$, the third one for the case where the domain is $\mathbb{R}^+$. Other possible choices based on the gamma and bilateral gamma distributions are contained in Filipović *et al.* (2013). Further choices for $p(x)$ and $P_i(x)$ are necessary[4] when alternative domains are considered, in particular Provost (2005) considers approximations based on Legendre polynomials when the domain is $[-1, 1]$ and approximations based on Laguerre polynomials when it is $[a, +\infty)$ with $a \geq 0$. Since in many cases, the approximating densities are more easily expressed in terms of the cumulants, instead of moments, we briefly recall the explicit expression for the $n-th$ moment (μ_n) in terms of the first n cumulants $(\{c_i\}_{i=1}^n)$, and vice versa. This relationship can be obtained by using Faá di Bruno's formula for higher derivatives of composite functions. In general, we have

$$\mu_n = \sum_{i=1}^{n} \mathrm{B}_{n,i}(c_1, ..., c_{n-i+1}), \tag{1.13}$$

$$c_n = \sum_{i=1}^{n} (-1)^{k-1}(k-1)!\mathrm{B}_{n,i}(\mu_1, ..., \mu_{n-i+1}) \tag{1.14}$$

where $\mathrm{B}_{n,i}$ are the incomplete Bell polynomials.

Expansion around standard normal density: the Gram-Charlier A series

We begin by defining the $i-th$ Hermite polynomial $He_i(x)$ as:

$$He_i(x) := (-1)^n \frac{\frac{\partial^i}{\partial x^i} n(x)}{n(x)} \tag{1.15}$$

[4]We don't report them since are not used inside this thesis.

where $n(x)$ denotes the standard normal density. Distinct Hermite polynomials $He_i(x)$ and $He_j(x)$, $i \neq j$, satisfy an orthogonality relation using the normal density as a weighting function, i.e. Hermite polynomials are orthogonal with respect to the normal density:

$$\langle He_i, He_j \rangle = \int_{-\infty}^{\infty} He_i(x) He_j(x) n(x) = 0.$$

The norm or weighted-average square of a Hermite polynomial is given by:

$$\langle He_i, He_i \rangle = i!,$$

in practice, Hermite polynomials are easy to compute recursively using the relation:

$$\begin{aligned} He_0(x) &= 1 \\ He_1(x) &= x \\ He_{i+1}(x) &= xHe_i(x) - iHe_{i-1}(x). \end{aligned}$$

Given a random variable X, its density can be expressed, according to (1.10), as:

$$f(x) = n(x) \left(\sum_{i=0}^{\infty} \frac{\mathrm{E}[He_i(x)]}{\langle He_i, He_i \rangle} He_i(x) \right). \tag{1.16}$$

In Table 1.1 we report the analytical expression of the first five Hermite polynomials together with their norm. Note that if X is a standardized distribution (i.e. with zero mean and unitary variance) then $\mathrm{E}[He_i(x)] = c_i$, hence $f(x)$ can be rewritten as:

$$f(x) = n(x) \left(\sum_{i=0}^{\infty} \frac{c_i}{i!} He_i(x) \right) = n(x) \left(1 + \sum_{i=3}^{\infty} \frac{c_i}{i!} He_i(x) \right).$$

Expansion around standard logistic density

Heston and Rossi (2017) introduce an analogous set of orthogonal polynomials based on the standardized logistic density:

$$l(x) = \frac{\pi}{\sqrt{3} \left(\exp\left(\frac{\pi x}{\sqrt{3}} \right) + 2 + \left(-\frac{\pi x}{\sqrt{3}} \right) \right)}.$$

The logistic polynomials are orthogonal with respect to the logistic density:

$$\langle Lo_i, Lo_j \rangle := \int_{-\infty}^{\infty} Lo_i(x) Lo_j(x) l(x) dx = 0.$$

We can generate the logistic polynomials recursively via the Gram-Schmidt procedure, but, according to Heston and Rossi (2017, Formula 31), the most computationally efficient

Table 1.1: Hermite and logistic polynomials along with their norms

i	$He_i(x)$	$\langle He_i, He_i \rangle$	$Lo_i(x)$	$\langle Lo_i, Lo_i \rangle$
0	1	1	1	1
1	x	1	x	1
2	$x^2 - 1$	2	$x^2 - 1$	$\frac{16}{5}$
3	$x^3 - 3x$	6	$x^3 - \frac{21}{5}x$	$\frac{3888}{175}$
4	$x^4 - 6x^2 + 3$	24	$x^4 - \frac{78}{7}x^2 + \frac{243}{35}$	$\frac{331776}{1225}$
5	$x^5 - 10x^3 + 15x$	120	$x^5 - \frac{70}{3}x^3 + \frac{407}{7}x$	$\frac{2764800}{539}$

approach is to use the following relation:

$$Lo_{i+1}(x) = xLo_i(x) - \frac{3i^4}{(2i+1)(2i-1)}Lo_{i-1}(x),$$

while the norms or weighted-average-squares of the logistic polynomials are:

$$\langle Lo_i, Lo_j \rangle = \frac{3^i i!^4}{(2i-1)!!(2i+1)!!}.$$

Finally, the true density of X is given by:

$$f(x) = l(x)\left(\sum_{i=0}^{\infty} \frac{\mathrm{E}[Lo_i(x)]}{\langle Lo_i, Lo_i \rangle} Lo_i(x)\right). \tag{1.17}$$

The first five logistic polynomials are reported, together with their norms, in Table 1.1. Note that the moments of X must be used in order to compute $\mathrm{E}[Lo_i(x)]$.

Expansion around log-normal density

In the case where the target distribution is defined on $\mathbb{R}^+$ an orthogonal polynomial expansion based on the log-normal density has been proposed by Willems (2019). In this case, the weight function is given by the density of a log-normal distribution:

$$w(x) = \frac{1}{\sqrt{2\pi}\sigma x} \exp\left(-\frac{(\ln(x) - \mu)^2}{2\sigma^2}\right),$$

with $\mu \in \mathbb{R}$ and $\sigma > 0$. Note that we have written the densities in terms of infinite sums (see for example equations (1.16) and (1.17)), in this case, in order to use a matrix notation, we consider a finite number N of terms in (1.10). Following Filipović *et al.*

(2013), orthonormal polynomial basis is built as follows:

$$\begin{bmatrix} b_0(x) \\ b_1(x) \\ \vdots \\ b_N(x) \end{bmatrix} = L^{-1} \begin{bmatrix} 1 \\ x \\ \vdots \\ x^N \end{bmatrix}$$

where $M = LL^T$ (i.e. L is computed by applying Cholesky decomposition on the matrix M) and M is the Hankel moment matrix:

$$M_{ij} = \int_0^\infty x^{i+j} w(x) dx = e^{(i+j)\mu + \frac{1}{2}(i+j)^2\sigma^2},$$

with the subscript "ij" denoting $i-th$ row and $j-th$ column of the matrix, μ and σ are selected in such a way that the unknown distribution shares with the weight function the first two moments. Given the orthonormal polynomial basis $b_n(x)$ is possible to approximate the true density $f(x)$ of the unknown distribution X by using the first n integer moments as follows:

$$f_n(x) = w(x) \sum_{i=0}^{n} l_i b_i(x), \tag{1.18}$$

where $\begin{bmatrix} l_0 \\ l_1 \\ \vdots \\ l_n \end{bmatrix} = L^{-1} \begin{bmatrix} 1 \\ \mu_1 \\ \vdots \\ \mu_n \end{bmatrix}$ and $\mu_i = \mathrm{E}[X^i]$.

1.3 Error bounds

In this section we tackle the problem of finding an appropriate bound to the error one commits when approximating an unknown random variable X with another one sharing the same first $2n$ integer moments. Two different error bounds are provided in literature. The first one is defined by the following:

Theorem 1.2. *Akhiezer (1965, pag. 66)*

Let $F_X(x)$ be the unknown distribution function and let $G_X(x)$ a distribution that shares with $F_X(x)$ the same $2n$ moments, then:

$$|F_X(x) - G_X(x)| \leq \zeta_n(x), \tag{1.19}$$

where

$$\frac{1}{\zeta_n(x)} = \begin{pmatrix} 1 & x & ... & x^n \end{pmatrix} \begin{pmatrix} 1 & \mu_1 & ... & \mu_n \\ \mu_1 & ... & ... & \mu_{n+1} \\ \vdots & \vdots & \vdots & \vdots \\ \mu_n & \mu_{n+1} & ... & \mu_{2n} \end{pmatrix}^{-1} \begin{pmatrix} 1 \\ x \\ \vdots \\ x^n \end{pmatrix}.$$

A positive feature of this result is that it is very easy to check (only the moment sequence $\{\mu_i\}_{i=1}^{2n}$ is needed), but, unfortunately, Lindsay and Basak (2000) show that this bound results to be tight only in the tails of the distribution. This means that, in practical applications, the true error will be typically extremely smaller than the error upper bound.

A second theoretical result is given by the following

Theorem 1.3. *Klebanov and Mkrtchyan (1985)*

Let $F_X(x)$ be the unknown distribution function and let $G_X(x)$ a distribution that shares with $F_X(x)$ the same $2n$ moments, denote the sub-quantity $C_n := \sum_{i=1}^{n} \mu_{2k}^{-\frac{1}{2k}}$, then

$$L(F, G) \leq c(\mu_2) \frac{\ln(1 + C_{n-1})}{C_{n-1}^{\frac{1}{4}}} \tag{1.20}$$

where $L(F, G) := \inf\{\epsilon > 0 : F(x - \epsilon) - \epsilon \leq G(x) \leq F(x + \epsilon) + \epsilon\}$ is the Lévy distance between the distribution functions and $c(\mu_2)$ is a function that depends on m_2.

Note the relationship with Criterion 2 (Carleman condition), if it is satisfied then $C_\infty = \sum_{i=1}^{\infty} \mu_{2k}^{-\frac{1}{2k}} = \infty$ and $L(F, G) = 0$, $\forall c(\mu_2)$. The main limitations of this result are that it holds only for random variables defined on $\mathbb{R}$ (Hamburger moment problem) and the ambiguity about the form of the function $c(\cdot)$, which makes it not easily applicable in practise.

1.4 Using moments in finance: a literature review

In this section we provide a literature review on the usage of moments and moment based approximations in finance.

We start by taking into account problems related to the pricing of financial derivatives, where unknown distributions are ubiquitous and approximations based on their moments have been largely adopted. The most emblematic case concerns the pricing of Asian options. This kind of instruments are particularly difficult to price since their payoff depends on the arithmetic average of prices which the underlying's assumes during the life of the contract, whose distribution is unknown even under simple model assumptions. We will devote entirely the next section to the usage of moments to price arithmetic Asian options

under the Black-Scholes model. Considering more complicated underlying's dynamics, moment matching has been adopted in Ballotta (2010) for Asian options valuation in the cases where the underlying evolves according to a Variance Gamma process and in Albrecher and Predota (2004) in a Normal Inverse Gaussian (NIG) economy. In Chapter 2 we tackle the more general problem of pricing Asian options in a context where the underlying evolves according to a mean-reverting exponential Lévy driven Ornstein-Uhlenbeck process and propose, among others, moment matching techniques. For what concerns other derivative instruments, Brigo *et al.* (2004) and Stace (2007) use moment matching to price, respectively, basket options and volume weighted average price options in the Black-Scholes model, Privault and Yu (2016) price bonds in the case where the short rate evolves according to the Dothan (1978) model, Pellegrino and Sabino (2014) propose the usage of moment matching to price multi-asset spread options (see the original paper for the underlying's dynamics specification) and Prayoga and Privault (2017) for pricing yield options in the CIR model[5]. Moreover, moment matching has been adopted also for real options valuation in project management, we mention, among others, Creemers (2018), which computes the Net Present Value (NPV) of a project with multiple stages that are executed in sequence.

For what concerns series expansion, Jarrow and Rudd (1982) pioneered the use of Edgeworth expansions for valuation of derivative securities and Corrado and Su (1996) introduced Gram-Charlier expansions. More recently, Filipović *et al.* (2013) developed pricing formulas for European options under affine models based on orthogonal polynomials expansions, Heston and Rossi (2017) derive an alternative series expansion which can be applied for models where the characteristic function of log-returns in unknown, as, for example, the Hull and White (1987) stochastic volatility model.

Moments are also used to find option price bounds in a model-free framework, more specifically, Bertsimas *et al.* (2000) and Gotoh and Konno (2002) show that the lower and upper bounds to option prices can be found, exploiting the knowledge of the moments, by solving a semi-definite programming problem. Lasserre *et al.* (2006) extend this moment based semi-definite programming approach to the pricing of exotic options, such as Asians and barriers under simple dynamics for the price process. More recently, Lütkebohmert and Sester (forthcoming) find price bounds for some exotic options solving an optimal martingale transport problem with moments constraints.

Outside option pricing, usage of moments have also been suggested for model calibration purposes. Bakshi and Madan (2000) and Bakshi *et al.* (2003) show how to compute risk-neutral moments given a set of European call and put options prices, based on this, several attempts have been made in literature to calibrate model parameters using the information provided by the moments. Guillaume and Schoutens (2013) develop a very simple calibration procedure for Lévy models, in particular, risk neutral moments are

[5]see Cox *et al.* (1985).

computed from a real dataset of option prices and parameters are estimated by solving (analytically) a simple system of moments. Successively, Guillaume and Schoutens (2014) extends this moment matching market implied calibration procedure to Markov models. Furthermore, Feunou and Okou (2018) calibrate the Andersen *et al.* (2015) option valuation model on real data using the historical time series of risk-neutral moments.

Finally, moments are widely employed in other areas of finance such as portfolio management and forecasting. The idea of using moments for portfolio optimization dates back to Markowitz (1952) which selects the optimal portfolio according to the expected mean and variance of stock returns. Several attempts have been made in literature to take into account higher order moments in the portfolio selection problem, we mention among others, Harvey *et al.* (2010). Moreover, the idea that moments can be used to predict financial market behavior is widely studied in literature, Bates (1996b) investigates the possibility that option implied higher moments contain significant information for the future exchange rates, Navatte and Villa (2000) find that the moments contain a substantial amount of information for future moments, with kurtosis contributing less to forecasting power than skewness and volatility. Carson *et al.* (2006) find that the implied volatility skew has strong predictive power in forecasting short-term market declines. However, Doran *et al.* (2007) find that the predictability is not economically significant. For individual stocks, Diavatopoulos *et al.* (2008) look at changes in implied skewness and kurtosis prior to earnings announcements and find that both have strong predictive power for future stock and option returns. DeMiguel *et al.* (2011) propose using implied volatility, skewness, correlation and variance risk premium in portfolio selection, and find that the inclusion of skewness and the variance risk premium improves the performance of the portfolio significantly.

1.5 Example: Asian option pricing in the Black-Scholes model

In this section we test moment matching and series expansion techniques against other moment based approximations proposed in literature in the context of pricing arithmetic average Asian options.

Asian options are derivative instruments whose payoff depends on the average value of the asset price over some time period. They have had a very large success in the last years, because they reduce the possibility of market manipulation near the expiry date and offer a better hedge to firms having a stream of positions, a discussion about this is presented in Chapter 2. Actually there is no closed form solution for the price of this option because in the usual Black-Scholes framework, the arithmetic average is a sum of correlated lognormal distributions for which there is no recognizable density function. In

order to price such options, several attempts in the literature have been made based on Monte Carlo simulation, moments based approximations, Partial Differential Equations (PDEs), binomial trees, Laplace transform inversion and lower and upper bounds for the option price (we refer to Fusai and Tagliani, 2002 for a detailed literature review). With the scope of testing the approximation techniques illustrated throughout this section, we consider approximations based on the integer moments of the unknown distribution of the arithmetic average.

Alternative approximations based on the moments of transformations of the arithmetic average have also been suggested. Dufresne (2000) uses Laguerre expansions of the price in terms of the moments of $\frac{1}{A(T)}$, Fusai and Tagliani (2002) propose approximations based on the moments of $\ln(A(T))$, while D'Amico *et al.* (2003) consider the fractional moments of the arithmetic average. All these approaches are able to produce extremely accurate results due to the fact that moment problem is determinate for such transformations of $A(T)$, but, unfortunately, moments are not easy to be computed and time consuming numerical techniques are required even under the simple assumption of a geometric Brownian motion as driving process for the stock price[6].

We start by briefly recalling the Black-Scholes model, then we show how to compute the moments of the arithmetic average and finally we show how to implement moment based approximations to price arithmetic Asian options under this model.

1.5.1 Black-Scholes model

In the Black-Scholes model the underlying asset price evolves, under the risk-neutral measure, according to a Geometric Brownian Motion:

$$dS(t) = rS(t)dt + \sigma S(t)dW(t) \tag{1.21}$$

where r is the instantaneous risk free rate, σ is the instantaneous volatility and $W(t)$ is a Brownian motion. Solution of equation (1.21) is

$$S(T) = S(0)e^{\left(r-\frac{\sigma^2}{2}\right)T+\sigma W(T)}, \tag{1.22}$$

where T is the final date and $S(0)$ is the stock price at the initial date. Assuming zero dividend yield and that the arithmetic average is computed continuously in time in the period $[0, T]$, we define:

$$A(T) = \frac{1}{T}\int_0^T S(t)dt = \frac{S(0)}{T}\int_0^T e^{\left(r-\frac{\sigma^2}{2}\right)t+\sigma W(t)}dt. \tag{1.23}$$

[6]For example, the computation of the moments of $\frac{1}{A(T)}$ requires to solve numerically differential-difference equations.

The payoff of the arithmetic average Asian call option with fixed strike K is given by $(A(T)-K)^+$, hence the price can be computed as

$$p = e^{-rT}\mathrm{E}\left[(A(T)-K)^+\right] = e^{-rT}\mathrm{E}\left[\left(\frac{S(0)}{T}Y(T)-K\right)^+\right]$$
$$= e^{-rT}\frac{S(0)}{T}\int_{\frac{KT}{S(0)}}^{\infty}\left(y-\frac{KT}{S(0)}\right)f_Y(y)dx, \tag{1.24}$$

where $Y(T) := \int_0^T e^{\left(r-\frac{\sigma^2}{2}\right)t+\sigma W(t)}dt$ and $f_Y(\cdot)$ is its density. Since the distribution of $Y(T)$ is unknown the pricing problem is essentially reduced to the determination of $f_Y(\cdot)$.

1.5.2 Moments of $Y(T)$

The most used approximations in pricing Asian options are those based on the tentative of recovering the density of the average from its moments. In order to do that an expression for the moments of the arithmetic average is needed and can be found in Geman and Yor (1993, pag. 359):

$$\mu_n = \mathrm{E}\left[Y^n(T)\right] = \frac{n!}{\sigma^{2n}}\left\{\sum_{j=0}^{n} d_j^{\left(\frac{v}{\sigma}\right)}\exp\left(\left(\frac{\sigma^2 j^2}{2}+\sigma j v\right)T\right)\right\} \tag{1.25}$$

where

$$d_j^{(\beta)} = 2^n \prod_{\substack{i\neq j\\ 0\leq i\leq n}}\left((\beta+j)^2-(\beta+i)^2\right)^{-1}, \quad v = \frac{r-\frac{\sigma^2}{2}}{\sigma}.$$

An alternative way to compute such moments based on the theory of polynomial processes has been recently suggested by Willems (2019).

On one hand, since the moment problem for the log-normal density is indeterminate, one might expect that approximations of the arithmetic average based on a sequence of algebraic moments might either fail to converge, or converge to another distribution with the same moments. On the other hand, in the case of the arithmetic average we have a convolution of an infinite number of log-normal distributions and this convolution can change the distribution from a heavy tail density (the log-normal) to a light-tail density (the arithmetic average) and so there could be a (little) possibility that the moments determine uniquely the distribution. But we need to remark that Geman and Yor (1993) have shown that the Carleman's criterion is not satisfied in the case of the average of the geometric Brownian motion and so nothing can be said about the determinacy problem. Despite that, several approximations based on the moments of the arithmetic average have been proposed in literature, a detailed review is given next.

1.5.3 Approximations based on the first 2 moments

When only the first two integer moments are available moment matching is the most popular approach. Approximations based on the log-normal and the reciprocal gamma distributions have been proposed.

Log-normal approximation

The idea suggested by Turnbull and Wakeman (1991) and Levy (1992) is to approximate the unknown distribution of the arithmetic average with the known one of the log-normal distribution, whose parameters are estimated by moment matching. In other words, the density of $Y(T)$ is approximated through

$$f_{LN}(y;\mu,\sigma) = \frac{1}{y\sqrt{2\pi}\sigma} e^{-\frac{(\ln y-\mu)^2}{2\sigma^2}}, \tag{1.26}$$

where μ and σ are computed as:

$$\begin{cases} \mathrm{E}[Y(T)] = e^{\mu+\frac{\sigma^2}{2}} \\ \mathrm{E}[Y^2(T)] = e^{2\mu+2\sigma^2} \end{cases} \Rightarrow \begin{cases} \sigma^2 = \ln \frac{\mathrm{E}[Y^2(T)]}{\mathrm{E}[Y(T)]^2} \\ \mu = \ln(\mathrm{E}[Y(T)]) - \frac{\sigma^2}{2} \end{cases}.$$

Substituting (1.26) into (1.24) one gets

$$\begin{aligned} p \approx p_{LN} &:= e^{-rT}\frac{S(0)}{T}\int_{\frac{KT}{S(0)}}^{\infty}\left(y-\frac{KT}{S(0)}\right)f_{LN}(y)dy \\ &= e^{-rT}\frac{S(0)}{T}\left(e^{\mu+\frac{\sigma^2}{2}}\Phi\left(\frac{\mu+\sigma^2-\ln(K^\star)}{\sigma}\right) - K^\star\Phi\left(\frac{\mu-\ln(K^\star)}{\sigma}\right)\right), \end{aligned} \tag{1.27}$$

where $K^\star = \frac{KT}{S(0)}$ and $\Phi(\cdot)$ is the cumulative distribution function of the standard normal.

Reciprocal gamma approximation

Milevsky and Posner (1998) have proved that the stationary density for the arithmetic average of a geometric Brownian motion is given by a reciprocal gamma density, i.e. the reciprocal of the average has a gamma density. Consequently, the authors propose to approximate $f_Y(Y)$ through a moment matched inverse gamma density

$$f_{RG}(y;a,b) = \frac{b^a}{\Gamma(a)} y^{-a-1} e^{-\frac{b}{y}} \tag{1.28}$$

whose parameters are computed by solving the system of moments

$$\begin{cases} \mathrm{E}[Y(T)] = \frac{b}{a-1} \\ \mathrm{Var}[Y(T)] = \frac{b^2}{(a-2)(a-1)^2} \end{cases} \Rightarrow \begin{cases} a = \frac{\mathrm{E}[Y(T)]^2}{\mathrm{Var}[Y(T)]} + 2; \\ b = (a-1)\mathrm{E}[Y(T)] \end{cases}.$$

Substituting (1.28) into (1.24) one gets

$$\begin{aligned} p \approx p_{RG} &:= e^{-rT}\frac{S(0)}{T}\int_{\frac{KT}{S(0)}}^{\infty}\left(y - \frac{KT}{S(0)}\right) f_{RG}(y)dy \\ &= e^{-rT}\frac{S(0)}{T}\left(\mathrm{E}[Y(T)]G\left(\frac{b}{K^\star}, a-1, 1\right) - K^\star G\left(\frac{b}{K^\star}, a, 1\right)\right), \end{aligned} \tag{1.29}$$

where $G(x; a, b) = \int_0^x f_{RG}(y; a, b)dy$ is the cumulative distribution function of a Gamma random variable.

1.5.4 Approximations based on the first 3 moments

In the case where the first three integer moments are available, more sophisticated approximating random variables have been suggested by Lo *et al.* (2014). We provide here a brief review and refer to the original paper for more details.

Shifted log-normal

Milevsky and Posner (1998) and Lo *et al.* (2014) propose to add a third shifting parameter to the standard log-normal approximation of Levy (1992) and Turnbull and Wakeman (1991) and approximate $Y(T)$ by the following density

$$f_{SLN}(y; \mu, \sigma, h) = \frac{1}{(y-h)\sqrt{2\pi}\sigma} e^{-\frac{(\ln(y-h)-\mu)^2}{2\sigma^2}}, \quad y > h \tag{1.30}$$

whose parameters are estimated by solving the system of moments

$$\begin{cases} \mathrm{E}[Y(T)] = h + e^{\mu+\frac{\sigma^2}{2}} \\ \mathrm{Var}[Y(T)] = e^{2\mu+\sigma^2}\left(e^{\sigma^2} - 1\right) \\ \mathrm{Skew}[Y(T)] = \left(e^{\sigma^2} + 2\right)\sqrt{e^{\sigma^2} - 1} \end{cases} \Rightarrow \begin{cases} h = \mathrm{E}[Y(T)] - \frac{\sqrt{\mathrm{Var}[Y(T)]}}{\mathrm{Skew}[Y(T)]}\left(1 + B^{\frac{1}{3}} + B^{-\frac{1}{3}}\right) \\ \sigma^2 = \ln\left(1 + \frac{\mathrm{Var}[X]}{(\mathrm{E}[Y(T)]-h)^2}\right) \\ \mu = \ln\left(\mathrm{E}[Y(T)] - h\right) - \frac{\sigma^2}{2} \end{cases}$$

where $B := \frac{1}{2}\left(\text{Skew}[Y(T)]^2 + 2 - \sqrt{\text{Skew}[Y(T)]^4 + 4\text{Skew}[Y(T)]^2}\right) \in (0,1]$. Substituting (1.30) into (1.24) one gets

$$\begin{aligned} p \approx p_{SLN} &:= e^{-rT}\frac{S(0)}{T}\int_{\frac{KT}{S(0)}}^{\infty}\left(y - \frac{KT}{S(0)}\right) f_{SLN}(y)dy \\ &= e^{-rT}\frac{S(0)}{T}\left((\text{E}[Y(T)] - h)\Phi(d_1) - (K^\star - h)\Phi(d_2)\right), \end{aligned} \tag{1.31}$$

where $d_{1,2} = \frac{\ln\left(\frac{\text{E}[Y(T)]-h}{K^\star - h}\right) \pm \frac{\sigma^2}{2}}{\sigma}$ and $\Phi(\cdot)$ as in (1.27).

Shifted Gamma

Chang and Tsao (2011) propose a three-parameter shifted gamma distribution to approximate the sum of log-normal distributions. Its probability density function is

$$f_{SG}(y; a, b, h) = \frac{(y-h)^{a-1}}{b^a \Gamma(a)} e^{-\frac{y-h}{b}}, \quad y > h, b > 0 \tag{1.32}$$

with parameters computed according to

$$\begin{cases} \text{E}[Y(T)] = h + ab \\ \text{Var}[Y(T)] = ab^2 \\ \text{Skew}[Y(T)] = \frac{2}{\sqrt{a}} \end{cases} \Rightarrow \begin{cases} a = \frac{4}{\text{Skew}[Y(T)]^2} \\ b = \sqrt{\frac{\text{Var}[Y(T)]}{a}} \\ h = \text{E}[Y(T)] - ab \end{cases}.$$

Substituting (1.32) into (1.24) we get

$$\begin{aligned} p \approx p_{SG} &:= e^{-rT}\frac{S(0)}{T}\int_{\frac{KT}{S(0)}}^{\infty}\left(y - \frac{KT}{S(0)}\right) f_{SG}(y)dy \\ &= e^{-rT}\frac{S(0)}{T}\left((\text{E}[Y(T)] - h)\left(1 - G\left(\frac{K^\star - h}{b}, a+1, 1\right)\right) + \right. \\ &\left. - (K^\star - h)\left(1 - G\left(\frac{K^\star - h}{b}, a, 1\right)\right)\right), \end{aligned} \tag{1.33}$$

with G as in (1.29).

Shifted reciprocal gamma

Lo *et al.* (2014) propose to extend the work of Milevsky and Posner (1998) by adding a shift parameter to the approximating reciprocal gamma distribution. The resulting

density is

$$f_{SRG}(y;a,b,h) = \frac{b^a}{\Gamma(a)}(y-h)^{-a-1}e^{-\frac{b}{y-h}}, \quad y > h, b > 0 \tag{1.34}$$

with parameters estimated through moment matching[7]

$$\begin{cases} \mathrm{E}[Y(T)] = h + \frac{b}{a-1} \\ \mathrm{Var}[Y(T)] = \frac{b^2}{(a-1)(a-2)} \\ \mathrm{Skew}[Y(T)] = \frac{4\sqrt{a-2}}{a-3} \end{cases} \Rightarrow \begin{cases} h = \mathrm{E}[Y(T)] - \frac{\sqrt{\mathrm{Var}[Y(T)]}}{\mathrm{Skew}[Y(T)]}\left(2 + \sqrt{4 + \mathrm{Skew}[Y(T)]^2}\right) \\ a = 2 + \frac{(\mathrm{E}[Y(T)]-h)^2}{\mathrm{Var}[Y(T)]} \\ b = (\mathrm{E}[Y(T)] - h)(a-1) \end{cases}.$$

Substituting (1.34) into (1.24) we get

$$\begin{aligned} p \approx p_{SRG} &:= e^{-rT}\frac{S(0)}{T}\int_{\frac{KT}{S(0)}}^{\infty}\left(y - \frac{KT}{S(0)}\right)f_{SRG}(y)dy \\ &= e^{-rT}\frac{S(0)}{T}\left((\mathrm{E}[Y(T)] - h)G\left(\frac{b}{K^\star - h}, a-1, 1\right) - (K^\star - h)G\left(\frac{b}{K^\star - h}, a, 1\right)\right), \end{aligned} \tag{1.35}$$

with G as in (1.29).

1.5.5 Approximations based on the first 4 moments

When the first four integer moments are available several methods have been proposed in literature to produce accurate approximations. We briefly consider moment matching, series expansion and maximum entropy methods. These approximations allow to avoid important differences in terms of skewness and kurtosis between the approximating and true distributions. We stress that series expansion and maximum entropy methods are more general and allow to take into account more than four moments.

Johnson's and Pearson's systems

Moment matching can be implemented by using the Johnson's and Pearson's system of distributions. The procedure for family selection and density approximation have been outlined in Section 1.2.1. To the best of our knowledge, there are not results in literature concerning Asian option pricing by using the Johnson's or Pearson's system of distributions. Despite that, implementation is straightforward in the Black-Scholes model since moments of $Y(T)$ can be computed easily. Denoting with $f_J(y)$ and $f_P(y)$ the densities of the moment matched Johnson's and Pearson's system of distributions,

[7]Note that in order the first three integer moments to exist we need that $a > 3$.

the price can be computed according to

$$p \approx p_J := e^{-rT} \frac{S(0)}{T} \int_{\frac{KT}{S(0)}}^{\infty} \left(y - \frac{KT}{S(0)} \right) f_J(y) dy. \tag{1.36}$$

$$p \approx p_P := e^{-rT} \frac{S(0)}{T} \int_{\frac{KT}{S(0)}}^{\infty} \left(y - \frac{KT}{S(0)} \right) f_P(y) dy. \tag{1.37}$$

It is not said that the integrals in (1.36) and (1.37) can be solved analytically but depends on which distribution of the family is selected. In any case, the price can be obtained easily through numerical integration.

Polynomial expansions

We consider two different polynomial expansions, the first around the standard normal density (i.e. Gram-Charlier expansion), the second around the log-normal.

- Yamazaki (2014) proposes to use a Gram-Charlier expansion around the standard normal distribution to price Asian options. Since $Y(T)$ is defined on $\mathbb{R}^+$ while the standard normal density on $\mathbb{R}$, the author proposes to work with the standardized version of $Y(T)$, i.e. $x := (Y(T) - E[Y(T)])/\sqrt{\text{Var}[Y(T)]}$ and approximate its unknown distribution through (1.16). The resulting pricing formula is obtained by plugging (1.16) into (1.24):

$$\begin{aligned} p \approx p_{GC-N} \quad := \quad & \frac{S(0)}{T} \left[(c_1 - KT) \Phi \left(\frac{c_1 - KT}{\sqrt{c_2}} \right) + \sqrt{c_2} \phi \left(\frac{c_1 - KT}{\sqrt{c_2}} \right) \right. \\ & \left. + \sum_{n=3}^{\infty} \sqrt{c_2} (-1)^n q_n \text{He}_{n-2} \left(\frac{c_1 - KT}{\sqrt{c_2}} \right) \phi \left(\frac{c_1 - KT}{\sqrt{c_2}} \right) \right], \end{aligned}$$

  where $q_3 := c_3/(3! c_2^{3/2})$, $q_4 := c_4/(4! c_2^2)$, $q_5 := c_5/(5! c_2^{5/2})$, $q_6 := (c_6 + 10 c_3^2)/(6! c_2^3)$, etc. (refer to Yamazaki, 2014, pag. 87 for the general formula)

- The expansion based on polynomials that are orthogonal with respect to the log-normal distribution derived by Willems (2019) can be used to price continuously monitored arithmetic Asian options in the Black-Scholes setting. Is interesting to note that all terms in the series are fully explicit and no numerical integration nor any special functions are involved in pricing formulas. The procedure to derive the approximating density function has been already outlined in Section 1.2.2, hence, by substituting (1.18) into (1.24) one gets the pricing formula:

$$p \approx p_{OP-LN} := e^{-rT} \frac{S(0)}{T} \int_{\frac{KT}{S(0)}}^{\infty} \left(y - \frac{KT}{S(0)} \right) f_{OP-LN}(y) dy \tag{1.38}$$

where $f_{OP-LN}(\cdot)$ is given by (1.18). Willems (2019) also show that the integral can be solved analytically, interested reader may refer to Willems (2019, Formula 5).

Edgeworth expansion

Turnbull and Wakeman (1991) and Ritchken *et al.* (1990) propose to use a fourth-order Edgeworth series expansion. Given $f_{LN}(y;\mu,\sigma)$ defined as in (1.26) the Edgeworth approximation to the true density is given by

$$f_{EDG}(y;\mu,\sigma) = f_{LN}(y;\mu,\sigma) + \sum_{j=1}^{4} \frac{k_j}{j!} \frac{\partial^j f_{LN}(y;\mu,\sigma)}{\partial y^j} \tag{1.39}$$

where k_j is the difference between the $i-th$ cumulant of the exact distribution and the approximate distribution. Plugging (1.39) into (1.24) we get

$$p \approx p_{EDG} := e^{-rT} \frac{S(0)}{T} \int_{\frac{KT}{S(0)}}^{\infty} \left(y - \frac{KT}{S(0)} \right) f_{EDG}(y) dy. \tag{1.40}$$

The main problem of the Edgeworth series is that increasing the number of matched moments does not ensure an improvement in the resulting approximation, moreover, it can lead to negative densities. In formula (1.40) Edgeworth expansion is implemented around the log-normal density because the arithmetic average of the stock price is defined on $\mathbb{R}^+$, Ju (2002) considers the Edgeworth series for approximating the distribution of $\ln(Y(T))$ with a normal distribution and obtains a very efficient pricing formula (see Roncoroni *et al.*, 2015, Chapter 18), but, since its range of application is restricted to the Black-Scholes setting we don't enter in details of this approximation technique.

Maximum entropy

Another well known and widely diffused method for distribution approximation is the maximum entropy principle, developed by Jaynes (1978) and Golan *et al.* (1996). Assuming the given moments as known information, the maximum entropy (ME) principle chooses, out of the distributions consistent with the given partial information, the one having maximum entropy, or equivalently the most uncertain, accomplishing a principle of scientific honesty. In our context, we can price Asian options given the first N integer moments of $Y(T)$ by approximating $f_Y(\cdot)$ with the ME density:

$$f_{ME}(y) = \exp\left(\sum_{j=0}^{N} \lambda_j y^j \right)$$

where $\{\lambda_j\}_{j=0}^N$ are Lagrange's multipliers that solve the minimization problem

$$\min_{\lambda_1,\dots,\lambda_N} \sum_{j=1}^{N} \lambda_j \mathrm{E}[Y^j(T)] + \ln\left(\int_0^\infty \exp\left(-\sum_{j=1}^{N} \lambda_j y^j\right) dx\right) \tag{1.41}$$

and λ_0 is chosen such that $\int_0^\infty f_{ME}(x)dx = 1$. Then, plugging (1.41) into (1.24) one gets

$$p \approx p_{ME} := e^{-rT}\frac{S(0)}{T}\int_{\frac{KT}{S(0)}}^{\infty}\left(y - \frac{KT}{S(0)}\right) f_{ME}(y)dy. \tag{1.42}$$

The main drawback of this method is the computational efficiency, note indeed that, in order to approximate the unknown distribution is necessary to solve an optimization problem (which is convex but existence of the solution is not ensured, see Kesavan and Napur, 1992) involving an integral to be computed numerically. Moreover, integral in (1.42) can be computed only numerically. Since computational efficiency is a crucial aspect of this thesis, ME approximation does not find application outside this example.

1.5.6 Numerical experiment

We evaluate the performances of the various approximations examined throughout this chapter by pricing fixed strike continuously monitored Asian options. The different approximations can be compared in several ways:

a) evaluating with the Kolmogorov-Smirnov criterion the distance between the approximating distribution and the distribution obtained by Monte Carlo simulation or the Laplace transform inversion of Geman and Yor (1993);

b) comparing the different approximations with the lower and the upper bound to the option price as given in Rogers and Shi (1992) and Thompson (1998);

c) evaluating the difference (mean, absolute, percentage) between the option price coming from the different approximations and the one obtained by the Laplace transform inversion of Geman and Yor (1993).

For brevity, exploiting the fact that lower bound appears to be very tight, we only consider the criterion *b*), but also report the result of the Laplace transform inversion as further benchmark. Parameters are taken from Fusai and Tagliani (2002) and Lo *et al.* (2014), numerical results are reported in Table 1.2.

Some comments are in order, numerical results show that approximations based on the first three integer moments outperform the ones based on the first two, especially in a context of high volatility (i.e. the third parameter setting). We note that the shifted gamma is the worst performing among the ones based on the first three integer moments,

Table 1.2: Price of Asian options in the Black-Scholes model.

Method	$r = 0.09$, $\sigma = 0.1$	$r = 0.09$, $\sigma = 0.3$	$r = 0.15$, $\sigma = 0.5$
Benchmarks			
Laplace transform inversion	4.91512	8.82876	14.10024
Lower bound	4.91508	8.82755	14.09498
Upper bound	4.91541	8.83329	14.12496
2 moments approximations			
Log-normal	4.92310	8.88576	14.30234
Reciprocal gamma	4.90938	8.78216	13.92346
3 moments approximations			
Shifted log-normal	4.91514	8.83183	14.10653
Shifted gamma	4.91549	8.85200	14.15791
Shifted reciprocal gamma	4.91510	8.82572	14.09664
4 moments approximations			
Johnson	4.91514	8.82832	14.09313
Pearson	4.91512	8.82949	14.10716
Edgeworth	4.90938	8.80190	13.87252
Gram-Charlier (normal)	4.91500	8.71351	13.38673
Polynomial expansion (log-normal)	4.91505	8.81929	14.06508
Maximum entropy	4.95559	8.80854	14.00206
6 moments approximations			
Gram-Charlier (normal)	4.91598	8.95100	16.09646
Polynomial expansion (log-normal)	4.91402	8.82767	14.08110
Maximum entropy	4.95408	8.82602	14.07074

Legend: Contract parameters: $S(0) = K = 100$, $T = 1$.

while shifted log-normal always produces pricing approximations which are inside the bounds.

When the fourth moment is considered, impressive performances are reported by Johnson's and Pearson's systems of distributions, also in contexts of high volatility. Note indeed that the price of the option computed by using the Pearson's approximation always falls between the lower and upper bounds. About Edgeworth approximation, for high volatility levels we obtain a bimodal density with negative values, hence the performances of this kind of approximations are very poor and we don't recommend their usage for problems in which the moment problem is not determined. The polynomial expansion around log-normal distribution largely outperforms the one based on the standard normal. This is particularly evident for high volatility levels, where the latter diverges when six moments are used. Moreover, this result is consistent with Filipović *et al.* (2013) which suggest to choose the weight function as close as possible to the unknown density function, in this case, the moment matched log-normal density appears much closer than the standard normal. Maximum entropy approximation is not only less accurate than the polynomial expansion (around log-normal density) but also computationally slower. Hence, polynomial expansion around log-normal density seems to be the best option when many moments are available.

1.6 An experiment on moment problem

In this section we implement a further numerical experiment related to the moment problem. More specifically, we investigate what happens when replacing the correct distribution with another one which is totally different but shares with the true one the same identical sequence of moments. To this aim we consider the problem of pricing an European call option in the Black-Scholes model (see Section 1.5.1). Under this model, indeed, the stock price at maturity can be written as[8] $S(T) = S(0)X(T)$ where $X(T) = e^{\left(r-\frac{\sigma^2}{2}\right)T+\sigma W(T)}$. Note that $X(T)$ is log-normally distributed, i.e. its density is:

$$f(x) = \frac{1}{x\sqrt{2\pi v}} e^{-\frac{(\ln(x)-m)^2}{2v}}, \tag{1.43}$$

where $m = \mathrm{E}[\ln X(T)] = \left(r - \frac{\sigma^2}{2}\right) T$ and $v = \mathrm{Var}[\ln X(T)] = \sigma^2 T$. The price of the European call option is given by

$$C = \mathrm{E}[(S(0)X(T) - K)^+] = \int_0^\infty (S(0)x - K)^+ f(x)dx. \tag{1.44}$$

[8]Compare with (1.22).

Figure 1.1: $f_a(x)$ for different levels of a.

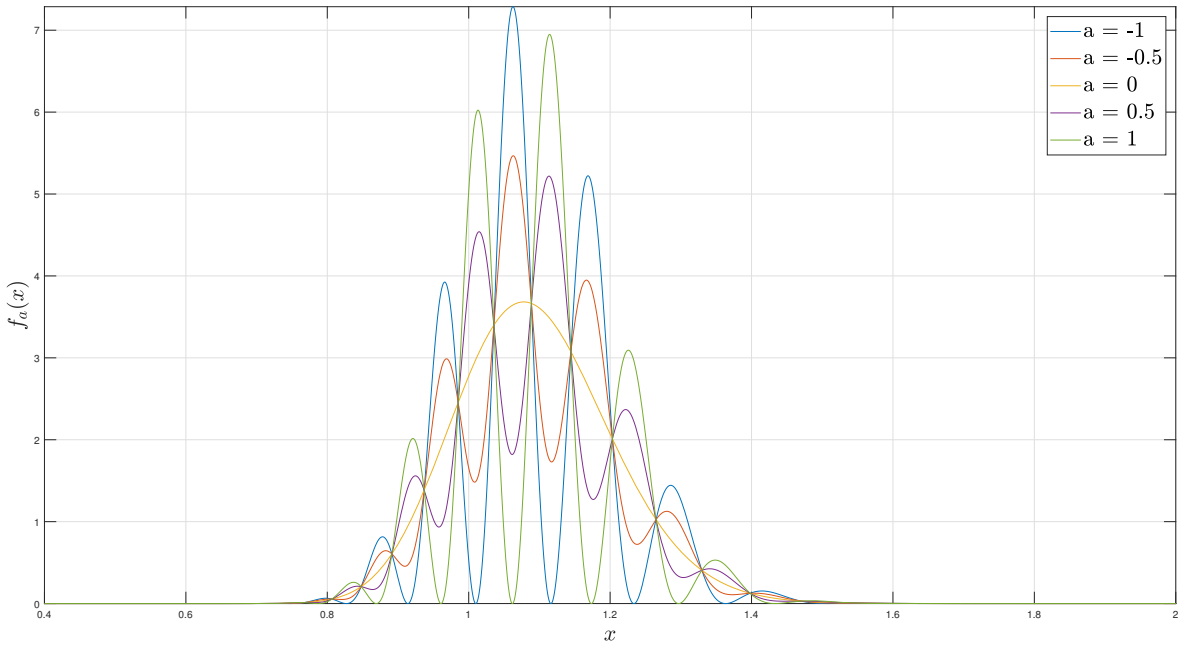

This equation can be solved explicitly, giving rise to the well known Black-Scholes formula for European call option price

$$C = S(0)\Phi(d_1) - Ke^{-rT}\Phi(d_2), \tag{1.45}$$

where $d_1 = \frac{\ln\left(\frac{S(0)}{K}\right)+\left(r+\frac{\sigma^2}{2}\right)T}{\sigma\sqrt{T}}$, $d_2 = d_1 - \sigma\sqrt{T}$ and $\Phi(\cdot)$ is the cumulative distribution function of the standard normal. As pointed out in Section 1.1, the log-normal distribution represent the classical case for which the moment problem is indeterminate, i.e. there are infinite distributions with exactly the same moment sequence. For example, one can consider the following class of distributions (cfr. Stoyanov, 1997, pag. 103):

$$f_a(x) = f(x)\left(1 + a\sin\left(2\pi\left(\frac{\ln x - m}{\sqrt{v}}\right)\right)\right), \quad -1 \leq a \leq 1 \tag{1.46}$$

which is plotted for different values of a in Figure 1.1.

It is possible to show that $\int_0^\infty x^k f_a(x)dx = \int_0^\infty x^k f(x)dx$, i.e. these distributions share exactly the same sequence of moments. In this experiment, we replace $f(x)$ with $f_a(x)$ into (1.44) and compare with the exact solution computed through (1.45). Numerical results are reported in Table 1.3 and show that, despite densities are totally different, the computed price does not fall so far from the true one, with absolute error in % that is steadily below 2%. Moreover, from Figure 1.1 is possible to appreciate how the plotted

Table 1.3: Prices of European call options computed using the wrong density

	$r = 0.09$, $\sigma = 0.1$		$r = 0.09$, $\sigma = 0.3$		$r = 0.15$, $\sigma = 0.5$	
a	Price	Abs. err (%)	Price	Abs. err (%)	Price	Abs. err (%)
-1	9.6310	0.6766	15.9985	1.3610	26.0345	0.3751
-0.8	9.6180	0.5413	16.0427	1.0888	26.0541	0.3001
-0.6	9.6051	0.4060	16.0868	0.8166	26.0737	0.2250
-0.4	9.5922	0.2706	16.1310	0.5444	26.0933	0.1500
-0.2	9.5792	0.1353	16.1751	0.2722	26.1129	0.0750
0	9.5663	-	16.2193	-	26.1325	-
0.2	9.5533	0.1353	16.2634	0.2722	26.1521	0.0750
0.4	9.5404	0.2706	16.3076	0.5444	26.1717	0.1500
0.6	9.5274	0.4060	16.3517	0.8166	26.1913	0.2250
0.8	9.5145	0.5413	16.3959	1.0888	26.2109	0.3001
1	9.5015	0.6766	16.4400	1.3610	26.2305	0.3751

Legend: Contract parameters: $S(0) = K = 100$, $T = 1$, true price corresponds to the case where $a = 0$.

random variables are similar in the tails but present large differences around the mean; this finding is consistent with Lindsay and Basak (2000) that show that the error upper bound presented in Section 1.3 is sharp only in the tails of the distributions. Finally, we stress how, imposing an additional constraint of unimodality, can help a lot in obtaining good approximations, note indeed that distributions sharing the same moments of $X(T)$ are multimodal.

Chapter 2

Asian options valuation under non–Gaussian Ornstein–Uhlenbeck dynamics

In this chapter, we contemplate distribution approximations for the arithmetic average of prices when the driving dynamics is given by non-Gaussian mean-reverting processes, which are omnipresent in financial, insurance and commodity markets. We revisit previous approximations and suggest new ones. We then derive moment-based average price approximations attuned to Asian option prices using a model-generic formula for the moments of the arithmetic average. We highlight the speed-accuracy benefits of the proposed methods by benchmarking their performances against price lower bounds and Monte Carlo price estimates.

2.1 Introduction

We devise accurate closed-form expressions for arithmetic Asian options with an underlying exponential Lévy-driven Ornstein–Uhlenbeck (OU) asset price process. The key points of our approach are its modelling capability of mean reversion and presence of jumps in commodity markets, but also its generality in the sense that its sole requirement is the availability of closed-form expression for the cumulant generating function of the background driving process hence the extensibility of its scope to other markets or areas of potential interest outlined later. Mean reversion is a principal feature of commodity prices, meaning that prices typically concentrate around a mean level for demand and supply reasons. Interested readers may refer, for example, to Bessembinder *et al.* (1995), Eydeland and Wolyniec (2003), Geman (2005, 2008), for more information about this subject including empirical corroboration and implications of mean reversion. Along with this, price discontinuities are another ubiquitous feature of commodity and energy

markets (see, e.g., Hilliard and Reis, 1999, Deng, 1999, Geman and Roncoroni, 2006 for empirical evidence of jumps in commodity and energy prices).

Although a large volume of the commodities' literature has focused on price and basic derivatives' modelling, the case of exotic payout structures has received less attention as, by nature, they affect the mathematical tractability rendering the valuation problem quite challenging. We focus on average-based derivatives, which are prevalent in commodity markets and whose trading volume has increased considerably over the recent years with important commodity exchanges offering such derivatives. For example, charterers operating in the freight market typically face freight rate exposure during a voyage and, as the freight revenue process for a ship in the physical spot market is given by the prices in this period, most freight derivatives are settled against average spot freight rates. Also, traded average price options in the London Metal Exchange give the metal community a flexible way of hedging against fluctuations in the monthly average settlement price for several metals. Crude oil consumers, whose supply price is not fixed, can use average options to hedge against spikes in oil prices during the supply period. Finally, in Europe, contracts on the CME Cumulative Average Temperature Index, based on the accumulated daily average temperatures over a calendar month, are available for summer months; these allow businesses to hedge against monthly volatility by tracking average daily temperature in a given city.

In light of the above discussion, we focus on Asian options and refer, for example, to Fusai *et al.* (2008), Cai *et al.* (2014) and Sesana *et al.* (2014) based on different driving commodity price dynamics, such as the Cox–Ingersoll–Ross and Constant Elasticity of Variance diffusions, Marena *et al.* (2013) with an added independent jump component, and Shiraya and Takahashi (2011) and Kyriakou *et al.* (2016) under stochastic volatility. In this chapter, we consider an exponential Lévy-driven OU process for the underlying asset price, that is, a Schwartz (1997) type model with Lévy-distributed innovations. This model choice is corroborated by previous literature that comes to a standstill when start thinking of exotic nonlinear payoff structures. More specifically, Benth and Šaltytė-Benth (2004) model energy spot prices with exponential non-Gaussian OU processes, the modelling philosophy being based on the fact that large price fluctuations frequently observed in energy, such as oil and natural gas, markets lead to non-normal deviations from the long-term mean towards which the prices revert. It turns out to be the case that the normal inverse Gaussian (NIG) is an appropriate driving noise for the returns. The same model has been used for the spot price of electricity (e.g., see Benth *et al.*, 2018 and earlier references therein). Börger *et al.* (2009) extend to a multivariate setting across different commodities, including power, oil, gas, coal and carbon, whereas Grønborg and Lunde (2016) model the term structure of futures contracts on oil within the GARCH model setting with NIG innovations. Finally, Benth and Šaltytė-Benth (2005) use a NIG-driven OU process for the time evolution of temperature, highlighting also the importance

of a multidimensional model for temperature across different locations of interest.

In this chapter, we derive the characteristic function of the discretely monitored arithmetic average of the log-returns of the underlying in the case where it evolves according to a Lévy driven OU process. Using this result as building block, we derive characteristic functions of log-returns and integrated log-returns and the moments of the arithmetic average of the price. These results enable, first, to price European and geometric Asian options through standard characteristic function inversion methods (see e.g. Carr and Madan, 1999 and Fang and Oosterlee, 2008). Then, we restrict our attention to the problem of pricing arithmetic Asian options. We propose moment matching, series expansion and lower bound pricing approximations. The latter is obtained by extending the lower bound approximation of Fusai and Kyriakou (2016), originally designed for exponential Lévy models. For what concerns moment based approximations, several methods have been proposed in literature to price options under exponential Lévy models: Ballotta (2010) propose moment matching in the variance gamma model, Albrecher and Predota (2004) adopt Edgeworth expansion in the case of NIG. Our work differs from their under several aspects: first for the underlying price process specification, which is more general, allowing for mean reversion; second, for the choice of the approximating distributions; third for the way of computing moments, Ballotta (2010) and Albrecher and Predota (2004) exploit independence and stationarity of increments under Lévy models, but, in the present case, these hypothesis are not valid anymore due to the presence of mean-reversion, requiring some extra labour for moments derivation.

For practical implementation of moment matching, we reconsider approximations for the unknown distribution law of the arithmetic average by moment matching of the standard approximating laws outlined in Section 1.5.4, i.e. the shifted versions of log-normal, gamma and reciprocal gamma. These have been applied originally by Lo *et al.* (2014) in the traditional geometric Brownian motion model setting widely used in equities. Aiming to account for non-Gaussian driving dynamics, we also come up with new suggestions, modified log-normal power-law distribution and the Johnson's and Pearson's system of distributions (see Section 1.2.1). The last two will produce approximations that take into account also the kurtosis of the unknown distribution of the arithmetic average, resulting, expectantly, more accurate for jump models. In addition, we also investigate the usage of the orthogonal polynomials expansion proposed in Willems (2019). Finally, we adapt the lower bound of Fusai and Kyriakou (2016) to the proposed model framework. We end up with a full battery of closed-form expressions for the option prices with grounded cornerstone the moments of the arithmetic average which we derive under general underlying model assumptions. The applicability of the proposed approximations is transferable to expectations of any nonlinear function of linear combination of asset prices. This is of practical importance as arithmetic averages see broader application in finance, such as bond pricing (Privault and Yu, 2016), insurance (Cummins and Geman, 1993), economic

project valuation (Zahra and Reza, 2012 and Creemers, 2018), real option valuation for commodity projects (Jaimungal *et al.*, 2013), and optimal capacity problems under demand uncertainty (Driouchi *et al.*, 2006).

In this research, we aim for a balance between market realism and rigorous model analytics that are very attractive for computational scientists. So, what are the sought merits of closed-form formulae? First, they are easy and can be better understood by practitioners rather than numerical algorithms, are fast to implement, and expectantly accurate. Second, replicating the payoff of an option leads to a perfect hedge for the risk associated with the sale of this option. Therefore, traders and risk managers favour closed-form formulae for option prices as they also yield closed formulae for the price sensitivities with respect to changes of various model parameters that constitute the components of the replicating portfolio. Pricing formulae, indeed, open the door for risk management as they can be more efficient, from a computational burden perspective, to implement than a numerical scheme (e.g., see Ballotta *et al.*, 2017).

The remainder of this chapter is structured as follows. In Section 2.2, we present the underlying model assumptions and basic result about the moment generating function of the arithmetic average of log-returns of a Lévy driven OU process required for the mathematical treatment that follows. Section 2.3 includes the analytical derivation of the characteristic function of log-returns and their arithmetic averages, which are used to price, respectively, European and geometric Asian options under the specified model. In Section 2.4 we first derive the moments of the arithmetic average of the underlying price process and show how to price Asian options exploiting knowledge of the first three-four integer moments; second, we extend the lower bound of Fusai and Kyriakou (2016) to the present model. In Section 2.5, we assess the accuracy of the different pricing approaches on numerical simulations. Section 2.6 concludes the chapter.

2.2 Model and main result

The payoff of the Asian option is given by a suitably defined average of the price process $S(t)$. In particular, we consider throughout this chapter discretely and continuously monitored geometric and arithmetic Asian options. In the case of a discrete monitoring we consider a set of dates $0 =: t_0 < t_1 < t_2 < ... < t_n := T$ and define the geometric average as $G_n(T) := \exp\left(\frac{1}{n}\sum_{j=1}^{n}\ln(S(t_j))\right)$, the price of the discretely monitored geometric Asian option is given by:

$$p_{G_n} = e^{-rT}\mathrm{E}[(G_n(T) - K)^+]. \tag{2.1}$$

In the same way, we define the discrete arithmetic average as $A_n(T) := \frac{1}{n}\sum_{j=1}^{n} S(t_j)$, then the price of the discretely monitored arithmetic Asian option is given by:

$$p_{A_n} = e^{-rT}\mathrm{E}[(A_n(T) - K)^+]. \tag{2.2}$$

In the case of continuous monitoring the geometric average is $G(T) := \exp\left(\frac{1}{T}\int_0^T \ln S(t)dt\right)$ and the corresponding price is

$$p_G = e^{-rT}\mathrm{E}[(G(T) - K)^+] \tag{2.3}$$

while the arithmetic average is $A(T) := \frac{1}{T}\int_0^T S(t)dt$ and the price of the continuously monitored arithmetic Asian option is given by:

$$p_A = e^{-rT}\mathrm{E}[(A(T) - K)^+]. \tag{2.4}$$

Expectations in (2.1), (2.2), (2.3) and (2.4) are computed under the risk neutral measure and $x^+ := \max(x, 0)$. Changing to a put-type option is straightforward.

We assume a general (non) Gaussian OU process for the (log) asset returns dynamics under the historical measure,

$$d\tilde{X}(t) = \alpha(\beta - \tilde{X}(t))dt + dL(t), \tag{2.5}$$

where $\alpha > 0$ is the speed of mean reversion, β is the long-run mean, and L is a general background driving Lévy process. The solution of the stochastic differential equation (2.5) is

$$\tilde{X}(t) = \tilde{X}(0)e^{-\alpha t} + \beta(1 - e^{-\alpha t}) + \int_0^t e^{-\alpha(t-s)}dL(s). \tag{2.6}$$

The asset price process is given by

$$S(t) = S(0)e^{(r-\tilde{\omega}(t))t+\tilde{X}(t)}, \quad 0 \le t \le T \tag{2.7}$$

where r is the constant continuously compounded interest rate[1], and $\tilde{\omega}(t)$ is chosen so that the discounted price process of the (tradable) asset is a martingale under some risk neutral measure, i.e. $\tilde{\omega}(t) := \frac{\ln \mathrm{E}[e^{X(t)}]}{t}$. After some simple algebraic manipulations we get:

$$S(t) = S(0)e^{(r-\omega(t))t+X(t)}, \tag{2.8}$$

[1]We assume, without loss of generality, that the dividend yield is constant and equal to 0.

where

$$X(t) := \int_0^t e^{-\alpha(t-s)} dL(s), \quad \omega(t) := \frac{1}{t} \ln \mathrm{E}[e^{\int_0^t e^{-\alpha(t-s)} dL(s)}]. \tag{2.9}$$

Note that the stock price process under the risk neutral measure does not depend on the long run mean β, moreover, quantity $\omega(t)$ depends on the specification of the background driving Lévy process, we present, later, its general analytical expression.

We state here the main theoretical result of this chapter which will be used to compute the quantity $\omega(\cdot)$ and to price aforementioned derivative instruments.

Proposition 2.1. *Given $X(\cdot)$ as in (2.9), the following holds*

$$\mathrm{E}\left[e^{\sum_{j=1}^n \gamma_j X(t_j)}\right] = \exp\left\{\sum_{j=1}^n \int_{t_{j-1}}^{t_j} \psi\left(\sum_{k=j}^n \gamma_k e^{-\alpha(t_k - s)}\right) ds\right\}, \tag{2.10}$$

where $\gamma_j \in \mathbb{C}\ \forall j \in \{1, n\}$ and $\psi(\cdot)$ is the logarithm of the moment generating function of $L(1)$, i.e. $\psi(u) := \ln E[\exp(uL(1))]$.

Proof.

$$\begin{aligned}
\mathrm{E}\left[e^{\sum_{j=1}^n \gamma_j X(t_j)}\right] &= \mathrm{E}\left[e^{\sum_{j=1}^n \int_0^{t_j} \gamma_j e^{-\alpha(t_j - s)} dL(s))}\right] = \mathrm{E}\left[e^{\sum_{j=1}^n \int_{t_{j-1}}^{t_j} \sum_{k=j}^n \gamma_k e^{-\alpha(t_k - s)} dL(s)}\right] \\
&= \mathrm{E}\left[\prod_{j=1}^n e^{\int_{t_{j-1}}^{t_j} \sum_{k=j}^n \gamma_k e^{-\alpha(t_k - s)} dL(s)}\right] = \prod_{j=1}^n \mathrm{E}\left[e^{\int_{t_{j-1}}^{t_j} \sum_{k=j}^n \gamma_k e^{-\alpha(t_k - s)} dL(s)}\right],
\end{aligned} \tag{2.11}$$

where the last passage is possible because Lévy processes have independent increments and intervals of integration are disjoint. In order to solve the last expectation in (2.11), we register the following theoretical result

Lemma 2.1. *Eberlein and Raible (1999)*

Let L be a Lévy process. If $f : \mathbb{R}_+ \to \mathbb{C}$ is a complex valued, left continuous function with limits from the right, such that $|Re(f)| \leq M$, then

$$\mathrm{E}\left[\exp\left(\int_{t_0}^{t_n} f(s) dL(s)\right)\right] = \exp\left(\int_{t_0}^{t_n} \psi(f(s)) ds\right),$$

where $\psi(\cdot)$ is the logarithm of the moment generating function of $L(1)$.

Hence, by applying Lemma 2.1 and substituting $f(s)$ with $\sum_{k=j}^n \gamma_k e^{-\alpha(t_k - s)}$ one gets:

$$\mathrm{E}\left[e^{\int_{t_{j-1}}^{t_j} \sum_{k=j}^n \gamma_k e^{-\alpha(t_k - s)} dL(s)}\right] = \exp\left(\int_{t_{j-1}}^{t_j} \psi\left(\sum_{k=j}^n \gamma_k e^{-\alpha(t_k - s)}\right) ds\right). \tag{2.12}$$

Finally, substituting (2.12) into (2.11) one gets:

$$\mathrm{E}\left[e^{\sum_{j=1}^{n}\gamma_j X(t_j)}\right] = \prod_{j=1}^{n} \exp\left(\int_{t_{j-1}}^{t_j} \psi\left(\sum_{k=j}^{n} \gamma_k e^{-\alpha(t_k-s)}\right) ds\right)$$

from which the thesis follows. ■

From (2.10), setting $n = 1$, $t_1 = t$ and $\gamma_1 = 1$ we get the general analytic expression for $\omega(t)$:

$$\omega(t) = \frac{1}{t} \ln \mathrm{E}[e^{\int_0^t e^{-\alpha(t-s)} dL(s)}] = \frac{1}{t} \int_0^t \psi\left(e^{-\alpha(t-s)}\right) ds \tag{2.13}$$

For practical applications one needs to specify a dynamics for the background Lévy process. This choice impacts on tractability of the problem because determines whether or not the integral in (2.10) can be solved analytically. For sake of generality, we postpone discussing the choice of the dynamics of the background driving Lévy process to Section 2.5.1, where we also provide analytical expression for $\psi(\cdot)$ under various Lévy models and show whenever (2.10) can be solved explicitly.

Proposition 2.1 opens doors to pricing options under the specified model. On one hand it allows to obtain the characteristic function of log-returns and arithmetic average of log-returns (both discrete and continuous) as special cases, thus (2.1) and (2.3) can be computed through standard inversion algorithms such as FFT and COS methods (see Carr and Madan, 1999 and Fang and Oosterlee, 2008), on the other hand computing (2.2) and (2.4) by means of an exact closed-form solution under standard driving dynamics is an unsolvable problem. For this, we present, next, important results based on Proposition 2.1 related to the moments of $A(T)$ and $A_n(T)$ that will form the building block of our proposed solution for the case of the arithmetic Asian options. In particular, we aim to provide suitable approximations of the distribution of the arithmetic average, exploiting knowledge of its moments.

2.3 Geometric Asian option pricing

In this section we derive the characteristic functions of the log-returns and arithmetic average of log-returns. Given these quantities, we can price European and geometric Asian options under the model specified in equation (2.5) through standard inversion methods, we use the COS method developed by Fang and Oosterlee (2008), which is briefly summarized in Appendix A. Considering the imaginary unit $i := \sqrt{-1}$, we state the following theoretical results.

Proposition 2.2. *The characteristic function of* $X(T)$

$$\mathrm{E}\left[e^{iuX(T)}\right] = \exp\left(\int_0^T \psi\left(iue^{-\alpha(T-s)}\right) ds\right) \tag{2.14}$$

Proof. Follows from Proposition 2.1 considering the special case where $n = 1$, $\gamma_1 = iu$ and $t_1 = T$. ■

Proposition 2.3. *The characteristic function of* $\frac{1}{T}\int_0^T X(t)dt$

$$\mathrm{E}\left[e^{\frac{iu}{T}\int_0^T X(t)dt}\right] = \exp\left(\int_0^T \psi\left(\frac{iu}{T}\left(\frac{1-e^{-\alpha(T-s)}}{\alpha}\right)\right) ds\right). \tag{2.15}$$

Proof.

$$\begin{aligned}\int_0^T X(t)dt &= \int_0^T \left(\int_0^t e^{-\alpha(t-s)}dL(s)\right) dt = \int_0^T \int_s^T e^{-\alpha(t-s)}dtdL(s)\\ &= \int_0^T \frac{1-e^{-\alpha(T-s)}}{\alpha}dL(s)\end{aligned}$$

Hence

$$\mathrm{E}\left[e^{\frac{iu}{T}\int_0^T X(t)dt}\right] = \mathrm{E}\left[e^{\int_0^T \frac{iu}{T}\left(\frac{1-e^{-\alpha(T-s)}}{\alpha}\right)dL(s)}\right] = e^{\int_0^T \psi\left(\frac{iu}{T}\left(\frac{1-e^{-\alpha(T-s)}}{\alpha}\right)\right)ds},$$

where the second equation follows again from Lemma 2.1. ■

Proposition 2.4. *The characteristic function of* $\frac{1}{n}\sum_{j=1}^n X(t_j)$

$$\mathrm{E}\left[e^{\frac{iu}{n}\sum_{j=1}^n X(t_j)dt}\right] = \exp\left(\sum_{j=1}^n \int_{t_{j-1}}^{t_j} \psi\left(\sum_{k=j}^n \frac{iu}{n}e^{-\alpha(t_k-s)}\right) ds\right). \tag{2.16}$$

Proof. Follows from Proposition 2.1 substituting γ_j with $\frac{iu}{n}$ $\forall j$. ■

These results enables pricing European and geometric Asian (continuously and discretely monitored) options in an accurate and fast way, defining

$$\begin{aligned}R &:= (r-\omega(T))T + X(T)\\ Z &:= \frac{1}{T}\left(r\frac{T^2}{2} - \int_0^T t\omega(t)dt\right) + \frac{1}{T}\int_0^T X(t)dt\\ Z_n &:= \frac{1}{n}\sum_{j=1}^n (r-\omega(t_j))t_j + X(t_j)\end{aligned}$$

we get the following pricing formulas for, respectively, European, geometric continuous

and geometric discrete Asian options:

$$p_E = e^{-rT}\mathrm{E}\left[(S(T)-K)^+\right] = e^{-rT}\int_{\ln\frac{K}{S(0)}}^{\infty}(S(0)e^r - K)f_R(r)dr$$
$$p_G = e^{-rT}\mathrm{E}\left[(G(T)-K)^+\right] = e^{-rT}\int_{\ln\frac{K}{S(0)}}^{\infty}(S(0)e^z - K)f_Z(z)dz$$
$$p_{G_n} = e^{-rT}\mathrm{E}\left[(G_n(T)-K)^+\right] = e^{-rT}\int_{\ln\frac{K}{S(0)}}^{\infty}(S(0)e^z - K)f_{Z_n}(z)dz$$

where the probability density functions $f_R(\cdot)$, $f_Z(\cdot)$ and $f_{Z_n}(\cdot)$ can be obtained through numerical inversion of their characteristic functions:

$$\mathrm{E}[e^{iuR}] = e^{iu(r-\omega(T))T}\mathrm{E}[e^{iuX(T)}]$$
$$\mathrm{E}[e^{iuZ}] = e^{\frac{iu}{T}\left(r\frac{T^2}{2}-\int_0^T t\omega(t)dt\right)}\mathrm{E}[e^{\frac{iu}{T}\int_0^T X(t)dt}]$$
$$\mathrm{E}[e^{iuZ_n}] = e^{\frac{iu}{n}\sum_{j=1}^n (r-\omega(t_j))t_j}\mathrm{E}[e^{\frac{iu}{n}\sum_{j=1}^n X(t_j)}].$$

2.4 Arithmetic Asian option pricing

Since pricing arithmetic Asian options by means of exact closed form solutions is an unsolvable problem we consider some approximations. First, we derive formulas for the moments of the arithmetic average (both in the continuous and discrete setting) and then we revisit some pricing approximation techniques illustrated in Section 1.5. Finally, exploiting again Proposition 2.1 we derive a very sharp lower bound price approximation for the arithmetic Asian options.

2.4.1 Moments of the arithmetic average

Next, we show how to obtain the moments of the arithmetic average within the general model framework defined in the previous section. For notational convenience, we decide to work with the following transformation of the arithmetic average[2]: $Y_n(T) := \frac{A_n(T)}{S(0)}n$ and $Y(T) := \frac{A(T)}{S(0)}T$. Given the moments of $Y_n(T)$ and $Y(T)$, recovering the moments of $A_n(T)$ and $A(T)$ is straightforward.

Proposition 2.5. *The m-th moment of $Y_n(T)$ is given by*

$$\mathrm{E}[Y_n^m(T)] = \sum_{\gamma_1+\gamma_2+\ldots+\gamma_n=m}\binom{m}{\gamma_1,\gamma_2,\ldots,\gamma_n}e^{\sum_{j=1}^n\gamma_j((r-\omega(t_j))t_j)+\int_{t_{j-1}}^{t_j}\psi\left(\sum_{k=j}^n\gamma_k e^{-\alpha(t_k-s)}\right)ds}. \tag{2.17}$$

[2]Note that notation now coincides with the one of Section 1.5.

Proof. Since $Y_n(T) = \sum_{j=1}^{n} e^{(r-\omega(t_j))t_j + X(t_j)}$ then

$$\begin{aligned}
\mathrm{E}\left[Y_n^m(T)\right] &= \mathrm{E}\left[\left(\sum_{j=1}^{n} e^{(r-\omega(t_j))t_j + X(t_j)}\right)^m\right] \\
&= \mathrm{E}\left[\sum_{\gamma_1+\gamma_2+\ldots+\gamma_n=m} \binom{m}{\gamma_1, \gamma_2, \ldots, \gamma_n} \prod_{j=1}^{n} e^{((r-\omega(t_j))t_j + X(t_j))\gamma_j}\right] \\
&= \sum_{\gamma_1+\gamma_2+\ldots+\gamma_n=m} \binom{m}{\gamma_1, \gamma_2, \ldots, \gamma_n} e^{\sum_{j=1}^{n} \gamma_j((r-\omega(t_j))t_j)} \mathrm{E}\left[e^{\sum_{j=1}^{n} X(t_j)\gamma_j}\right],
\end{aligned}$$

where we have used the multinomial theorem for the second step. As expectation in the last equation coincides with the result of Proposition 2.1 the thesis follows. ■

Remark 2.1. *The term $\sum_{\gamma_1+\gamma_2+\ldots+\gamma_n=m}$ indicates that the sum is taken for any combination of $\{\gamma_j\}_{j=1}^n$ such that their sum is equal to m. Hence, despite no numerical methods are required at any stage when computing moments of $A_n(T)$, computational complexity increases for high n and m because of elevated number of possible combinations of $\{\gamma_j\}_{j=1}^n$ which determines the number of evaluations of $\mathrm{E}\left[e^{\sum_{j=1}^{n} X(t_j)\gamma_j}\right]$.*

We consider now the continuous arithmetic average.

Proposition 2.6. *The m-th moment of $Y(T)$*

$$\begin{aligned}
\mathrm{E}[Y^m(T)] &= m! \int_0^T dt_1 \int_{t_1}^T dt_2 \cdots \int_{t_{m-1}}^T \exp\left\{\sum_{j=1}^{m} (r-\omega(t_j))t_j + \right. \\
&\quad \left. + \int_{t_{j-1}}^{t_j} \psi\left(\sum_{k=j}^{m} e^{-\alpha(t_k - s)}\right) ds\right\} dt_m, \qquad (2.18)
\end{aligned}$$

Proof. From Bharucha-Reid (1960, pag. 344–345),

$$\begin{aligned}
\mathrm{E}[Y^m(T)] &= \int_{t_0}^T \cdots \int_{t_0}^T e^{\sum_{j=1}^{m} (r-\omega(t_j))t_j} \mathrm{E}[\exp(X(t_1) + \cdots + X(t_m))] dt_1 \cdots dt_m \\
&= m! \int_{t_0}^T dt_1 \int_{t_1}^T dt_2 \cdots \int_{t_{m-1}}^T e^{\sum_{j=1}^{m} (r-\omega(t_j))t_j} \mathrm{E}[\exp(X(t_1) + \cdots + X(t_m))] dt_m.
\end{aligned}$$

The thesis follows Proposition 2.1 considering the special case where $\gamma_j = 1 \; \forall j \in \{1, m\}$. ■

Finally, the moments of the arithmetic average are computed according to:

$$\mathrm{E}[A_n^m(T)] = \left(\frac{S(0)}{n}\right)^m \mathrm{E}[Y_n^m(T)]$$
$$\mathrm{E}[A^m(T)] = \left(\frac{S(0)}{T}\right)^m \mathrm{E}[Y^m(T)].$$

.

2.4.2 Pricing using moments

The price of the fixed strike arithmetic average Asian call options is

$$p = e^{-rT}\mathrm{E}\left[\left(\frac{S(0)}{T}Y(T) - K\right)^+\right] = e^{-rT}\frac{S(0)}{T}\int_{\frac{KT}{S(0)}}^{\infty}\left(y - \frac{KT}{S(0)}\right)f_Y(y)dx, \tag{2.19}$$

while in the discrete case

$$p_n = e^{-rT}\mathrm{E}\left[\left(\frac{S(0)}{T}Y_n(T) - K\right)^+\right] = e^{-rT}\frac{S(0)}{T}\int_{\frac{KT}{S(0)}}^{\infty}\left(y - \frac{KT}{S(0)}\right)f_{Y_n}(y)dx, \tag{2.20}$$

Hence, we aim to approximate the unknown distribution of $Y(T)$ and $Y_n(T)$ through their moments, which have been derived in Section 2.4.1. Moment matching and series expansion are considered. We start by taking into account the approximations proposed in Lo *et al.* (2014), i.e. the shifted log-normal, shifted gamma and shifted reciprocal gamma. For these cases we have already shown in Section 1.5.4 how to estimate the parameters of the approximating distribution by using the moments of $Y(T)$ and obtained the corresponding closed form approximations, which are given in formulas (1.31), (1.33) and (1.35). Then we also come up with a new suggestion: the modified log-normal power law distribution (MLP). This random variable is a generalization of the log-normal distribution with a third parameter controlling the tail behavior. Indeed, contrarily to Lo *et al.* (2014) that operate in a classical Black-Scholes framework, we consider jump models, which can possibly lead to extreme events and heavier tails in the distribution of the arithmetic average. A brief description of the MLP distribution is given next, for brevity, we omit the details of the forms of the associated probability density and cumulative distribution functions, which can be found in Basu *et al.* (2015), and rather merely present the resulting pricing expressions following from the general formula. All these approximations are based on the first three integer moments, but, in order to improve pricing accuracy, we also include the fourth moment and approximate the value of the option through Johnson's and Pearson's systems of distributions, this is important when dealing with jump models since allows to take into account also the kurtosis of the unknown distribution. In these cases we implement moment matching by following the procedure described in Section 1.2.1 and then compute pricing approximations through formulas (1.36) and (1.37). In addition, we also consider the orthogonal polynomial expansion proposed by Willems (2019), which has been described in Section 1.2.2 with corresponding pricing formula given in (1.38). Alternatively, we could consider the methodology developed by Yamazaki (2014), see Section 1.5.5, but performances of this approach are worse than the alternative orthogonal polynomial expansion based on the

log-normal density[3]. This is for a theoretical reason: Filipović *et al.* (2013) suggest that polynomial expansion is more efficient when implemented around a distribution as close as possible to the unknown density, in this case, the moment matched log-normal density appears much closer than the standard normal. This is also confirmed by the numerical test reported in Section 1.5 (see Table 1.2).

Modified lognormal power-law (MLP)

Finally, we consider the case of the modified lognormal power-law distribution with initial lognormal distribution parameters m, s and parameter a controlling the power law behaviour, which we calculate by matching raw moments given by

$$\mathrm{E}[Y^k(T)] = \frac{a}{a-k}\exp\left(\frac{s^2k^2}{2} + mk\right), \quad a > k$$

(see Basu *et al.*, 2015). Parameter a can be calculated from

$$\frac{(a-2)^3 a \mathrm{E}[Y^2(T)]^3}{(a-3)(a-1)^3\mathrm{E}[Y(T)]^3} = \mathrm{E}[Y^3(T)].$$

This equation can be solved explicitly (we use Mathematica®) and possesses four different solutions. The value of a will be the only real solution such that $a > 3$. Given a, the remaining parameters are given by

$$s^2 = \ln\frac{a(a-2)\mathrm{E}[Y^2(T)]}{(a-1)^2\mathrm{E}[Y(T)]^2}, \quad m = -\frac{s^2}{2} + \ln\frac{(a-1)\mathrm{E}[Y(T)]}{a}.$$

The relevant pricing formula is

$$\begin{aligned}\tilde{p}_0^{\mathrm{MLP}} \quad := \quad & \int_K^\infty \frac{a e^{am+\frac{a^2s^2}{2}}x}{2x^{1+a}}\mathrm{erfc}\left\{\frac{as^2 - \ln x + m}{s\sqrt{2}}\right\}dx \\ & -K\left(1 - \frac{1}{2}\mathrm{erfc}\left\{\frac{-\ln K + m}{s\sqrt{2}}\right\} - \frac{e^{am+\frac{a^2s^2}{2}}}{2K^a}\mathrm{erfc}\left\{\frac{as^2 - \ln K + m}{s\sqrt{2}}\right\}\right),\end{aligned}$$

where

$$\mathrm{erfc}(z) = \frac{2}{\sqrt{\pi}}\int_z^\infty e^{-t^2}dt$$

is the complementary error function. The probability density function of the MLP distribution is displayed for different values of a in Figure 2.1.

[3]We have also considered to price the Asian option by standardizing the unknown distribution of the arithmetic average and implementing polynomial expansion around the standard normal and logistic distributions, see Section 1.2.2, but this approach has been largely outperformed by the polynomial expansion around the moment matched log-normal density, hence we don't propose that approach in this thesis.

Figure 2.1: Probability density function of the modified log-normal power law distribution for different levels of a

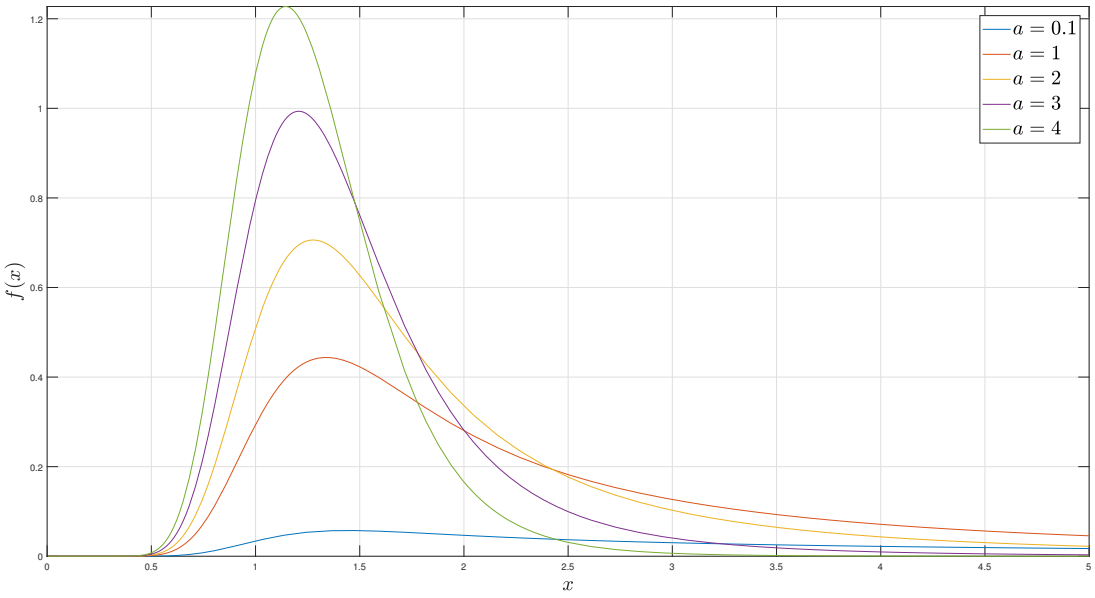

Legend: other parameters $m = 0.1$, $s = 0.25$.

2.4.3 Error upper bound

In order to establish an upper bound to the error committed when approximating an unknown distribution Y with another one $\tilde{Y}$ sharing the same $2n$ moments, we recall the result from Akhiezer (1965, pag. 66) which have been outlined in Section 1.3, given two cumulative distribution functions $F_Y(x)$ and $F_{\tilde{Y}}(x)$ sharing the same first $2n$ integer moments:

$$|F_Y(x) - F_{\tilde{Y}}(x)| \leq \zeta_n(x), \tag{2.21}$$

where

$$\frac{1}{\zeta_n(x)} = \begin{pmatrix} 1 & x & \dots & x^n \end{pmatrix} \begin{pmatrix} 1 & \mu_1 & \dots & \mu_n \\ \mu_1 & \dots & \dots & \mu_{n+1} \\ \vdots & \vdots & \vdots & \vdots \\ \mu_n & \mu_{n+1} & \dots & \mu_{2n} \end{pmatrix}^{-1} \begin{pmatrix} 1 \\ x \\ \vdots \\ x^n \end{pmatrix}$$

and μ_n is the nth moment of the unknown distribution. The error bound (2.21) is then applicable to expected values of functions of the underlying random quantity.

Example 2. *The price of the Asian put option with fixed strike price K is given by*

$$e^{-rT}\mathrm{E}\left[(K - Y(T))^+\right] = e^{-rT}\int_0^K F(x)dx \approx e^{-rT}\int_0^K \tilde{F}(x)dx.$$

Figure 2.2: Error upper bound Error upper bounds for a continuum of strike prices

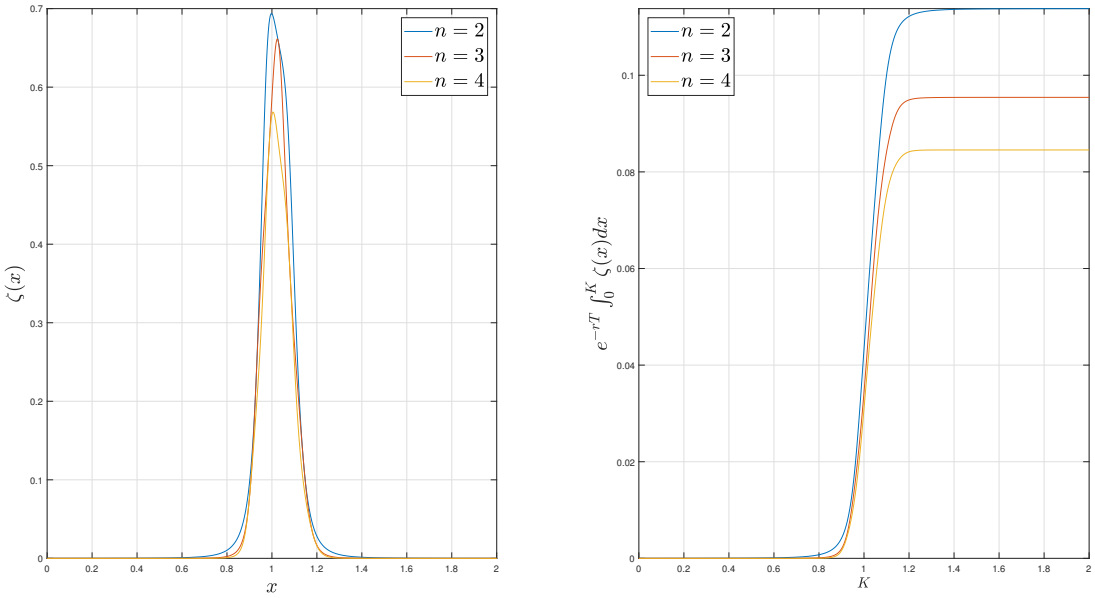

Legend: $\zeta_n(x)$ (left plot): the case of an approximating distribution function that shares $2n$ moments with the original distribution function (see 2.21). $e^{-rT}\int_0^K \zeta(x)dx$ (right plot): the case of the fixed-strike Asian put option price with the unknown distribution function of the arithmetic average approximated by a distribution function that has the first $2n$ moments matched (see 2.22).

Then, from (2.21),

$$e^{-rT}\int_0^K \left|F_Y(x) - F_{\tilde{Y}}(x)\right| dx \leq e^{-rT}\int_0^K \zeta_n(x)dx. \tag{2.22}$$

Figure 2.2 shows a simple implementation of (2.21)–(2.22) based on the moments of the discrete arithmetic average (12 monitoring dates) in the case where the background driving Lévy process is a Brownian motion. Two comments are in order. The error upper bound becomes tighter the more moments we take into account. This becomes particularly sharp with decreasing option moneyness, consistently with Lindsay and Basak (2000) who show that this bound is sharp only in the tails of the distributions.

2.4.4 Lower bound price approximation

In this section we consider a price approximation for Asian options in the form of a lower bound (LB). More specifically, we adapt the lower bound of Fusai and Kyriakou (2016) to the case of the underlying asset price dynamics (2.5) and present an analytical expression for it in the Fourier domain.

Discrete monitoring

For notational convenience, we split the time interval according to $0 < \Delta < 2 \cdot \Delta < ... < n \cdot \Delta := T$, note that $X(\Delta j)$ is thus equivalent to what we called $X(t_j)$ throughout the rest of this chapter. The lower bound for the discretely monitored arithmetic Asian option is given by:

$$\begin{aligned} p_0^{\mathrm{LB}} &:= \mathrm{E}\left[e^{-rT}\left(\frac{S(0)}{n}\sum_{j=1}^{n} e^{(r-\omega(\Delta j))\Delta j + X(\Delta j)} - K\right)\mathbf{1}_{\left\{\frac{S(0)}{n}\sum_{j=1}^{n}(r-\omega(\Delta j))\Delta j + X(\Delta j) > \lambda\right\}}\right] \\ &\leq \mathrm{E}\left[e^{-rT}\left(\frac{S(0)}{n}\sum_{j=1}^{n} e^{(r-\omega(\Delta j))\Delta j + X(\Delta j)} - K\right)^{+}\right] \end{aligned}$$

Multiplying and dividing by $S(0)$ we get

$$p_0^{\mathrm{LB}} := S(0) p_1^{\mathrm{LB}}$$

where

$$p_1^{\mathrm{LB}} := \mathrm{E}\left[e^{-rT}\left(\frac{1}{n}\sum_{j=1}^{n} e^{(r-\omega(\Delta j))\Delta j + X(\Delta j)} - K^{\star}\right)\mathbf{1}_{\left\{\frac{1}{n}\sum_{j=1}^{n}(r-\omega(\Delta j))\Delta j + X(\Delta j) > \lambda^{\star}\right\}}\right]$$

where $K^{\star} = \frac{K}{S(0)}$ and $\lambda^{\star} = \frac{\lambda}{S(0)}$ satisfies

$$\begin{aligned} \int_{\mathbb{R}} e^{-i\lambda^{\star}u}\Bigg(\sum_{k=1}^{n} \mathrm{E}\left[e^{(r-\omega(\Delta k))\Delta k + X(\Delta k) + \frac{iu}{n}\sum_{j=1}^{n}(r-\omega(\Delta j))\Delta j + X(\Delta j)}\right] + \\ -K^{\star} n \mathrm{E}\left[e^{\frac{iu}{n}\sum_{j=1}^{n}(r-\omega(\Delta j))\Delta j + X(\Delta j)}\right]\Bigg) du = 0. \end{aligned}$$

The optimal lower bound is then given by

$$p_1^{\mathrm{LB}} = \frac{e^{-\delta\lambda^{\star} - rT}}{2\pi}\int_{\mathbb{R}} e^{-iu\lambda^{\star}}\Phi(u;\delta)du$$

where $\delta > 0$ ensures integrability and

$$\begin{aligned} \Phi(u;\delta) = \frac{1}{iu+\delta}\Bigg(\frac{1}{n}\sum_{k=1}^{n} e^{(r-\omega(\Delta k))\Delta k + \frac{i(u-i\delta)}{n}\sum_{j=1}^{n}(r-\omega(\Delta j))\Delta j}\mathrm{E}\left[e^{X(\Delta k) + \frac{i(u-i\delta)}{n}\sum_{j=1}^{n} X(\Delta j)}\right] + \\ - K^{\star} e^{\frac{i(u-i\delta)}{n}\sum_{j=1}^{n}(r-\omega(\Delta j))\Delta j}\mathrm{E}\left[e^{\frac{i(u-i\delta)}{n}\sum_{j=1}^{n} X(\Delta j)}\right]\Bigg). \end{aligned} \tag{2.23}$$

We aim now to find the analytical expressions of the expectations in (2.23). Let's define $X(j\Delta) := \int_0^{j\Delta} e^{-\alpha(j\Delta - s)}dL(s)$, we find two alternative representations for $X(\Delta j)$, which

will be used next:

$$X(j\Delta) = \int_0^{j\Delta} e^{-\alpha(j\Delta-s)}dL(s) = \sum_{m=1}^{j}\int_{(m-1)\Delta}^{m\Delta} e^{-\alpha(j\Delta-s)}dL(s) \tag{2.24}$$

$$= \sum_{m=1}^{j}\int_0^{m\Delta} e^{-\alpha(j\Delta-s)}dL(s) - \int_0^{(m-1)\Delta} e^{-\alpha(j\Delta-s)}dL(s)$$

$$= \sum_{m=1}^{j}\left(\int_0^{m\Delta} e^{-\alpha(m\Delta-s)}dL(s) - \int_0^{(m-1)\Delta} e^{-\alpha\Delta}e^{-\alpha((m-1)\Delta-s)}dL(s)\right)e^{-(j-m)\alpha\Delta}$$

$$= \sum_{m=1}^{j}(X(m\Delta) - X((m-1)\Delta)e^{-\alpha\Delta})e^{-(j-m)\alpha\Delta} = \sum_{m=1}^{j} Z_m e^{-(j-m)\alpha\Delta} \tag{2.25}$$

where $Z_m := X(m\Delta) - X((m-1)\Delta)e^{-\alpha\Delta}$. From which follows:

$$\sum_{j=1}^{n} X(j\Delta) = \sum_{j=1}^{n}\sum_{m=1}^{j} Z_m e^{-(j-m)\alpha\Delta} = \sum_{j=1}^{n} Z_j \sum_{m=1}^{n-j+1} e^{-\alpha\Delta(m-1)} = \sum_{j=1}^{n} Z_j C_j \tag{2.26}$$

where $C_j := \frac{e^{\alpha\Delta}-e^{-\alpha\Delta(n-j)}}{e^{\alpha\Delta}-1}$. Recalling that

$$Z_j = X(j\Delta) - X((j-1)\Delta)e^{-\alpha\Delta}$$

$$= \int_0^{j\Delta} e^{-\alpha(j\Delta-s)}dL(s) - \int_0^{(j-1)\Delta} e^{-\alpha\Delta}e^{-\alpha((j-1)\Delta-s)}dL(s)$$

$$= \int_0^{j\Delta} e^{-\alpha(j\Delta-s)}dL(s) - \left(\int_0^{j\Delta} e^{-\alpha(j\Delta-s)}dL(s) - \int_{(j-1)\Delta}^{j\Delta} e^{-\alpha(j\Delta-s)}dL(s)\right)$$

$$= \int_{(j-1)\Delta}^{j\Delta} e^{-\alpha(j\Delta-s)}dL(s),$$

we can compute the following quantity:

$$X(k\Delta) + \frac{i(u-i\delta)}{n}\sum_{j=1}^{n} X(j\Delta) = \sum_{j=1}^{k}\int_{(j-1)\Delta}^{j\Delta} e^{-\alpha(k\Delta-s)}dL(s) + \frac{i(u-i\delta)}{n}\sum_{j=1}^{n} Z_j C_j$$

$$= \sum_{j=1}^{k}\int_{(j-1)\Delta}^{j\Delta}\left(e^{-\alpha(k\Delta-s)} + \frac{i(u-i\delta)}{n}C_j e^{-\alpha(j\Delta-s)}\right)dL(s) +$$

$$\sum_{j=k+1}^{n}\int_{(j-1)\Delta}^{j\Delta}\frac{i(u-i\delta)}{n}C_j e^{-\alpha(j\Delta-s)}dL(s)$$

Taking exponential:

$$e^{X(k\Delta)+\frac{i(u-i\delta)}{n}\sum_{j=1}^{n}X(j\Delta)} = \prod_{j=1}^{k} e^{\int_{(j-1)\Delta}^{j\Delta}\left(e^{-\alpha(k\Delta-s)}+\frac{i(u-i\delta)}{n}C_j e^{-\alpha(j\Delta-s)}\right)dL(s)} \times \\ \times \prod_{j=k+1}^{n} e^{\int_{(j-1)\Delta}^{j\Delta}\frac{i(u-i\delta)}{n}C_j e^{-\alpha(j\Delta-s)}dL(s)}$$

Exploiting the fact that Lévy increments are independent and intervals of integration are disjoint we take expectation and get the following

$$\begin{aligned}
\mathrm{E}\left[e^{X(k\Delta)+\frac{i(u-i\delta)}{n}\sum_{j=1}^{n}X(j\Delta)}\right] &= \prod_{j=1}^{k}\mathrm{E}\left[e^{\int_{(j-1)\Delta}^{j\Delta}\left(e^{-\alpha(k\Delta-s)}+\frac{i(u-i\delta)}{n}C_j e^{-\alpha(j\Delta-s)}\right)dL(s)}\right]\times \\
&\times \prod_{j=k+1}^{n}\mathrm{E}\left[e^{\int_{(j-1)\Delta}^{j\Delta}\frac{i(u-i\delta)}{n}C_j e^{-\alpha(j\Delta-s)}dL(s)}\right] \\
&= \prod_{j=1}^{k} e^{\int_{(j-1)\Delta}^{j\Delta}\psi\left(iue^{-\alpha(k\Delta-s)}+\frac{i(u-i\delta)}{n}C_j e^{-\alpha(j\Delta-s)}\right)ds}\times \\
&\times \prod_{j=k+1}^{n} e^{\int_{(j-1)\Delta}^{j\Delta}\psi\left(\frac{i(u-i\delta)}{n}C_j e^{-\alpha(j\Delta-s)}\right)ds} \\
&= \exp\left(\sum_{j=1}^{k}\int_{(j-1)\Delta}^{j\Delta}\psi\left(iue^{-\alpha(k\Delta-s)}+\frac{i(u-i\delta)}{n}C_j e^{-\alpha(j\Delta-s)}\right)ds+\right. \\
&\left.+\sum_{j=k+1}^{n}\int_{(j-1)\Delta}^{j\Delta}\psi\left(\frac{i(u-i\delta)}{n}C_j e^{-\alpha(j\Delta-s)}\right)ds\right),
\end{aligned}$$

where we have applied again Lemma 2.1 for the second passage.

Same reasoning applies to $\mathrm{E}\left[e^{\frac{i(u-i\delta)}{n}\sum_{j=1}^{n}X(\Delta j)}\right]$ which is obtained by following the same procedure but neglecting the term $X(k\Delta)$.

Continuous monitoring

For the continuously monitored Asian call option LB is given by

$$\begin{aligned}
\tilde{p}_0^{\mathrm{LB}} &:= \mathrm{E}\left[e^{-rT}\left(\frac{S(0)}{T}\int_0^T e^{(r-\omega(t))t+X(t)}dt-K\right)\mathbf{1}_{\left\{\frac{S(0)}{T}\int_0^T(r-\omega(t))t+X(t)dt>\lambda\right\}}\right] \\
&\leq \mathrm{E}\left[e^{-rT}\left(\frac{S(0)}{T}\int_0^T e^{(r-\omega(t))t+X(t)}dt-K\right)^{+}\right], \qquad (2.27)
\end{aligned}$$

Multiplying and dividing by $S(0)$ we get

$$\tilde{p}_0^{\mathrm{LB}} := S(0)\tilde{p}_1^{\mathrm{LB}}, \qquad (2.28)$$

where

$$\tilde{p}_1^{LB} := \mathrm{E}\left[e^{-rT}\left(\frac{1}{T}\int_0^T e^{(r-\omega(t))t+X(t)}dt - K^\star\right)\mathbf{1}_{\left\{\frac{1}{T}\int_0^T (r-\omega(t))t+X(t)dt>\lambda^\star\right\}}\right] \tag{2.29}$$

where $K^\star = \frac{K}{S(0)}$ and $\lambda^\star = \frac{\lambda}{S(0)}$ satisfies

$$\int_{\mathbb{R}} e^{-i\lambda u}\left(\int_0^T \mathrm{E}\left[e^{(r-\omega(t))t+X(t)+\frac{iu}{T}\int_0^T (r-\omega(t))t+X(t)dt}\right]dt - K^\star T\mathrm{E}\left[e^{\frac{iu}{T}\int_0^T (r-\omega(t))t+X(t)dt}\right]\right)du = 0.$$

This lower bound has the following inverse Fourier transform representation:

$$\tilde{p}_1^{\mathrm{LB}} = \frac{e^{-\delta\lambda^\star - rT}}{2\pi}\int_{\mathbb{R}} e^{-iu\lambda^\star}\Phi(u;\delta)du, \tag{2.30}$$

where the constant $\delta > 0$ ensures integrability and

$$\begin{aligned}\Phi(u;\delta) := \frac{1}{iu+\delta}\Bigg(&\frac{1}{T}\int_0^T e^{(r-\omega(t))t+\frac{i(u-i\delta)}{T}(r\frac{T^2}{2}-\int_0^T \omega(t)tdt)}\mathrm{E}\left[e^{X(t)+\frac{i(u-i\delta)}{T}\int_0^T X(t)dt}\right]dt + \\ &- K^\star e^{\frac{i(u-i\delta)}{T}\int_0^T (r-\omega(t))tdt}\mathrm{E}\left[e^{\frac{i(u-i\delta)}{T}\int_0^T X(t)dt}\right]\Bigg).\end{aligned} \tag{2.31}$$

Expectations in (2.31) can be computed analytically exploiting Proposition (2.1):

$$\mathrm{E}\left[e^{\frac{i(u-i\delta)}{T}\int_0^T X(t)dt}\right] = \mathrm{E}\left[e^{\frac{i(u-i\delta)}{T}\int_0^T X(t)dt}\right] = e^{\int_0^T \psi\left(\frac{i(u-i\delta)}{T}\left(\frac{1-e^{-\alpha(T-t)}}{\alpha}\right)\right)dt} \tag{2.32}$$

and

$$\begin{aligned}\mathrm{E}\left[e^{X(t)+\frac{i(u-i\delta)}{T}\int_0^T X(t)dt}\right] &= \mathrm{E}\left[e^{\int_0^t e^{-\alpha(t-s)}+\frac{i(u-i\delta)}{T}\left(\frac{1-e^{-\alpha(T-s)}}{\alpha}\right)dL(s)+\int_t^T \frac{i(u-i\delta)}{T}\left(\frac{1-e^{-\alpha(T-s)}}{\alpha}\right)dL(s)}\right] \\ &= e^{\int_0^t \psi\left(e^{-\alpha(t-s)}+\frac{i(u-i\delta)}{T}\left(\frac{1-e^{-\alpha(T-s)}}{\alpha}\right)\right)ds+\int_t^T \psi\left(\frac{i(u-i\delta)}{T}\left(\frac{1-e^{-\alpha(T-s)}}{\alpha}\right)\right)ds}\end{aligned} \tag{2.33}$$

where, for last passage, we have exploited independence of increments of Lévy processes and Lemma 2.1.

2.5 Numerical analysis

In this section we perform an extensive numerical study in order to test the proposed pricing formulas. We start by specifying a dynamics for the underlying's price process. Next, we show numerical performances of the proposed formulas, with model parameters taken from literature concerning option pricing under Lévy models. Finally, we summarize and

comment results.

2.5.1 The background driving Lévy process

Theoretical results stated in the previous sections are valid for a generic background driving Lévy process (BDLP), but for practical implementation one needs to specify a dynamics for such process. Numerical efficiency depends on the key quantity

$$\int_{t_{j-1}}^{t_j} \psi\left(\sum_{k=j}^{n} \gamma_k e^{-\alpha(t_k-s)}\right) ds, \tag{2.34}$$

which appears (under several forms) in any pricing formula. The symbolic computing language Mathematica® is used to solve the integral in (2.34). Codes for implementing the general formula (2.10) are given in Appendix C.1. We obtain full explicit solutions for the cases where the BDLP is a Brownian motion (BM), double exponential jump diffusion (DEJD), hyper-exponential jump diffusion (HEJD)[4] and normal inverse gaussian (NIG). In the cases of variance gamma (VG) and CGMY the integral can still be solved but the solution is only in terms of special functions, i.e. the polylogarithm function (for VG) and Gaussian hypergeometric function (for CGMY). Finally, (2.34) can not be solved analytically in the cases of the Merton jump diffusion (MJD), Meixner and generalized hyperbolic (GH) models. This findings are summarized in Table 2.1. Even in the cases where (2.34) does not possess analytical solution, option pricing can still be implemented by solving the integral numerically. In what follows we restrict our attention to the cases where (2.34) can be solved analytically, i.e. BM, DEJD, NIG, VG and CGMY. For sake of simplicity and brevity, we don't consider the more general HEJD model for numerical experiments but restrict our attention to the DEJD model.

2.5.2 Asian options pricing

Since characteristic functions of log-returns and their arithmetic averages (both continuous and discrete) are known analytically, European and geometric Asian option pricing is implemented through the COS method (which is briefly summarized in Appendix A), with infinite summations truncated at the $2^7 - th$ element. Results are reported in Table 2.2. We consider in the discrete case, $n = 12$ monitoring dates, but the formula can be modified to take into account a different number of dates. Since the method is exact, we don't report any benchmark (correctness has been checked through comparison with Monte Carlo simulation[5]).

[4]This is a generalization of the DEJD (see Cai and Kou, 2011).

[5]Monte Carlo simulation of the CGMY model is not a trivial task, we employ the simulation scheme proposed by Ballotta and Kyriakou (2014) for the simulation of the BDLP in that case.

Table 2.1: Features of the Background driving Lévy processes

BDLP	$\psi(u)$	Solution of (2.34)
BM	$\frac{\sigma^2u^2}{2}$	Full explicit
DEJD	$\lambda\left(\frac{\eta_1 p}{\eta_1-u}+\frac{\eta_2(1-p)}{\eta_2+u}-1\right)+\frac{\sigma^2u^2}{2}$	Full explicit
HEJD	$\lambda\left(\sum_{i=1}^{m}\frac{p_i\eta_i}{\eta_i-u}+\sum_{j=1}^{n}\frac{(1-p_j)\theta_j}{\theta_j+u}-1\right)+\frac{\sigma^2u^2}{2}$	Full explicit
MJD	$\lambda\left(e^{\frac{\delta^2u^2}{2}+\mu u}-1\right)+\frac{\sigma^2u^2}{2}$	No analytical solution
NIG	$\frac{1-\sqrt{-k\sigma^2u^2-2k\theta u+1}}{k}$	Full explicit
VG	$-\frac{\ln\left(-\frac{1}{2}k\sigma^2u^2-k\theta u+1\right)}{k}$	In terms of polylogarithm function
CGMY	$C\Gamma(-Y)\left((G+u)^Y-G^Y-M^Y+(M-u)^Y\right)$	In terms of hypergeometric function
Meixner	$\log\left(\left(\cos\left(\frac{b}{2}\right)\operatorname{sech}\left(\frac{1}{2}(-iau-ib)\right)\right)^{2\delta}\right)$	No analytical solution
GH	$\left(\frac{\alpha^2-\beta^2}{\alpha^2-(\beta+u)^2}\right)^{\frac{\lambda}{2}}\frac{K_\lambda(\delta\sqrt{\alpha^2-(\beta+u)^2})}{K_\lambda(\delta\sqrt{\alpha^2-\beta^2})}$	No analytical solution

Legend: parameterization as in Cont and Tankov (2004) for BM, DEJD, MJD, NIG, VG, Meixner; as in Cai and Kou (2011) for HEJD; as in Eberlein and Prause (2002) for GH. $K_\lambda(\cdot)$ denotes the modified Bessel function of the second kind.

Next, we focus on assessing the accuracy of our moment-based approximations of the arithmetic average price distribution in the context of Asian call option pricing. In this analysis, we consider three examples of background driving Lévy processes for (2.5): Brownian motion, DEJD, and NIG process, i.e. the cases for which (2.34) can be solved explicitly (see Table 2.1). Proposition 2.6 contains a formula for the moments of the continuous arithmetic average of the stock price. This formula is in the form of an iterated integral, meaning that $m-$dimensional integration is required in order to compute the $m-th$ moment. As part of this research, we have considered several numerical integration techniques and found that the best performing is the Gauss-Legendre quadrature method (see Press *et al.*, 1992) or Abramowitz and Stegun (1968, Formula 25.4.29) which largely outperformed the Matlab's built-in global adaptive quadrature. For practical implementation one needs to specify how many Gaussian nodes must be considered to approximate the integral, this choice impacts both on accuracy and efficiency of the method. In Tables 2.3, 2.4, 2.5 and 2.6 we report the prices of continuously monitored arithmetic Asian options for various BDLPs, levels of the speed of mean reversion and number of Gauss-Legendre quadrature nodes. In order to test the accuracy we also report the absolute error in % of the pricing approximation with respect to a benchmark for the true option price. This is generated by a very accurate Monte Carlo simulation strategy using the lower bound with known expected value given by (2.28) as control variate (henceforth referred to as CV-LB)[6]. To this end, we employ standard CV Monte Carlo setup

[6]Fu *et al.* (1999) have implemented previously a similar efficient simulation approach for pricing

Table 2.2: Prices of European and geometric (continuous and discrete) Asian options for different levels of the speed of mean reversion α.

OU parameter: $\alpha = 0.1$	European		Geometric Asian (cts)		Geometric Asian ($n = 12$)	
BDLP	Price	CPU	Price	CPU	Price	CPU
BM $\sigma = 0.1$	5.8034	0.0076	3.1183	0.0105	3.3387	0.0357
BM $\sigma = 0.5$	20.3280	0.0036	10.5820	0.0077	11.3139	0.0038
DEJD $\left(\begin{smallmatrix}\sigma=0.1,\lambda=3,p=0.6\\ \eta_1=25,\eta_2=25\end{smallmatrix}\right)$	7.1235	0.0061	3.8196	0.0171	4.0876	0.1194
DEJD $\left(\begin{smallmatrix}\sigma=0.5,\lambda=5,p=0.6\\ \eta_1=25,\eta_2=25\end{smallmatrix}\right)$	20.8995	0.0040	10.8467	0.0088	11.5986	0.0046
NIG $\left(\begin{smallmatrix}k=0.1222,\theta=-0.4091\\ \sigma=0.2637\end{smallmatrix}\right)$	12.6149	0.0113	6.7396	0.0247	7.2015	1.0627
NIG $\left(\begin{smallmatrix}k=0.1222,\theta=-0.6819\\ \sigma=0.4395\end{smallmatrix}\right)$	19.2269	0.0040	10.0016	0.0117	10.6946	0.0120
VG $\left(\begin{smallmatrix}k=0.2470,\theta=-0.4671\\ \sigma=0.1967\end{smallmatrix}\right)$	12.5133	0.7297	6.6856	0.7843	7.1431	0.9445
VG $\left(\begin{smallmatrix}k=0.7940,\theta=-0.3053\\ \sigma=0.1669\end{smallmatrix}\right)$	12.1699	0.6967	6.3988	0.8522	6.8475	0.9370
CGMY $\left(\begin{smallmatrix}C=0.5,G=2\\ M=3.5,Y=0.5\end{smallmatrix}\right)$	17.0662	1.8525	8.6004	2.4374	9.2313	2.4916
CGMY $\left(\begin{smallmatrix}C=0.1,G=2\\ M=3.5,Y=1.5\end{smallmatrix}\right)$	18.7581	1.8084	9.7465	2.3342	10.4263	2.5394
OU parameter: $\alpha = 0.5$						
BM $\sigma = 0.1$	5.2414	0.0035	2.8563	0.0083	3.0510	0.0036
BM $\sigma = 0.5$	17.3382	0.0035	9.3373	0.0080	9.9301	0.0036
DEJD $\left(\begin{smallmatrix}\sigma=0.1,\lambda=3,p=0.6\\ \eta_1=25,\eta_2=25\end{smallmatrix}\right)$	6.3114	0.0042	3.4587	0.0090	3.6897	0.0056
DEJD $\left(\begin{smallmatrix}\sigma=0.5,\lambda=5,p=0.6\\ \eta_1=25,\eta_2=25\end{smallmatrix}\right)$	17.8185	0.0039	9.5692	0.0094	10.1776	0.0040
NIG $\left(\begin{smallmatrix}k=0.1222,\theta=-0.4091\\ \sigma=0.2637\end{smallmatrix}\right)$	10.9241	0.0042	6.0167	0.0106	6.4014	0.0121
NIG $\left(\begin{smallmatrix}k=0.1222,\theta=-0.6819\\ \sigma=0.4395\end{smallmatrix}\right)$	16.5101	0.0042	8.8900	0.0112	9.4591	0.0128
VG $\left(\begin{smallmatrix}k=0.2470,\theta=-0.4671\\ \sigma=0.1967\end{smallmatrix}\right)$	10.8880	0.6936	5.9975	0.7721	6.3817	0.9241
VG $\left(\begin{smallmatrix}k=0.7940,\theta=-0.3053\\ \sigma=0.1669\end{smallmatrix}\right)$	10.6713	0.8255	5.7970	0.9913	6.1797	1.0233
CGMY $\left(\begin{smallmatrix}C=0.5,G=2\\ M=3.5,Y=0.5\end{smallmatrix}\right)$	14.6675	1.6827	7.6849	2.3458	8.2080	2.7695
CGMY $\left(\begin{smallmatrix}C=0.1,G=2\\ M=3.5,Y=1.5\end{smallmatrix}\right)$	16.0267	1.9690	8.6216	2.2399	9.1751	2.9832

Legend: $S(0) = K = 100$, $r = 0.0367$, $T = 1$, parameters sets from Fusai and Kyriakou, 2016 (DEJD), Černý and Kyriakou, 2011 (NIG), Guillaume and Schoutens, 2013 (VG), Poirot and Tankov, 2006 (CGMY). CPU time is expressed in seconds.

with the CV coefficient estimated in a pilot run, e.g., Glasserman (2004) and Cont and Tankov (2004). Our choice of the Monte Carlo benchmark is justified by its high accuracy and flexible adaptability to different underlying model assumptions, with a, nevertheless, notable computational burden (refer to Tables 2.3, 2.4, 2.5, 2.6 for relevant reports).

Moments of the discrete arithmetic average does not require numerical methods (nor approximations) at any stage, but higher order moments are still computationally demanding for high number of monitoring dates, see Remark 2.1. We consider $n = 12$ monitoring dates and accuracy is measured by computing the absolute error in % with respect to a benchmark for the true option price which is computed by means of a Monte Carlo simulation where, in analogy with the continuous case, the lower bound price approximation is adopted as control variate (denoted CV-LB). We also include in our numerical experiments an approximation based on higher order moments, i.e. we implement the orthogonal polynomial expansion outlined in Section 1.2.2 considering six moments (OP-6). Numerical results for discrete Asian options are reported in Tables 2.7 and 2.8.

2.5.3 Results

Let us first consider the pricing of European and geometric Asian options. In these cases pricing procedure is exact but computational efficiency depends on the solution of (2.34): when it is full explicit (i.e. BM, DEJD and NIG) pricing procedure is almost instantaneous, with the discrete Asian options slightly more computationally demanding due to the more involved structure of the characteristic function of the arithmetic average of log-returns. In the cases of VG and CGMY, the solution of (2.34) is in terms of special functions, consequently, pricing procedure is more expensive passing from few milliseconds in the case of (for example) NIG to approximately 0.7 seconds in the case of VG and 2 seconds for CGMY (note, indeed, that evaluation of polylogarithm function is less expensive than hypergeometric), see Table 2.2 for exact prices and computing times.

Next, we consider pricing continuously monitored arithmetic average Asian options. Lower bound is certainly the most accurate approximation but also the most computational intensive, see for example Table 2.4: in the case of NIG, produced pricing approximation is very accurate but computing time is enormous (1119.1574 seconds). Hence, the lower bound is used only to compute CV-LB, i.e. the benchmark for the true price of the option. About performances of moment based approximations for continuously monitored arithmetic average Asian options we start by noting the computational-accuracy trade-off implicit in the choice of the number of Gauss-Legendre quadrature nodes, i.e., the higher the number of nodes, the higher the (expected) accuracy and the computing burden[7].

continuous arithmetic Asian options using, instead, the continuous geometric Asian option as control variate

[7]Unfortunately, since we are dealing with approximations and not exact solutions, it may happen

Table 2.3: Arithmetic Asian options prices computed through various moment based approximations for $\alpha = 0.1$ and different number of Gauss-Legendre quadrature nodes (Part 1)

	No. nodes = 6			No. nodes = 12			No. nodes = 24		
Method	Price	Abs err. %	CPU	Price	Abs err. %	CPU	Price	Abs err. %	CPU
	BDLP: BM with $\sigma = 0.1$								
	Benchmarks: CV-LB (s.e., CPU) = 3.1768 (7.7522e-08, 8.3918), LB (CPU) = 3.1766 (0.6050)								
SLN	3.1875	0.3372	0.0023	3.1797	0.0925	0.0076	3.1776	0.0252	0.0157
SG	3.1883	0.3620	0.0016	3.1805	0.1171	0.0056	3.1784	0.0497	0.0155
SRG	3.1873	0.3288	0.0015	3.1794	0.0842	0.0035	3.1773	0.0168	0.0159
MLP	3.1863	0.2998	0.0075	3.1785	0.0549	0.0122	3.1764	0.0126	0.0253
OP-3	3.1867	0.3125	0.0021	3.1789	0.0677	0.0074	3.1768	0.0004	0.0204
J	3.1875	0.3373	0.0160	3.1797	0.0926	0.0508	3.1776	0.0253	0.5826
P	3.1874	0.3334	0.0200	3.1796	0.0887	0.0621	3.1775	0.0214	0.5800
OP-4	3.1873	0.3291	0.0042	3.1795	0.0844	0.0391	3.1773	0.0170	0.5602
	BDLP: DEJD with $\sigma = 0.1$, $\lambda = 3$, $p = 0.6$, $\eta_1 = 25$, $\eta_2 = 25$								
	Benchmarks: CV-LB (s.e., CPU) = 3.9255 (2.2836e-07, 19.4010), LB (CPU)= 3.9253 (2.8928)								
SLN	4.0039	1.9564	0.0026	3.9928	1.6855	0.0088	3.9898	1.6109	0.0368
SG	4.0109	2.1280	0.0036	3.9998	1.8564	0.0080	3.9968	1.7816	0.0397
SRG	4.0016	1.9014	0.0034	0.0048	1.6307	0.0089	3.9876	1.5562	0.0411
MLP	3.9871	1.5430	0.0052	3.9762	1.2728	0.0106	3.9732	1.1984	0.0410
OP-3	3.9945	1.7272	0.0048	3.9836	1.4577	0.0094	3.9806	1.3835	0.0396
J	3.9307	0.1309	0.0213	3.9204	0.1310	0.0977	3.9176	0.2031	1.4224
P	3.9430	0.4418	0.0270	3.9325	0.1775	0.1044	3.9297	0.1047	1.4434
OP-4	3.9238	0.0435	0.0103	3.9137	0.3039	0.0804	3.9109	0.3755	1.3971
	BDLP: NIG with $\theta = -0.4091$, $k = 0.1222$, $\sigma = 0.2637$								
	Benchmarks: CV-LB (s.e., CPU) = 7.0756 (1.7888e-06, 51.9735), LB (CPU)= 7.0726 (21.2278)								
SLN	7.1847	1.5190	0.0070	7.1608	1.1905	0.0228	7.1543	1.1000	0.1126
SG	7.1854	1.5287	0.0075	7.1615	1.2004	0.0205	7.1550	1.1099	0.1155
SRG	7.1845	1.5156	0.0091	7.1606	1.1871	0.0219	7.1540	1.0965	0.1128
MLP	7.1847	1.5190	0.0101	7.1608	1.1905	0.0225	7.1543	1.1000	0.1087
OP-3	7.2828	2.8450	0.0095	7.2576	2.5083	0.0223	7.2507	2.4154	0.1148
J	7.0978	0.3128	0.0500	7.0750	0.0078	0.2974	7.0688	0.0962	4.6101
P	7.1007	0.3543	0.0424	7.0779	0.0332	0.3323	7.0717	0.0552	4.5797
OP-4	7.1968	1.6845	0.0402	7.1722	1.3466	0.2840	7.1654	1.2535	4.4710

Legend: CV-LB = control variate lower bound (assumed to be the true option price), LB = lower bound, SLN = shifted log-normal, SG = shifted gamma, SRG = shifted reciprocal gamma, MLP = modified log-normal power law, OP-3 = orthogonal polynomial expansion (based on the first three moments), J = Johnson, P = Pearson, OP-4 = orthogonal polynomial expansion (based on the first four moments). Further notes: refer to Tables 2.1 and 2.2.

Table 2.4: Arithmetic Asian options prices computed through various moment based approximations for $\alpha = 0.1$ and different number of Gauss-Legendre quadrature nodes (Part 2)

	No. nodes = 6			No. nodes = 12			No. nodes = 24		
Method	Price	Abs err. %	CPU	Price	Abs err. %	CPU	Price	Abs err. %	CPU
	BDLP: BM with $\sigma = 0.5$								
	Benchmarks: CV-LB (s.e., CPU) = 11.6954 (5.1753e-06,7.4397), LB (CPU)= 11.6809 (0.3509)								
SLN	11.7572	0.5258	0.0025	11.7154	0.1706	0.0087	11.7039	0.0725	0.0156
SG	11.8472	1.2813	0.0019	11.8047	0.9262	0.0090	11.7930	0.8283	0.0153
SRG	11.7317	0.3094	0.0017	11.6900	0.0461	0.0060	11.6785	0.1443	0.0154
MLP	11.7310	0.3036	0.0095	11.6890	0.0549	0.0290	11.6774	0.1539	0.0171
OP-3	11.7144	0.1626	0.0023	11.6722	0.1988	0.0096	11.6606	0.2985	0.0157
J	11.7384	0.3668	0.0190	11.6968	0.0123	0.0453	11.6854	0.0856	0.5708
P	11.7500	0.4652	0.0214	11.7083	0.1100	0.0560	11.6968	0.0120	0.5746
OP - 4	11.6935	0.0164	0.0052	11.6516	0.3755	0.0423	11.6401	0.4746	0.5571
	BDLP: DEJD with $\sigma = 0.5$, $\lambda = 5$, $p = 0.6$, $\eta_1 = 25$, $\eta_2 = 25$								
	Benchmarks: CV-LB (s.e., CPU) = 12.0331 (5.9699e-06,19.5054), LB (CPU)= 12.0165 (3.0071)								
SLN	12.0983	0.5392	0.0036	12.0552	0.1830	0.0080	12.0433	0.0846	0.0391
SG	12.1958	1.3343	0.0039	12.1520	0.9784	0.0081	12.1400	0.8802	0.0363
SRG	12.0713	0.3162	0.0035	12.0283	0.0403	0.0083	12.0164	0.1388	0.0388
MLP	12.0720	0.3218	0.0053	12.0286	0.0378	0.0105	12.0166	0.1370	0.0427
OP-3	12.0542	0.1751	0.0048	12.0106	0.1878	0.0093	11.9986	0.2880	0.0432
J	12.0724	0.3257	0.0223	12.0295	0.0296	0.0864	12.0178	0.1277	1.4077
P	12.0879	0.4534	0.0290	12.0448	0.0971	0.1090	12.0330	0.0012	1.4787
OP-4	12.0276	0.0462	0.0113	11.9844	0.4068	0.0907	11.9725	0.5064	1.4614
	BDLP: NIG with $\theta = -0.6819$, $k = 0.1222$, $\sigma = 0.4395$								
	Benchmarks: CV-LB (s.e., CPU) = 10.8344 (5.7110e-06,2247.8054), LB (CPU) = 10.8200 (1119.1574)								
SLN	11.0249	1.7281	0.0073	10.9852	1.3727	0.0842	10.9743	1.2747	0.0943
SG	11.0564	2.0080	0.0079	11.0165	1.6530	0.0683	11.0056	1.5551	0.0983
SRG	11.0145	1.6352	0.0092	10.9749	1.2797	0.0581	10.9640	1.1816	0.0991
MLP	11.0249	1.7281	0.0104	10.9852	1.3727	0.0505	10.9743	1.2747	0.0944
OP-3	11.1034	2.4222	0.0097	11.0627	2.0633	0.0607	11.0515	1.9642	0.1026
J	10.8682	0.3110	0.0502	10.8306	0.0355	0.3413	10.8202	0.1311	4.0930
P	10.8881	0.4928	0.0464	10.8502	0.1451	0.2487	10.8398	0.0492	4.4408
OP-4	11.1369	2.7162	0.0464	11.0945	2.3439	0.2494	11.0828	2.2410	4.4602

Legend: refer to Table 2.3 for further notes.

Table 2.5: Arithmetic Asian options prices computed through various moment based approximations for $\alpha = 0.5$ and different number of Gauss-Legendre quadrature nodes (Part 1)

	No. nodes = 6			No. nodes = 12			No. nodes = 24		
Method	Price	Abs err. %	CPU	Price	Abs err. %	CPU	Price	Abs err. %	CPU
	BDLP: BM with $\sigma = 0.1$								
	Benchmarks: CV-LB (s.e., CPU) = 2.9075 (2.8542e-07, 7.4839), LB (CPU)= 2.9074 (0.3227)								
SLN	2.9196	0.4143	0.0015	2.9108	0.1125	0.0031	2.9084	0.0293	0.0148
SG	2.9201	0.4304	0.0023	2.9113	0.1284	0.0030	2.9088	0.0452	0.0148
SRG	2.9195	0.4089	0.0012	2.9106	0.1071	0.0030	2.9082	0.0239	0.0150
MLP	2.9189	0.3910	0.0112	2.9101	0.0891	0.0054	2.9077	0.0058	0.0170
OP-3	2.9192	0.3996	0.0031	2.9104	0.0978	0.0039	2.9079	0.0146	0.0168
J	2.9197	0.4183	0.0375	2.9108	0.1125	0.0425	2.9084	0.0294	0.5528
P	2.9195	0.4121	0.0335	2.9107	0.1103	0.0532	2.9083	0.0271	0.6020
OP-4	2.9195	0.4098	0.0044	2.9107	0.1080	0.0338	2.9082	0.0248	0.5663
	BDLP: DEJD with $\sigma = 0.1$, $\lambda = 3$, $p = 0.6$, $\eta_1 = 25$, $\eta_2 = 25$								
	Benchmarks: CV-LB (s.e., CPU) = 3.5504 (5.3655e-07, 18.0723), LB (CPU)= 3.5502 (2.5307)								
SLN	3.6193	1.9038	0.0036	3.6068	1.5632	0.0067	3.6034	1.4692	0.0319
SG	3.6239	2.0288	0.0026	3.6113	1.6870	0.0061	3.6079	1.5928	0.0324
SRG	3.6178	1.8634	0.0025	3.6053	1.5231	0.0062	3.6019	1.4293	0.0318
MLP	3.6070	1.5679	0.0051	3.5946	1.2292	0.0081	3.5912	1.1358	0.0338
OP-3	3.6134	1.7430	0.0034	3.6010	1.4040	0.0071	3.5976	1.3105	0.0328
J	3.5604	0.2808	0.0155	3.5489	0.0438	0.0777	3.5457	0.1332	1.2552
P	3.5694	0.5327	0.0179	3.5577	0.2043	0.0784	3.5545	0.1138	1.2473
OP-4	3.5553	0.1389	0.0093	3.5440	0.1807	0.0749	3.5409	0.2688	1.2707
	BDLP: NIG with $\theta = -0.4091$, $k = 0.1222$, $\sigma = 0.2637$								
	Benchmarks: CV-LB (s.e., CPU) = 6.3024 (4.9978e-06,43.3353), LB (CPU)= 6.2996 (17.1755)								
SLN	6.4031	1.5731	0.0091	6.3760	1.1539	0.0179	6.3685	1.0381	0.0969
SG	6.4032	1.5733	0.0069	6.3760	1.1541	0.0173	6.3685	1.0383	0.0948
SRG	6.4031	1.5731	0.0070	6.3760	1.1539	0.0176	6.3685	1.0381	0.0950
MLP	6.4031	1.5731	0.0071	6.3760	1.1539	0.0176	6.3685	1.0381	0.0949
OP-3	6.4930	2.9346	0.0070	6.4643	2.5045	0.0173	6.4564	2.3856	0.0980
J	6.3326	0.4768	0.0384	6.3068	0.0698	0.2420	6.2997	0.0425	3.9672
P	6.3343	0.5036	0.0344	6.3085	0.0960	0.2417	6.3014	0.0165	3.9584
OP-4	6.3982	1.4964	0.0276	6.3706	1.0705	0.2396	6.3631	0.9530	3.9718

Legend: refer to Table 2.3 for further notes.

Table 2.6: Arithmetic Asian options prices computed through various moment based approximations for $\alpha = 0.5$ and different number of Gauss-Legendre quadrature nodes (Part 2)

	No. nodes = 6			No. nodes = 12			No. nodes = 24		
Method	Price	Abs err. %	CPU	Price	Abs err. %	CPU	Price	Abs err. %	CPU
	BDLP: BM with $\sigma = 0.5$								
	Benchmarks: CV-LB (s.e., CPU) = 10.2898 (1.6291e-05,8.0249), LB (CPU)= 10.2748 (0.4136)								
SLN	10.3551	0.6303	0.0017	10.3070	0.1674	0.0031	10.2938	0.0394	0.0152
SG	10.4170	1.2216	0.0016	10.3684	0.7579	0.0030	10.3550	0.6296	0.0150
SRG	10.3363	0.4501	0.0013	10.2885	0.0126	0.0029	10.2753	0.1407	0.0147
MLP	10.3325	0.4131	0.0034	10.2844	0.0528	0.0051	10.2711	0.1817	0.0166
OP-3	10.3205	0.2973	0.0021	10.2723	0.1701	0.0036	10.2591	0.2995	0.0158
J	10.3444	0.5278	0.0099	10.2965	0.0657	0.0384	10.2834	0.0622	0.5554
P	10.3495	0.5769	0.0182	10.3015	0.1142	0.0465	10.2884	0.0139	0.5573
OP-4	10.3172	0.2653	0.0046	10.2693	0.1991	0.0336	10.2562	0.3276	0.5418
	BDLP: DEJD with $\sigma = 0.5$, $\lambda = 5$, $p = 0.6$, $\eta_1 = 25$, $\eta_2 = 25$								
	Benchmarks: CV-LB (s.e., CPU) = 10.5839 (1.6726e-05,17.9512), LB (CPU)= 10.5669 (2.5846)								
SLN	10.6529	0.6550	0.0026	10.6033	0.1907	0.0063	10.5897	0.0622	0.0445
SG	10.7209	1.2853	0.0026	10.6706	0.8201	0.0062	10.6568	0.6914	0.0377
SRG	10.6326	0.4654	0.0025	10.5832	0.0011	0.0061	10.5696	0.1274	0.0349
MLP	10.6286	0.4285	0.0048	10.5790	0.0390	0.0081	10.5653	0.1684	0.0368
OP-3	10.6151	0.3016	0.0036	10.5654	0.1677	0.0071	10.5517	0.2975	0.0360
J	10.6371	0.5076	0.0142	10.5878	0.0444	0.0786	10.5742	0.0838	1.2365
P	10.6441	0.5730	0.0231	10.5946	0.1090	0.0879	10.5810	0.0194	1.2308
OP-4	10.6092	0.2462	0.0096	10.5599	0.2200	0.0792	10.5463	0.3490	1.2173
	BDLP: NIG with $\theta = -0.6819$, $k = 0.1222$, $\sigma = 0.4395$								
	Benchmarks: CV-LB (s.e., CPU) = 9.6307 (1.7127e-05,44.5368), LB (CPU)= 9.6164 (17.4205)								
SLN	9.7757	1.4828	0.0077	9.7307	1.0275	0.0173	9.7183	0.9016	0.0963
SG	9.7907	1.6343	0.0072	9.7456	1.1791	0.0173	9.7332	1.0532	0.0931
SRG	9.7706	1.4314	0.0067	9.7256	0.9760	0.0168	9.7133	0.8501	0.0937
MLP	9.7757	1.4828	0.0068	9.7307	1.0275	0.0171	9.7183	0.9016	0.0936
OP-3	9.8722	2.4464	0.0067	9.8259	1.9862	0.0173	9.8131	1.8588	0.0946
J	9.6528	0.2286	0.0320	9.6103	0.2123	0.2386	9.5986	0.3342	3.9466
P	9.6632	0.3364	0.0303	9.6205	0.1059	0.2383	9.6088	0.2281	3.9655
OP-4	9.8617	2.3426	0.0265	9.8141	1.8684	0.2344	9.8010	1.7372	3.9517

Legend: refer to Table 2.3 for further notes.

Table 2.7: Discretely monitored ($n = 12$ monitoring dates) Arithmetic average Asian option prices (Part 1)

	$\alpha = 0.1$			$\alpha = 0.5$		
Method	Price	Abs. err. (%)	CPU	Price	Abs. err. (%)	CPU
	BDLP: BM with $\sigma = 0.1$					
CV-LB	3.3970	–	5.7706	3.1023	–	5.8132
std. err.	0.1145e-06			0.1012e-06		
LB	3.3968	0.0043	0.0470	3.1021	0.0044	0.0322
SLN	3.3970	0.0008	0.3268	3.1022	0.0030	0.1175
SG	3.3978	0.0259	0.1839	3.1027	0.0129	0.1528
SRG	3.3967	0.0078	0.2100	3.1020	0.0084	0.1219
MLP	3.3960	0.0286	0.3026	3.1016	0.0202	0.1585
OP-3	3.3963	0.0205	0.3291	3.1018	0.0149	0.1191
J	3.3970	0.0008	0.3942	3.1022	0.0030	0.2143
P	3.3969	0.0030	0.4409	3.1021	0.0051	0.2178
OP-4	3.3967	0.0066	0.2743	3.1020	0.0069	0.1707
OP-6	3.3968	0.0038	0.8321	3.1021	0.0055	0.5102
	BDLP: DEJD with $\sigma = 0.1$, $\lambda = 3$, $p = 0.6$, $\eta_1 = 25$, $\eta_2 = 25$					
CV-LB	4.1933	–	27.8876	3.7816	–	27.9909
std. err.	0.5880e-04			0.5102e-04		
LB	4.1929	0.0085	2.8473	3.7812	0.0099	4.3401
SLN	4.2574	1.5056	0.5439	3.8334	1.3522	0.1635
SG	4.2647	1.6746	0.2031	3.8381	1.4727	0.2065
SRG	4.2551	1.4515	0.2594	3.8319	1.3132	0.1698
MLP	4.2409	1.1236	0.2731	3.8216	1.0469	0.1794
OP-3	4.2472	1.2687	0.1828	3.8271	1.1884	0.1672
J	4.1838	0.2279	0.3786	3.7753	0.1680	0.2453
P	4.1961	0.0674	0.4669	3.7841	0.0669	0.2406
OP-4	4.1812	0.2895	0.4209	3.7734	0.2172	0.2356
OP-6	4.2179	0.5829	2.2203	3.8005	0.4977	1.0900
	BDLP: NIG with $\theta = -0.4091$, $k = 0.1222$, $\sigma = 0.2637$					
CV-LB	7.5363	–	9.9102	6.6864	–	9.9891
std. err.	0.4021e-03			0.3362e-03		
LB	7.5348	0.0200	2.5214	6.6848	0.0235	2.7389
SLN	7.6145	1.0270	0.3832	6.7512	0.9597	0.3476
SG	7.6156	1.0414	0.3185	6.7513	0.9606	0.3345
SRG	7.6141	1.0219	0.3332	6.7512	0.9594	0.3147
MLP	7.6145	1.0270	0.3290	6.7512	0.9597	0.3336
OP-3	7.7192	2.3692	0.3424	6.8462	2.3333	0.3214
J	7.5279	0.1120	1.0178	6.6820	0.0656	1.0143
P	7.5309	0.0720	0.9602	6.6837	0.0405	0.9396
OP-4	7.6419	1.3812	0.9766	6.7569	1.0434	1.0636
OP-6	7.4320	1.4042	1.0323	6.5901	1.4614	0.9731

Legend: CV-LB = Control variate with lower bound (assumed to be the true option price), OP-6 = orthogonal polynomial expansion (based on the first six moments). Further notes: refer to Tables 2.2 and 2.3.

Table 2.8: Discretely monitored ($n = 12$ monitoring dates) Arithmetic average Asian option prices (Part 2)

	$\alpha = 0.1$			$\alpha = 0.5$		
Method	Price	Abs. err. (%)	CPU	Price	Abs. err. (%)	CPU
	BDLP: BM with $\sigma = 0.5$					
CV-LB	12.4356	–	5.9083	10.8942	–	5.6833
std. err.	0.0021			0.0018		
LB	12.4154	0.1625	0.1581	10.8723	0.2014	0.0514
SLN	12.4358	0.0017	0.1397	10.8880	0.0577	0.1136
SG	12.5325	0.7733	0.1457	10.9537	0.5432	0.1607
SRG	12.4087	0.2169	0.1313	10.8682	0.2399	0.1284
MLP	12.4142	0.1728	0.1427	10.8696	0.2269	0.1148
OP-3	12.4031	0.2625	0.1382	10.8604	0.3117	0.1177
J	12.4160	0.1584	0.2093	10.8771	0.1578	0.1884
P	12.4289	0.0537	0.2455	10.8825	0.1077	0.1876
OP-4	12.3781	0.4646	0.2268	10.8546	0.3653	0.1844
OP-6	12.4070	0.2309	0.5827	10.8755	0.1727	0.4952
	BDLP: DEJD with $\sigma = 0.5$, $\lambda = 5$, $p = 0.6$, $\eta_1 = 25$, $\eta_2 = 25$					
CV-LB	12.7912	–	11.2023	11.2023	–	24.6128
std. err.	0.0019			0.0019		
LB	12.7715	0.1547	3.1382	11.1807	0.1928	1.7359
SLN	12.7956	0.0343	0.1723	11.1999	0.0209	0.1465
SG	12.9001	0.8442	0.1373	11.2720	0.6188	0.1372
SRG	12.7670	0.1899	0.1469	11.1786	0.2123	0.1311
MLP	12.7740	0.1353	0.1844	11.1800	0.1991	0.1430
OP-3	12.7627	0.2236	0.1605	11.1698	0.2907	0.1408
J	12.7684	0.1788	0.2457	11.1840	0.1640	0.2397
P	12.7856	0.0440	0.2671	11.1914	0.0974	0.2460
OP-4	12.7319	0.4663	0.2390	11.1614	0.3662	0.2514
OP-6	12.7601	0.2441	1.0254	11.1835	0.1681	1.0303
	BDLP: NIG with $\theta = -0.6819$, $k = 0.1222$, $\sigma = 0.4395$					
CV-LB	11.5623	–	10.3423	10.1895	–	9.9255
std. err.	0.0013			0.0013		
LB	11.5551	0.0625	3.4587	10.1890	0.0048	2.6305
SLN	11.6663	0.8912	0.3926	10.2863	0.9414	0.3375
SG	11.7024	1.1969	0.3409	10.3035	1.1067	0.3781
SRG	11.6545	0.7903	0.3411	10.2805	0.8855	0.3116
MLP	11.6663	0.8912	0.3233	10.2863	0.9414	0.3231
OP-3	11.7484	1.5838	0.3359	10.3891	1.9209	0.3157
J	11.5097	0.4575	1.0318	10.1660	0.2314	0.9418
P	11.5311	0.2712	0.9745	10.1769	0.1240	0.9453
OP-4	11.8058	2.0623	0.9552	10.3956	1.9831	0.9358
OP-6	11.5813	0.1634	0.9516	10.1521	0.3681	0.9711

Legend: refer to Tables 2.2, 2.3 and 2.7 for further notes.

Moreover, we note a significant upward shift in total computing time whenever we pass from 3 parameters approximations to 4. Indeed, computing time for fourth moment is much higher than for third, this fact prevents us from considering further approximations based on more than four moments, which would be much slower. Despite a bit more computational demanding, approximations based on first four integer moments are much more accurate, in particular, impressive are the performances of the Johnson's (J) and Pearson's (P) system of distributions which largely outperforms the orthogonal polynomial expansion implemented around the log-normal distribution (OP-4). Note indeed that absolute error in % is far below 1% throughout all the parameter settings explored (even for a small number of Gaussian quadrature nodes for which pricing procedure is extremely fast). The benefit of including the fourth moment becomes more prominent in models with jumps and with low speed of mean reversion. Moreover, the Pearson's system approximation outperforms the Johnson's one throughout all the parameter settings and seems to be preferable in general. Among three parameters approximations we have that the shifted gammma (SG) is certainly the worst performing, this is consistent with Lo *et al.* (2014) which draw the same conclusion under the Black-Scholes model. SLN, SRG and MLP have similar performances, with MLP outperforming the others throughout parameter settings explored in Tables 2.3 and 2.5.

In the following section, we summarize and present our conclusions.

2.6 Conclusions

We propose and survey different pricing expressions for the Asian option value for Lévy-driven OU processes that turn out to be appropriate to model returns in commodity markets and do not require special computing skills, hence Asian options become a viable hedging tool for various operators in these markets. Regarding geometric Asian options we derive the characteristic functions of log-returns and their arithmetic averages opening doors to exact option pricing through standard inversion algorithms. Furthermore, we consider a variety of Lévy models as background driving processes highlighting whether or not the problem becomes analytically tractable and implications for pricing performances.

For what concerns the more complicated case of arithmetic Asian options our approach relies on moment-based approximations that are flexible with conventional empirical regularities, such as mean reversion and discontinuous price movements. To this end, we present a general expression for the raw moments of both the continuous and discrete arithmetic average which we implement within our proposed model framework. Moreover, extending Fusai and Kyriakou (2016), we derive a very sharp lower bound to both

that accuracy does not increase with the number of nodes. A typical situation where this can happen is when the price approximation underestimate the true price and the approximated price decreases with the number of nodes considered.

continuously and discretely monitored arithmetic average Asian option price.

In light of the discussion in the previous section, we can draw some interesting conclusions. Despite the attention that series expansions have received in the literature of derivatives' pricing (e.g., see Tanaka *et al.*, 2010, Yamazaki, 2014 and Willems, 2019), they might not be a robust, hence an unreliable, method of choice for moment indeterminate problems and when only few moments are available (as in the present work). Having tested different background driving models under mild or stressed market conditions, the accuracy of these approximations seems to be the most susceptible to such changes. The lower bound is very sharp, but also more intricate, especially for non expert users, and less fast. Approximations based on moment-matching, on the other hand, are easy, fast to compute and accurate. Despite more time consuming, including the fourth moment into the pricing approximation entails an extra benefit in terms of accuracy, especially in jump models, where kurtosis plays a crucial role. This happens both in continuous and discrete monitoring settings. In particular, approximations implemented using four integer moments through the Johnson's and Pearson's distributions are the most accurate, this is also consistent with the results reported in Table 1.2. Among this two distributions, the Pearson's family is preferable resulting generally slightly more accurate with a similar computing time. Theoretical support to this evidence is given by the fact that, as stated in Section 1.2.1, the Johnson's system is more suited for quantile matching than moment matching (see Devroye, 1986).

Chapter 3

Wrong Way CVA for interest rates derivatives

In this chapter we show how to calculate Credit Value Adjustment (CVA) for interest rates derivatives in presence of Wrong Way Risk (WWR). Modeling the default intensity as in Hull and White (2012) we propose a procedure for parameters calibration based on moment matching and show how to compute Wrong Way CVA through the numerical integration of the solution of a Partial Differential Equation (PDE). Numerical experiments, conducted on a variety of interest rates derivatives such as bond options, caplets and swaptions, highlight the accuracy of the proposed method.

3.1 Introduction

Counterparty risk is a combination of market exposure and credit risk, in particular market factors determine the magnitude of the exposure and credit risk determines the default probability of the counterparty. According to Canabarro and Duffie (2003), its valuation is the first line of defense in credit risk management and Credit Value Adjustment (CVA), which consists in the adjustment to the value of derivatives to reflect the possibility of default of the counterparty before the expiry date, is the main tool to price credit risk. The financial crisis of 2007-2009 has highlighted the importance of this counterparty risk measure: according to the technical report of B. C. of Banking Supervision (2011), around two thirds of the credit losses were CVA losses. Ruiz *et al.* (2015) provide many practical examples on how CVA is of remarkable importance in many areas of finance, such as pricing of financial derivatives, calculation of margins and economic/regulatory capital.

For its calculation, the probability of default of the counterparty and the credit exposure are often considered independent but the efficacy of independent CVA is limited. Indeed, in many practical cases the credit exposure is related to the counterparty's default

time[1]. In particular, positive (negative) correlation among these two variables implies presence of Wrong (Right) Way Risk. Since the dependence between market factors and credit risk is a crucial aspect in CVA calculation, large part of literature has been devoted to its modelization. We refer to Li and Mercurio (2015) for an exhaustive list of the different methodologies and as source of references. For what concerns the specific case of interest rates markets, a way for incorporating wrong-way and right-way risk into CVA calculations is relating directly the dynamics of the short rate and the default intensity (or, equivalently, hazard rate), for example Brigo *et al.* (2013) use CIR (and CIR ++) process with and without jumps and Hull and White (2012) propose a log-normal setting for the default intensity.

We use an approach similar to the one proposed by Hull and White (2012). Their model links the default intensity of the counterparty to the value of the transactions outstanding between the dealer and the counterparty. In the original paper, the authors stress that this is not the only possible approach and suggest that alternative variables can be related to the default intensity. The chosen variable must *"affect the value of the counterparty's portfolio"* and *"have a big effect on the counterparty's health"*. The authors also suggest to use the short rate when dealing with interest rates derivatives. This is our choice. In particular, we model the short rate using a 1-factor Hull and White model and relate the default intensity with the diffusive component of the short rate. This choice allows us firstly to calculate explicitly the correlation between the default intensity and the short rate. Secondly, following the calibration scheme proposed by Hull and White (2012), to estimate the deterministic component of the default intensity from market data through a moment matching approach, and thirdly to reduce the problem of the calculation of Wrong Way CVA to the numerical integration of the solution of a PDE. The main advantage of our method is that it does not require Monte Carlo simulation in any step allowing for faster implementation. We stress, indeed, that the mathematical complexity of parameters calibration and CVA calculation (both with and without independence assumption) induced many authors to resort to Monte Carlo simulation, see for example Canabarro and Duffie (2003), Crépey (2015), Gregory (2012), Ghamami and Goldberg (2014), Glasserman and Yang (2016) and Ballotta *et al.* (2016). The usage of moment matching approximation introduces some approximation error but the mean reverting nature of the 1-factor Hull and White model mitigates it.

This chapter is organized as follows: Section 3.2 contains the description of the model, in Section 3.3 we derive an analytical representation of the correlation between the short rate and the default intensity, in Section 3.4 we describe moment matching method and show how to implement it to calibrate the parameters of the default intensity, in Section

[1]According to the International Swaps and Derivatives Association (ISDA), this happens typically when the probability of default of the counterparty is correlated with a macroeconomic variable which also affects the value of derivatives transactions.

3.5 we derive a general formula for the calculation of Wrong Way CVA for interest rates derivatives, Section 4.6 contains numerical results, conclusions are presented in the last section.

3.2 Model setup

We consider a 1-factor Hull and White (1990) model to describe the short rate dynamics:

$$r(t) = r(0)e^{-\gamma t} + \int_0^t e^{-\gamma(t-u)}\vartheta(u)du + \sigma\int_0^t e^{-\gamma(t-u)}dW(u), \tag{3.1}$$

where γ is the speed of reversion parameter, σ is the diffusion coefficient and $\vartheta(\cdot)$ is the deterministic long run mean and is chosen to fit the market discount curve. We set $Z(t) = \int_0^t e^{-\gamma(t-u)}dW(u)$ and we have that

$$Z(t) \sim \mathcal{N}\left(0, \frac{1-e^{-2\gamma t}}{2\gamma}\right).$$

As in Hull and White (2012) the default intensity (or equivalently the hazard rate) is assumed to be

$$\lambda(t) = e^{\alpha Z(t)+\beta(t)}. \tag{3.2}$$

Here the parameter α allows us to capture the dependence between the short rate and the hazard rate. The deterministic function $\beta(\cdot)$ allows us to fit the market term structure of default probability, extracted from quotations of defaultable bonds or from CDS spreads (see for example Ballotta *et al.*, 2016).

3.3 Correlation between default intensity and short rate

In order to understand the role of α, let us consider the correlation between $r(t)$, and $\lambda(t)$. We have

$$\begin{aligned}\mathrm{Cov}[r(t),\lambda(t)] &= \mathrm{Cov}\left[\sigma Z(t), e^{\alpha Z(t)+\beta(t)}\right] = \sigma e^{\beta(t)}\mathrm{Cov}\left(Z(t), e^{\alpha Z(t)}\right)\\ &= \sigma e^{\beta(t)}\mathrm{E}[Z(t)e^{\alpha Z(t)}] = \sigma e^{\beta(t)}\frac{\partial}{\partial\alpha}\mathrm{E}[e^{\alpha Z(t)}],\end{aligned}$$

where we have assumed that it is possible to interchange derivative and expectation. In the adopted Gaussian HJM model, we have

$$\mathrm{E}[e^{\alpha Z(t)}] = e^{\frac{1}{2}\alpha^2 \mathrm{Var}[Z(t)]},$$

where $\mathrm{Var}[Z(t)] = \frac{1-e^{-2\gamma t}}{2\gamma}$ in the 1-factor Hull and White model. Therefore

$$\mathrm{Cov}[r(t), \lambda(t)] = \sigma e^{\beta(t)} \alpha \mathrm{Var}[Z(t)] e^{\frac{1}{2}\alpha^2 \mathrm{Var}[Z(t)]},$$

and noting that

$$\mathrm{Var}[r(t)] = \sigma^2 \mathrm{Var}[Z(t)], \quad \mathrm{Var}[\lambda(t)] = e^{2\beta(t)+\alpha^2 \mathrm{Var}[Z(t)]} \left(e^{\alpha^2 \mathrm{Var}[Z(t)]} - 1 \right),$$

we get

$$\begin{aligned}
\rho(r(t), \lambda(t)) &= \frac{\sigma e^{\beta(t)} \left(e^{\frac{1}{2}\alpha^2 \mathrm{Var}[Z(t)]} \right) \alpha \mathrm{Var}[Z(t)]}{\sqrt{\sigma^2 \mathrm{Var}[Z(t)]} \sqrt{e^{2\beta(t)+\alpha^2 \mathrm{Var}[Z(t)]} (e^{\alpha^2 \mathrm{Var}[Z(t)]} - 1)}} \\
&= \frac{\sigma \left(e^{\frac{1}{2}\alpha^2 \mathrm{Var}[Z(t)]} \right) \alpha \mathrm{Var}[Z(t)]}{\sigma \sqrt{\mathrm{Var}[Z(t)]} \sqrt{e^{\alpha^2 \mathrm{Var}[Z(t)]} (e^{\alpha^2 \mathrm{Var}[Z(t)]} - 1)}} \\
&= \frac{\left(e^{\frac{1}{2}\alpha^2 \mathrm{Var}[Z(t)]} \right) \alpha \sqrt{\mathrm{Var}[Z(t)]}}{\sqrt{e^{\alpha^2 \mathrm{Var}[Z(t)]} (e^{\alpha^2 \mathrm{Var}[Z(t)]} - 1)}} = \frac{\alpha \sqrt{\mathrm{Var}[Z(t)]}}{\sqrt{e^{\alpha^2 \mathrm{Var}[Z(t)]} - 1}}
\end{aligned}$$

In conclusion, the parameter α controls the correlation between the short rate and the hazard rate and we notice that the full range of values in the interval $[-1, 1]$ can be recovered. This is shown in Figure 3.1, where the correlation between the short rate and the intensity process is plotted for different horizons and different values of α. Considering the limit of the correlation as α tends to zero, we have that it approaches $\frac{\alpha}{|\alpha|}$, i.e. ± 1 depending on the sign of α. So, for $\alpha \to 0$ we achieve the maximum positive or negative dependency between the short rate and the default intensity.

3.4 Calibration of $\beta(t)$ in the 1 factor Hull-White model

In order to calculate Wrong Way Risk CVA we are interested in calibrating α and $\beta(\cdot)$ in equation (3.2). Hull and White (2012) describe two different methods for the calculation of α based on historical time series of credit spread and then (assuming that α is known) propose a procedure that allows to estimate $\beta(\cdot)$ based on market data. The procedure can be summarized as follows:

Figure 3.1: Relationship between $\rho(r(t), \lambda(t))$ and α for different maturities and γ.

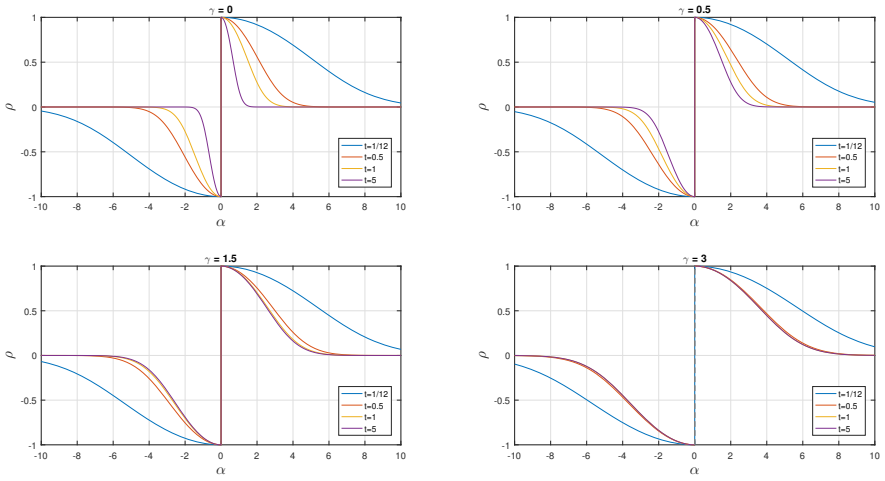

Legend: The first subplot is obtained with $\gamma = 0$ (which corresponds to the case where the short rate follows a Ho-Lee dynamics), otherwise we have the 1-factor Hull and White model.

1 Define $\beta(\cdot)$ as a piecewise constant function:

$$\beta(t) = \begin{cases} \beta_1 & \text{if} \quad 0 < t \leq t_1 \\ \beta_2 & \text{if} \quad t_1 < t \leq t_2 \\ \vdots & \\ \beta_n & \text{if} \quad t_{n-1} < t \leq t_n = T \end{cases}, \tag{3.3}$$

where $0 < t_1 < \cdots < t_j < \cdots < t_n := T$.

2 Let us suppose to have a term structure of survival probabilities $Q(0, t_j)$. Assuming that $\beta_1, \cdots, \beta_{j-1}$ are given, recursively solve the following equation:

$$Q(0, t_j) = \mathrm{E}_0 \left[e^{-\int_0^{t_j} e^{\alpha Z(s) + \beta(s)} ds} \right], \tag{3.4}$$

with respect to β_j. The authors calculate the expectation on the right hand side through a Monte Carlo simulation.

The drawback of this approach is that the numerical solution of an equation involving a Monte Carlo simulation can be quite heavy from a computational point of view. The aim of this section is to propose an alternative procedure for the estimation of $\beta(\cdot)$. In particular, we propose to approximate the expected value in equation (3.4) through a moment matching procedure.

3.4.1 Moment Matching

Let's denote $X(t) := \int_0^t e^{\alpha Z(s)+\beta(s)}ds$. We assume a parametric distribution for $X(t)$. Its parameters are estimated equaling moments of $X(t)$ with the ones implied by the supposed distribution. In particular, we define a new random variable $Y(t)$ having a parametric distribution $f_Y(y;\underline{\theta})$ and the parameter vector $\underline{\theta}$ is chosen so that $Y(t)$ has the same moments as $X(t)$. Therefore we approximate $\mathrm{E}\left[e^{-X(t)}\right]$ by $\mathrm{E}\left[e^{-Y(t)}\right]$. Notice the significant advantage of this procedure when the characteristic function of $Y(\cdot)$ is known analytically: the iterative solution of (3.4) does not require anymore Monte Carlo simulation.

In the following subsection we show how to implement the moment matching procedure in this context. In order to reduce the computational effort and improve the accuracy of the approximation we need to carefully choose the supposed distribution. In particular, we need a random variable with the following characteristics: its density must be unimodal and with positive support (note indeed that our problem is related to the difficult problem of determining the distribution of the sum of log-normal random variables); the system of moments must be solvable analytically; the approximating random variable must have moment generating (or alternatively characteristic) function. In addition, for simplifying the computational cost, we also require that the parameter vector to be bi-dimensional, so that we fit mean and variance, a standard procedure when we deal with approximating the sum of log-normal r.v.'s.

According to those criteria a possible approximation is based on the Gamma distribution. In principle, other distributions can be used (see, for example, Section 1.5) for other suitable distributions), but the Gamma ensures the best trade-off between accuracy and computational cost thanks to the simplicity of its characteristic function.

We recall here some properties of the Gamma distribution that will be used in the next subsection for the calibration of $\beta(\cdot)$: if $Y \sim \Gamma(\theta, k)$ then $\theta = \frac{\mathrm{Var}[Y]}{\mathrm{E}[Y]}$ and $k = \frac{\mathrm{E}[Y]}{\theta}$; the characteristic function is $\mathrm{E}[e^{-itY}] = (1 - it\theta)^{-k}$ and $e^{\beta}Y \sim \Gamma(k, e^{\beta}\theta)$. See also Example 1.

Finally, let us denote $X(t_j, \beta_j) := \int_0^{t_j} e^{\alpha Z(s)+\beta(s)}ds$ where we have put in evidence the dependence of $X(\cdot,\cdot)$ on β_j only, assuming that $\beta_1, \cdots, \beta_{j-1}$ have already been computed. Moments can be computed numerically according to the following:

Proposition 3.1. *The first two moments of $X(t_j, \beta_j)$ are given by:*

$$\begin{aligned}
\mathrm{E}\left[X(t_j,\beta_j)\right] &= \int_0^{t_j} e^{\beta(s)+\frac{\alpha^2}{4\gamma}(1-e^{-2\gamma s})}ds \\
\mathrm{E}\left[X^2(t_j,\beta_j)\right] &= \int_0^{t_j}\left(\int_0^{t_j} e^{\beta(s)+\beta(u)+\frac{\alpha^2}{4\gamma}(2-e^{-2\gamma s}-e^{-2\gamma u})+\frac{\alpha^2}{2\gamma}(e^{-\gamma|u-s|}-e^{-\gamma(u+s)})}ds\right)du,
\end{aligned}$$

where $\beta(t)$ is defined as in (3.3).

Proof. It is similar to the proof of Proposition 2.6. For the first moment, we have

$$\mathrm{E}\left[X(t_j,\beta_j)\right] = \mathrm{E}\left[\int_0^{t_j} e^{\alpha Z(s)+\beta(s)}ds\right] = \int_0^{t_j} \mathrm{E}\left[e^{\alpha Z(s)+\beta(s)}\right]ds = \int_0^{t_j} e^{\frac{1}{2}\alpha^2\left(\frac{1-e^{-2\gamma s}}{2\gamma}\right)+\beta(s)}ds.$$

For the second moment, following Bharucha-Reid (1960, pag. 344–345), we have

$$\mathrm{E}\left[X^2(t_j,\beta_j)\right] = \int_0^{t_j}\left(\int_0^{t_j} e^{\beta(s)+\beta(u)}\mathrm{E}\left[e^{\alpha(Z(s)+Z(u))}\right]ds\right)du.$$

The thesis follows by computing the inner expectation, which can be done easily using the properties of the normal distribution. ■

3.4.2 Methodology

We propose now an iterative method for a steepwise calibration of the function β. The first step is the calculation of β_1, which can be estimated solving the following equation:

$$Q(0,t_1) = \mathrm{E}_0\left[e^{-\int_0^{t_1} e^{\alpha Z(s)+\beta_1}ds}\right].$$

Implementing moment matching (we suppose that $\int_0^{t_1} e^{\alpha Z(s)}ds \sim \Gamma(\theta,k)$) we get a closed form approximation for β_1[2]:

$$\begin{aligned} Q(0,t_1) &\approx (1+\theta e^{\beta_1})^{-k} \\ \beta_1 &\approx \ln\left(\frac{Q(0,t_1)^{-1/k}-1}{\theta}\right). \end{aligned} \tag{3.5}$$

Once β_1 is known, the whole curve of $\beta(\cdot)$ can be estimated using an iterative procedure: at each step, starting from $j=2$[3], we have to solve the following equation:

$$Q(0,t_j) = \mathrm{E}_0[e^{-X(t_j,\beta_j)}].$$

Let us suppose that the approximating distribution of $X(t_j,\beta_j)$ is $Y \sim \Gamma(k(\beta_j),\theta(\beta_j))$[4]. Solving the system of moments we get:

$$\theta(\beta_j) = \frac{\mathrm{Var}[X(t_j,\beta_j)]}{\mathrm{E}[X(t_j,\beta_j)]}, \quad k(\beta_j) = \frac{\mathrm{E}[X(t_j,\beta_j)]}{\theta(\beta_j)}.$$

[2]Parameters are estimated equating theoretical moments of Gamma distribution with the moments of $\int_0^{t_1} e^{\alpha Z(s)}ds$ which are computed numerically according to Proposition 3.1.

[3]Note that at time t_j the variable β_j is the only unknown. For example, if $j=2$ then $\beta(t) = \begin{cases}\beta_1 & \text{if} \quad 0<t\le t_1 \\ \beta_2 & \text{if} \quad t_1<t\le t_2\end{cases}$, where β_1 has been calculated in the previous step, while β_2 is the unknown. More in general, if we consider t_j then $\beta_1,\beta_2,\cdots,\beta_{j-1}$ are known, β_j is the only unknown.

[4]We stress again the fact that the parameters depend on the unknown β_j.

Figure 3.2: Calibration of $\beta(t)$

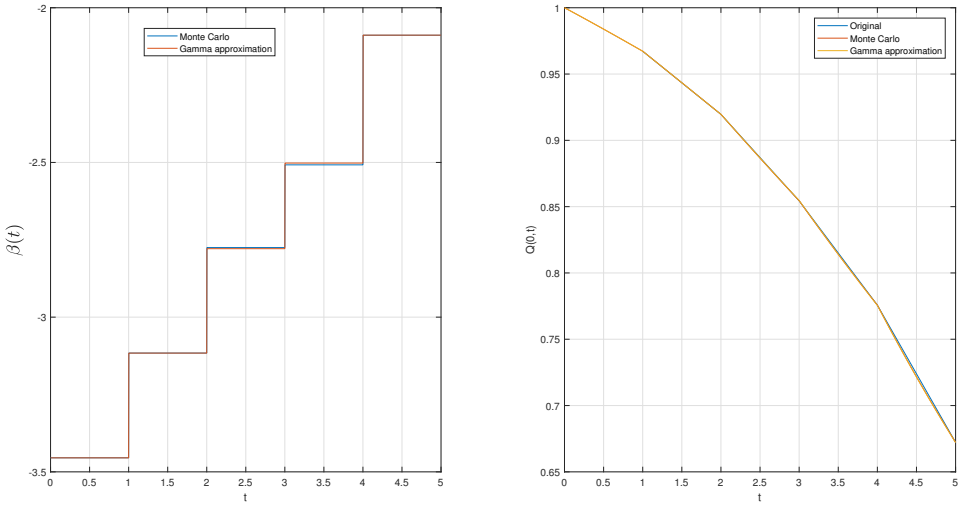

Legend: first subplot: estimation of $\beta(t)$ as in (3.3) using Monte Carlo (blue line) and moment matching (red line). Second subplot: comparison between the true market term structure of default probability and the ones obtained using $\beta(t)$ as estimated in the first subplot. Model parameters: $\alpha = 0.5$, $\gamma = 0.2$, maturities $= \{1, 2, 3, 4, 5\}$ years, $Q = \{0.9672, 0.9196, 0.8544, 0.7757, 0.6722\}$; Monte Carlo parameters: $N°$ of simulations=10^5, $N°$ of points in grid $= 2000$.

with the first two moments of X computed according to Proposition 3.1. Finally, exploiting the analytical expression of the characteristic function of the Gamma distribution, it is possible to solve numerically[5] the following equation with respect to β_j:

$$Q(0, t_j) = (1 + \theta(\beta_j))^{-k(\beta_j)}.$$

Repeating the procedure for every j we get the whole curve of $\beta(t)$ (see Figure 3.2).

Clearly, the goodness of the proposed method relies on the efficiency of the moment matching procedure. In particular, on one hand, when α is very high the above method performs poorly. On the other hand, a large mean reversion is of great help and the method produces very accurate results. In their paper Hull and White (2012) use, for numerical experiments, values of α not larger than 0.0423, for which the proposed method performs extremely well.

3.5 CVA estimation in presence of Wrong Way Risk

In this section we illustrate how to calculate the CVA of an interest rate derivative allowing for dependence between interest rate and default intensity. Following Ghamami

[5]for example using `fsolve` function in Matlab®(integrals are solved numerically using the Gauss-Legendre algorithm).

and Goldberg (2014) we calculate CVA in presence of WWR as follows:

$$CVA_{WWR} = \int_0^T \mathrm{E}_0 \left[D(t)V(r(t))\lambda(t)e^{-\int_0^t \lambda(s)ds} \right] dt, \tag{3.6}$$

where $D(t) = e^{-\int_0^t r(s)ds}$ is the discount factor ($r(t)$ is as in formula 3.1), $V(r(t))$ denotes the credit exposure (i.e. $V(r(t)) = \max(0, \Pi(r(t)))$, where $\Pi(r(t))$ is the exposure of a generic interest rate derivative whose underlying is $r(t)$) and $\lambda(t)$ is as in (3.2). Denoting $\phi(t) := r(0)e^{-\gamma t} + \int_0^t e^{-\gamma(t-u)}\vartheta(u)du$, so that $r(t) = \phi(t) + \sigma Z(t)$ and substituting $r(t)$ and $\lambda(t)$ in formula (3.6) we obtain:

$$\begin{aligned} CVA_{WWR} &= \int_0^T \mathrm{E}_0 \left[e^{-\int_0^t r(s)ds} V(r(t)) e^{\alpha Z(t)+\beta(t)} e^{-\int_0^t e^{\alpha Z(s)+\beta(s)}ds} \right] dt \\ &= \int_0^T \mathrm{E}_0 \left[e^{-\int_0^t \phi(s)ds - \int_0^t \sigma Z(s)ds} V(r(t)) e^{\alpha Z(t)+\beta(t)} e^{-\int_0^t e^{\alpha Z(s)+\beta(s)}ds} \right] dt. \end{aligned}$$

Taking all the deterministic components outside the expectation one gets:

$$CVA_{WWR} = \int_0^T e^{-\int_0^t \phi(s)ds+\beta(t)} \mathrm{E}_0 \left[e^{-\int_0^t \sigma Z(s)ds} V(r(t)) e^{\alpha Z(t)} e^{-\int_0^t e^{\alpha Z(s)+\beta(s)}ds} \right] dt. \tag{3.7}$$

Now we restrict our attention to the expected value in the last equation. Let's start noting that:

$$\begin{aligned} \alpha Z(t) - \int_0^t \sigma Z(s)ds &= \alpha \int_0^t e^{-\gamma(t-u)}dW(u) - \sigma \int_0^t \left(\int_0^s e^{-\gamma(s-u)}dW(u) \right) ds \\ &= \alpha \int_0^t e^{-\gamma(t-u)}dW(u) - \sigma \int_0^t \left(\int_u^t e^{-\gamma(s-u)}ds \right) dW(u) \\ &= \alpha \int_0^t e^{-\gamma(t-u)}dW(u) - \int_0^t \frac{\sigma}{\gamma} \left(1 - e^{-\gamma(t-u)}\right) dW(u) \\ &= \int_0^t H(t,u)dW(u) \sim N\left(0, \int_0^t H^2(t,u)du\right) \end{aligned}$$

where $H(t,u) = \alpha e^{-\gamma(t-u)} - \frac{\sigma}{\gamma}(1 - e^{-\gamma(t-u)})$ and

$$\int_0^t H^2(t,u)du = \frac{2\sigma e^{-\gamma t}(\alpha\gamma+\sigma) - e^{-2\gamma t}(\alpha\gamma+\sigma)^2 - 4\sigma(\alpha\gamma+\sigma) + (\alpha\gamma+\sigma)^2 + 2\gamma\sigma^2 t}{4\gamma^3},$$

where the variance of the Gaussian distribution has been computed resorting to the isometry property of the Brownian motion. Consider now the following Radon-Nykodim derivative:

$$\mathcal{L}(t) = \frac{e^{\int_0^t H(t,u)dW(u)}}{\mathrm{E}_0[e^{\int_0^t H(t,u)dW(u)}]} = \frac{e^{\int_0^t H(t,u)dW(u)}}{e^{\frac{1}{2}\int_0^t H^2(t,u)du}} = e^{\int_0^t H(t,u)dW(u) - \frac{1}{2}\int_0^t H^2(t,u)du},$$

We can perform the following change of measure:

$$\begin{aligned}\mathrm{E}_0\left[e^{\alpha Z(t)-\int_0^t \sigma Z(s)ds}V(r(t))e^{-\int_0^t \lambda(s)ds}\right]dt &= \mathrm{E}_0[e^{\alpha Z(t)-\int_0^t \sigma Z(s)ds}]\mathrm{E}_0[\mathcal{L}(t)V(r(t))e^{-\int_0^t \lambda(s)ds}] \\ &= \mathrm{E}_0[e^{\alpha Z(t)-\int_0^t \sigma Z(s)ds}]\tilde{\mathrm{E}}_0[V(r(t))e^{-\int_0^t \lambda(s)ds}],\end{aligned}$$

and $\mathrm{E}_0[e^{\alpha Z(t)-\int_0^t \sigma Z(s)ds}] = e^{\frac{1}{2}\int_0^t H^2(t,u)du}$. Applying Girsanov's theorem we find the dynamics of the Brownian motion under the new measure. We have

$$\tilde{W}(t) = W(t) - \int_0^t H(t,u)du = W(t) - \left(\frac{\alpha\gamma + \sigma - e^{-\gamma t}(\alpha\gamma+\sigma) - \gamma\sigma t}{\gamma^2}\right),$$

and using Itô's lemma we get the dynamics of $\tilde{W}(t)$:

$$d\tilde{W}(t) = dW(t) + k(t)dt,$$

where

$$k(t) = \alpha e^{-\gamma t} - \frac{\sigma}{\gamma}\left(1 - e^{-\gamma t}\right).$$

So, we can rewrite the dynamics of $Z(t)$ under the new measure as follows:

$$\begin{aligned}dZ(t) &= (-\gamma Z(t))dt + dW(t) \\ &= (-\gamma Z(t))dt + d\tilde{W}(t) - k(t)dt \\ &= (-\gamma Z(t) - k(t))dt + d\tilde{W}(t).\end{aligned}$$

The calculation of the CVA allowing for the wrong-way risk is now related to the computation of the following integral

$$CVA_{WWR} = \int_0^T e^{-\int_0^t \phi(s)ds+\beta(t)}e^{-\frac{1}{2}\int_0^t H^2(t,u)du}\tilde{\mathrm{E}}_0\left[V(r(t))e^{-\int_0^t e^{\alpha Z(s)+\beta(s)}ds}\right]dt. \tag{3.8}$$

We now discuss how to compute the inner expectation. We set $r(t) = \phi(t) + x(t)$ where $x(t) = \sigma Z(t)$ and

$$dx(t) = (-\gamma x(t) - \sigma k(t))dt + \sigma d\tilde{W}(t).$$

The Feynman-Kac representation theorem ensures equivalence between

$$u(x,t) = \tilde{\mathrm{E}}_0[V(\phi(t) + x(t))e^{-\int_0^t \exp\left(\frac{\alpha}{\sigma}x(s)+\beta(s)\right)ds}]$$

and the solution of the following PDE:

$$\begin{cases}\frac{\partial u}{\partial t}(x,t) + (-\gamma x(t) - \sigma k(t))\frac{\partial u}{\partial x}(x,t) + \frac{1}{2}\sigma^2\frac{\partial^2 u^2}{\partial x^2}(x,t) - e^{\alpha\frac{x}{\sigma}+\beta(t)}u(x,t) = 0 \\ u(x,T) = V(\phi(T) + x)\end{cases}. \tag{3.9}$$

Table 3.1: Calibration of $\beta(t)$ through Monte Carlo simulation (MC) and moment matching (MM) for various parameter settings

	$\alpha = 0.05$, $\gamma = 0.1$		$\alpha = 0.05$, $\gamma = 0.3$		$\alpha = 0.15$, $\gamma = 0.1$		$\alpha = 0.15$, $\gamma = 0.3$	
t	MC	MM	MC	MM	MC	MM	MC	MM
1	-3.4003	-3.4013	-3.4001	-3.4012	-3.4050	-3.4059	-3.4039	-3.4053
2	-2.9870	-2.9880	-2.9865	-2.9876	-2.9991	-3.0000	-2.9954	-2.9967
3	-2.6110	-2.6154	-2.6103	-2.6147	-2.6279	-2.6322	-2.6205	-2.6259
4	-2.3382	-2.3376	-2.3371	-2.3366	-2.3572	-2.3564	-2.3475	-2.3478
5	-1.9446	-1.9550	-1.9435	-1.9540	-1.9623	-1.9724	-1.9527	-1.9638
CPU	51.4286	0.0590	51.0063	0.0557	51.5588	0.0511	51.4162	0.0626

Legend: parameters of Monte Carlo simulation and default probabilities are as in Figure 3.2, numerical integration is implemented using 30 nodes.

Table 3.2: Credit exposure for various derivative instruments.

Instrument	$V(r(t))$
Bond option	$(P(t,T) - K)^+$
Caplet	$(P(t,T_{i-1}) - P(t,T_i)(1 + K\tau_i))^+$
Swaption	$(\sum_{i=1}^{n}(P(t,T_{i-1}) - P(t,T_i)(1 + K\tau_i)))^+$

Legend: $P(t,T)$ denotes the price at time t of a bond with maturity T in the 1 factor Hull and White model, $\tau_i = T_i - T_{i-1}$ denotes the year fraction and K the strike.

We solve this PDE numerically for $0 \leq t \leq T$ using the `pdepe` solver in Matlab®. The time steps of the numerical solution of the PDE are dictated by the nodes of the Gauss-Legendre quadrature adopted to compute the integral in (3.8).

Finally, we note that the case of independent CVA can be obtained by posing $\alpha = 0$, the result will be that the default intensity becomes deterministic and formula (3.7) drastically simplifies.

3.6 Numerical results

In this section we present the numerical performance of the procedure proposed in Section 3.4 and the Wrong Way CVA calculation derived in Section 3.5.

We start by illustrating the results of the calibration of $\beta(t)$ proposed in Section 3.4[6]. These are reported in Table 3.1 where we compare the calibration via moment matching and via Monte Carlo. Numerical results show that moment matching is extremely accurate (even for large maturities) and much faster than Monte Carlo (which is implemented using 10^5 simulations). Moreover we note that $\beta(t)$ is only slightly sensitive to the choice of the model parameters α and γ.

[6]We are assuming that $\beta(t)$ is as in (3.3) with $T = 5$.

Figure 3.3: Bond yield in % and estimated $\phi(t)$

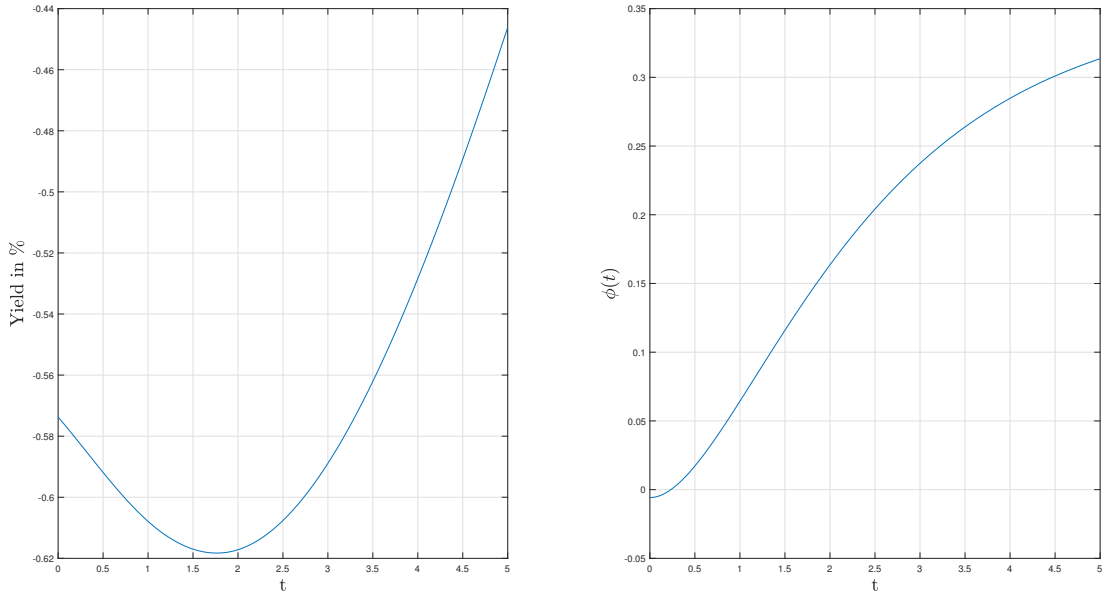

Legend: model parameters: $\sigma = 0.25$ and $\gamma = 0.3$.

Therefore, that bond pricing function of the 1-factor Hull-White model is required at various stages of the PDE solution. Closed form solution is available for this problem but note that, in our case, we need to evaluate $P(t,T)$ (for various $t \in [0,T]$) given the information at time 0, see for example equation (3.7):

$$P(t,T) = \mathrm{E}_t\left[e^{-\int_t^T r(s)ds}\right] = \mathrm{E}_t\left[e^{-\int_t^T \phi(s)ds - \int_t^T \sigma Z(s)ds}\right] = e^{-\int_t^T \phi(s)ds} e^{-B(t,T)x(t)+A(t,T)},$$

where $A(t,T) = -\frac{\sigma^2}{2\gamma^2}\left(B(t,T) - T + t\right) - \frac{\sigma^2}{4\gamma}B(t,T)^2$ and $B(t,T) = \frac{1}{\gamma}\left(1 - e^{-\gamma(T-t)}\right)$.

We calibrate $\phi(t)$ on market data following the procedure described in Brigo and Mercurio (2006, Chapter 1). As market data we use the yield curve at 7/05/2019 of the Euro area obtained using Government bond, nominal, all issuers whose rating is triple A (`https://www.ecb.europa.eu/stats/financial_markets_and_interest_rates/euro_area_yield_curves/html/index.en.html`), see Figure 3.3. Then $\int_t^T \phi(s)ds$ is computed numerically via the trapezoidal rule.

Finally, we compute Wrong Way CVA solving numerically equation (3.7). We start by defining the integrand in (3.7) as:

$$\Lambda(t) := e^{-\int_0^t \phi(s)ds + \beta(t)} \mathrm{E}_0\left[e^{-\int_0^t \sigma Z(s)ds} V(r(t)) e^{-\int_0^t e^{\alpha Z(s)+\beta(s)}ds}\right]$$

and plot $\Lambda(t)$ for different levels of α, see Figure 3.4.

In order to compute the integral in (3.8) we use the Gauss-Legendre quadrature

Table 3.3: Wrong Way CVA for various instruments and parameter settings

	MC	95% C.I.	PDE	Abs. diff.
		$\sigma = 0.05$, $\gamma = 0.1$, $\alpha = 0.05$		
Bond option	$7.7968 \cdot 10^{-3}$	$(7.7703, 7.8232) \cdot 10^{-3}$	$7.7482 \cdot 10^{-3}$	4.86e-05
Caplet	$1.0319 \cdot 10^{-3}$	$(1.0274, 1.0364) \cdot 10^{-3}$	$1.0102 \cdot 10^{-3}$	2.17e-05
Swaption	$5.6936 \cdot 10^{-3}$	$(5.6771, 5.7101) \cdot 10^{-3}$	$5.7075 \cdot 10^{-3}$	1.39e-05
		$\sigma = 0.25$, $\gamma = 0.3$, $\alpha = 0.05$		
Bond option	$12.7730 \cdot 10^{-3}$	$(12.6793, 12.8668) \cdot 10^{-3}$	$12.7060 \cdot 10^{-3}$	6.7e-05
Caplet	$14.3789 \cdot 10^{-3}$	$(14.3643, 14.39359) \cdot 10^{-3}$	$14.2596 \cdot 10^{-3}$	0.0001193
Swaption	$50.2793 \cdot 10^{-3}$	$(50.2406, 50.3180) \cdot 10^{-3}$	$50.3261 \cdot 10^{-3}$	4.68e-05
		$\sigma = 0.05$, $\gamma = 0.1$, $\alpha = 0.15$		
Bond option	$6.3211 \cdot 10^{-3}$	$(6.3008, 6.3414) \cdot 10^{-3}$	$6.2859 \cdot 10^{-3}$	3.52e-05
Caplet	$1.2916 \cdot 10^{-3}$	$(1.2857, 1.2975) \cdot 10^{-3}$	$1.2768 \cdot 10^{-3}$	1.48e-05
Swaption	$6.7030 \cdot 10^{-3}$	$(6.6825, 6.7234) \cdot 10^{-3}$	$6.7306 \cdot 10^{-3}$	2.76e-05
		$\sigma = 0.25$, $\gamma = 0.3$, $\alpha = 0.15$		
Bond option	$10.1650 \cdot 10^{-3}$	$(10.0941, 10.2359) \cdot 10^{-3}$	$10.0617 \cdot 10^{-3}$	0.0001033
Caplet	$15.1366 \cdot 10^{-3}$	$(15.1207, 15.1526) \cdot 10^{-3}$	$15.0530 \cdot 10^{-3}$	8.36e-05
Swaption	$52.8810 \cdot 10^{-3}$	$(52.8375, 52.9245) \cdot 10^{-3}$	$52.9969 \cdot 10^{-3}$	0.0001159

Legend: All the instruments have maturity $T = 5$. We consider bond option with strike $K = 1$, caplet with $K = 0.1$ and payment time $T_i = 4$ and a swaption with payment times $\{1, 2, 3, 4, 5\}$ and $K = 0.025$. Parameters of Monte Carlo simulation and default probabilities are as in Figure 3.2. We use 10 nodes to compute the integral in formula (3.6), for the solution of the PDE we use the following time discretization: 10001 equispaced points in $[0, T]$, space discretization: 2001 equispaced points in $[-2, 2]$. "Abs. diff." indicates the difference in absolute value between the Wrong Way CVA computed through Monte Carlo simulation (MC) and through PDE.

method. In Table 3.3 we report the results of the calculation of Wrong Way CVA through Monte Carlo and PDE approach for different parameter settings. Whatever the calibration procedure adopted in the calculation of $\beta(t)$, we smooth the piece-wise constant function via a spline interpolation at the Gauss-Legendre nodes dictated by the calculation of the integral.

Numerical results show that the PDE approach allows substantial improvements with respect to Monte Carlo simulation. In particular, the computational cost is drastically reduced and accuracy is guaranteed until the fourth significant digit. Finally, we compute the CVA for the caplet case varying the level of α. Results are reported in Table 3.4 and show the same behaviour as the results in Hull and White (2012, Tables 1-4).

3.7 Conclusions

In this chapter we have proposed an efficient method, combining moment matching and solution of a PDE, to compute the Wrong Way CVA for different interest rates derivatives. In this way, we avoid the time consuming Monte Carlo simulation proposed in Hull and

Figure 3.4: $\Lambda(t)$ for different levels of α

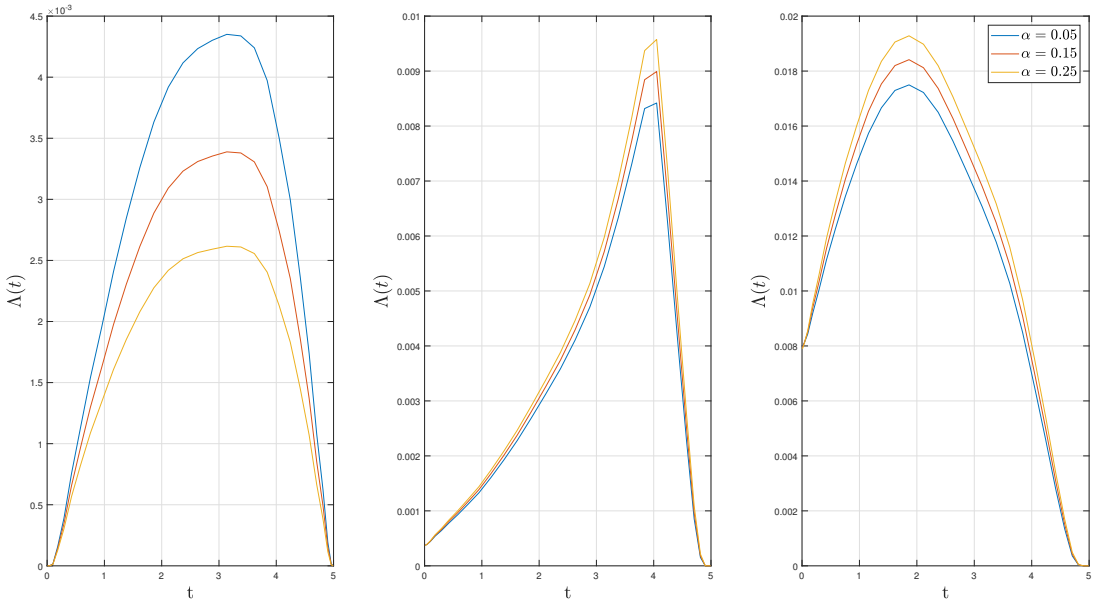

Legend: Bond option (left subplot), caplet (central subplot) and swaption (right subplot), parameters: $\sigma = 0.25$, $\gamma = 0.3$.

Table 3.4: Wrong Way CVA in the case of Caplet for different values of α

α	-0.05	-0.03	-0.01	-0.001	0.001	0.01	0.03	0.05
$CVA_{WWR} \cdot 10^3$	13.4484	13.6134	13.7776	13.8512	13.8676	13.9410	14.0367	14.2596

Legend: Other parameter: $\sigma = 0.25$, $\gamma = 0.3$. Further notes: see Table 3.3.

White (2012). Our approach requires firstly the implementation of a recursive procedure based on moment matching for the calibration of the deterministic function of time $\beta(t)$ to the survival probability term structure extracted from CDS quotes. Then, the Wrong Way CVA calculation is performed through a PDE approach exploiting a change of measure. Our method turns out to be much faster and accurate than Monte Carlo simulation (as shown in Table 3.1). This fact implies a significant advantage when default intensity of many different counterparties must be estimated. The calculation of the Wrong Way CVA can be done via Monte Carlo simulation or combining moment matching and the numerical integration of a PDE. Our numerical results show that the approximation is accurate at least to four significant digits (see Table 3.3) and allows a substantial reduction in the computational cost respect to the procedure proposed in Hull and White (2012).

Chapter 4

Conditional Monte Carlo methods under stochastic volatility models

The simulation of popular volatility models, such as Heston, stochastic alpha-beta-rho and Ornstein–Uhlenbeck type, represents a nontrivial longstanding problem with various solution attempts made in the literature, preponderated by stochastic differential equation discretization techniques with inevitable inherent biases. Alternatively, we have seen exact methods which are able to restore the convergence rate of unbiased simulation, while nevertheless being perceptibly computationally demanding. We propose a new solution for generating sample trajectories that turns out to be conceptually simple with a straightforward implementation based on moment-based probability distribution construction of the key random quantity, that is, the integrated stochastic variance conditional on the variance level at the endpoints of the given time period. Crucially, the method retains the exactness of some of its predecessors while improving the speed and flexibility across payoff structures, including options that are path-independent or dependent on the maximum (or minimum) of the underlying asset price process, such as barrier, lookback and hindsight options. Numerical experiments highlight the accuracy-runtime benefits of our proposed methodologies.

4.1 Introduction

In this chapter, we propose efficient Monte Carlo methods for simulation in the Heston, stochastic alpha-beta-rho (SABR) and Ornstein–Uhlenbeck stochastic volatility (OU-SV) models. The application is extendable to models that involve jumps. Stochastic volatility is a salient and well-documented feature of financial returns that constitutes a primary factor driving the option prices (e.g., see Bakshi *et al.*, 1997). To this end, various volatility models have been proposed in literature, including, among others, Hull and White (1990), Scott (1987), Stein and Stein (1991), Heston (1993), Schöbel and

Zhu (1999), Barndorff-Nielsen and Shephard (2001) and Hagan *et al.* (2002), which are generally capable of explaining in a self-consistent way the so-called volatility smile effect while assuming realistic dynamics for the underlying (see Gatheral, 2006).

They are usually specified by pairs of stochastic differential equations (SDEs), for the price of an asset and its variance (or volatility). Typically, these SDEs do not yield simple exact solutions rendering them notoriously difficult to simulate accurately. Because of the increased problem dimensionality, Monte Carlo simulation remains the method of choice for computing expected values of nonlinear functions of the driving processes on several occasions, including cases of path-dependence and advanced stochastic volatility models where Fourier or Laplace-transform solutions for the derivative's price are inexistent or slow to compute. Over the years, several discretization methods for SDEs have been proposed in literature (refer, for example, Chen *et al.*, 2012 for a review), inevitably yielding a bias, though, that can be hard to quantify accurately besides rendering the procedure particularly tedious. To circumvent this, a few attempts have been made to simulate exactly, or, perhaps, more precisely phrased, recover the $O(s^{-1/2})$ convergence rate of an unbiased Monte Carlo estimator for simulating derivative prices with a total computational budget s, such as Broadie and Kaya (2006), Cai *et al.* (2017) and Li and Wu (2019) for, respectively, the Heston model (and variants with jumps), SABR and OU-SV. These approaches have proved to be able to produce accurate results. At the core, these rely on simulation of the integral of the variance over a time interval conditional on the variance level at its endpoints, which appears in the stochastic price dynamics. Although accurate, a serious demerit of such an approach, as pointed out in the seminal work of Broadie and Kaya (2006), has been the implicit need to recover the unknown distribution function of the conditional integrated variance using obvious techniques, such as inversion of the associated Laplace transform, which becomes a heavy load and almost impracticable when generating entire sample trajectories. Additional complexities might arise due to bias arising in model-specific cases and which need to be treated with care, such as in SABR, where the conditional asset price distribution is not exactly known (see Islah, 2009 and Cai *et al.*, 2017) or a lognormal-based approximation of the integrated variance is used Chen *et al.*, 2012, or in Heston where a central discretization of the time integral might be implemented (Andersen, 2008) or alternative law representations of it might be considered (Glasserman and Kim, 2011) for potential speed-up.

The various runtime-precision concerns, in addition to the sophistication of implementation on several occasions, still hinder the way between a method and its end user, making space for further research. In this chapter, we aim to unify simulation in a stochastic volatility framework in a simple and practicable manner and unblock the road to universality for different models such as Heston, SABR and OU-SV with speed-up and accuracy advances. More specifically, first, we employ an adaptively modified moment generating function from Choudhury and Lucantoni (1996) to compute fast the first

four moments of the conditional integrated variance and, thereby, an accurate Pearson system to approximate its probability distribution over the entire range. This allows us to easily generate random samples from it, as well as fast bypassing computationally intensive Laplace transform inversion. In addition, our contribution extends to further refinements of the proposed method applicable to path-independent and special cases of path-dependent contracts, such as barrier and lookback, and model specifications as we explain later on. In particular, we obtain conditionally simplified pricing formulae for these options which are evaluated with the aid of Monte Carlo to result in improved price estimates.

The remainder of the chapter is structured as follows. In Section 4.2, we introduce the models under consideration in this chapter. Section 4.3 presents a succinct outline of the exact simulation of the volatility models in question and the associated conditional distribution arguments. Section 4.4 represents the core of this chapter where we portray our random number generation mechanism using an efficient moment-based probability distribution build-up. In Section 4.5, we move forward on conditional Monte Carlo methods for path-independent contracts or payoffs dependent on the maximum (or minimum) of the underlying asset price process during the life of the derivative. Section 4.6 presents our numerical study. In Section 4.7 we present some ideas for further research, concerning the pricing of alternative path dependent derivative instruments and extensions to more sophisticated stochastic volatility models. Section 4.8 concludes the chapter. Required explicit Laplace transform expressions are deferred to the appendix.

4.2 Stochastic volatility models

Consider a filtered probability space $(\Omega, \mathcal{F}, Q, \{\mathcal{F}_t\})$ on which two independent standard Brownian motions W_1 and W_2 are defined. We consider the following models which are given under the risk neutral measure Q by the solutions to the following SDEs:

- **Heston:**

$$dS(t) = rS(t)dt + \sigma(t)S(t)(\rho dW_2(t) + \sqrt{1-\rho^2}dW_1(t)), \tag{4.1}$$
$$d\sigma^2(t) = k(\theta - \sigma^2(t))dt + v\sigma(t)dW_2(t), \tag{4.2}$$

  where $S(t)$ in (4.1) gives the dynamics of the asset price at time t, r is the risk neutral drift given by the continuously compounded risk-free interest rate, and $\sigma(t)$ the volatility at time t represented by a square-root diffusion. In the defining dynamics (4.2) of $\sigma(t)$, θ is the long-run mean variance, k the speed of mean-reversion, v the parameter that controls the volatility of the variance process, and $\rho \in [-1, 1]$ the instantaneous correlation between the return and volatility (or variance) processes;

SABR:

$$dS(t) = \sigma(t)S(t)^{\beta}\left(\rho dW_2(t) + \sqrt{1-\rho^2}dW_1(t)\right), \tag{4.3}$$

$$d\sigma(t) = v\sigma(t)dW_2(t), \tag{4.4}$$

where $S(t)$ describes the dynamics of an asset's forward price at time t, constant $\beta \in [0,1]$, and volatility $\sigma(t)$ evolves according to a geometric Brownian motion;

OU-SV:

$$dS(t) = rS(t)dt + \sigma(t)S(t)\left(\rho dW_2(t) + \sqrt{1-\rho^2}dW_1(t)\right), \tag{4.5}$$

$$d\sigma(t) = k(\theta - \sigma(t))dt + vdW_2(t), \tag{4.6}$$

where the volatility process $\sigma(t)$ at time t (4.5) is now represented by a Gaussian OU model.

4.3 Unified simulation framework

For each of the models in the previous section, exact simulation schemes have been proposed to simulate the asset price at some future time t by conditioning on the values generated by the volatility (or variance) process and the asset price at time $u < t$.

Step 1 Simulate

$$\begin{cases} \sigma^2(t) = \frac{v^2(1-e^{-k(t-u)})}{4k}\chi'^2_d(\lambda), & \text{Heston} \\ \ln\sigma(t) \sim \mathcal{N}\left(\ln\sigma(u) - \frac{1}{2}v^2(t-u), v^2(t-u)\right), & \text{SABR} \\ \left(\sigma(t), \int_u^t \sigma(s)ds\right) \sim \mathcal{N}(\underline{\mu}, \Sigma), & \text{OU-SV} \end{cases}, \tag{4.7}$$

where for the Heston model $\chi'^2_d(\lambda)$ denotes the noncentral chi-squared distribution with $d := 4\theta k/v^2$ degrees of freedom and noncentrality parameter

$$\lambda := 4ke^{-k(t-u)}\sigma^2(u)/v^2(1-e^{-k(t-u)})$$

and for the OU-SV model the bivariate normal distribution has mean vector

$$\underline{\mu} := \begin{pmatrix} (\sigma(u)-\theta)e^{-k(t-u)} + \theta \\ \theta(t-u) + (\sigma(u)-\theta)\frac{1-e^{-k(t-u)}}{k} \end{pmatrix}$$

and covariance matrix

$$\Sigma := \begin{pmatrix} \frac{v^2}{2k}(1-e^{-2k(t-u)}) & \frac{v^2}{2k^2}(1-e^{-k(t-u)})^2 \\ \frac{v^2}{2k^2}(1-e^{-k(t-u)})^2 & -\frac{v^2}{2k^3}(1-e^{-k(t-u)})^2 + \frac{v^2}{k^2}(t-u-\frac{1-e^{-k(t-u)}}{k})^2 \end{pmatrix}$$

(for the latter, see Li and Wu, 2019).

Step 2 Simulate

$$\Psi(u,t) \overset{\mathcal{D}}{=} \begin{cases} \left(\int_u^t \sigma^2(s)ds \middle| \sigma(u), \sigma(t)\right), & \text{Heston} \\ \left(\left(\int_u^t \sigma^2(s)ds\right)^{-1} \middle| \sigma(u), \sigma(t)\right), & \text{SABR} \\ \left(\int_u^t \sigma^2(s)ds \middle| \sigma(u), \sigma(t), \int_u^t \sigma(s)ds\right), & \text{OU-SV} \end{cases} . \tag{4.8}$$

Hitherto in the literature, exact simulation of (4.8) relies on numerical inversion of the Laplace transform of the conditional integrated variance (refer to the appendix for the different models), which is nevertheless the hardest and most time-consuming step of the whole simulation scheme, and subsequent application of the inverse transform method for the simulation. In the following section, we present a new approach to this simulation problem that still hinges on the Laplace transform but circumvents its numerical inversion ensuring a balanced speed-accuracy. We postpone further discussion of this until then.

Step 3 Simulate

$$\left(S(t) \middle| \sigma(u), \sigma(t), \int_u^t \sigma^2(s)ds, S(u)\right)$$

in the

i) Heston model (Broadie and Kaya, 2006):

$$\begin{aligned} \ln S(t) \;\sim\; \mathcal{N}\Bigg(&\ln S(u) + r(t-u) - \frac{1}{2}\int_u^t \sigma^2(s)ds - \frac{\rho}{v}k\theta(t-u) \\ &+\frac{\rho}{v}\left(\sigma^2(t) - \sigma^2(u) + k\int_u^t \sigma^2(s)ds\right), (1-\rho^2)\int_u^t \sigma^2(s)ds\Bigg); \end{aligned} \tag{4.9}$$

ii) OU-SV model (Li and Wu, 2019):

$$\begin{aligned} \ln S(t) \;\sim\; \mathcal{N}\Bigg(&\ln S(u) + \left(r - \frac{\rho v}{2}\right)(t-u) + \frac{\rho}{2v}(\sigma^2(t) - \sigma^2(u)) + -\frac{\rho k\theta}{v}\int_u^t \sigma(s)ds \\ &+\left(\frac{\rho k}{v} - \frac{1}{2}\right)\int_u^t \sigma^2(s)ds, (1-\rho^2)\int_u^t \sigma^2(s)ds\Bigg); \end{aligned} \tag{4.10}$$

iii) SABR model with $\beta = 1$:

$$\ln S(t) \sim \mathcal{N}\left(\ln S(u) - \frac{1}{2}\int_u^t \sigma^2(s)ds + \frac{\rho}{v}(\sigma(t) - \sigma(u)), (1-\rho^2)\int_u^t \sigma^2(s)ds\right); \tag{4.11}$$

iv) SABR model with $\beta \in [0,1)$, $\rho = 0$ and $\{S(t)\}$ with an absorbing boundary at 0 (Islah, 2009, Cai *et al.*, 2017)

$$\begin{aligned} P\left(S(t)=0 \,\middle|\, \sigma(u), \sigma(t), \int_u^t \sigma^2(s)ds, S(u)\right) &= 1 - Q_{\chi^2}\left(A_0; \frac{1}{1-\beta}\right), \\ P\left(S(t)\le y \,\middle|\, \sigma(u), \sigma(t), \int_u^t \sigma^2(s)ds, S(u)\right) &= 1 - Q_{\chi'^2}\left(A_0; \frac{1}{1-\beta}, C_0(y)\right) \end{aligned} \tag{4.12}$$

for any $y > 0$, where

$$A_0 := \left(\int_u^t \sigma^2(s)ds\right)^{-1} \left(\frac{S(u)^{1-\beta}}{1-\beta}\right)^2, \quad C_0(y) := \left(\int_u^t \sigma^2(s)ds\right)^{-1} \left(\frac{y^{1-\beta}}{1-\beta}\right)^2,$$

$Q_{\chi^2}(\cdot; d)$ and $Q_{\chi'^2}(\cdot; d, \lambda)$ are, respectively, the chi-squared and noncentral chi-squared cumulative distribution functions;

v) SABR model with $\beta \in [0,1)$, $\rho \neq 0$ and $\{S(t)\}$ with an absorbing boundary at 0:

$$\begin{aligned} P\left(S(t)=0 \,\middle|\, \sigma(u), \sigma(t), \int_u^t \sigma^2(s)ds, S(u)\right) &\approx 1 - Q_{\chi^2}\left(A; 1 + \frac{\beta}{(1-\beta)(1-\rho^2)}\right), \\ P\left(S(t)\le y \,\middle|\, \sigma(u), \sigma(t), \int_u^t \sigma^2(s)ds, S(u)\right) &\approx 1 - Q_{\chi'^2}\left(A; 1 + \frac{\beta}{(1-\beta)(1-\rho^2)}, C(y)\right) \end{aligned} \tag{4.13}$$

for $y > 0$, where

$$A := \frac{\left(\frac{S(u)^{1-\beta}}{1-\beta} + \frac{\rho}{v}(\sigma(t) - \sigma(u))\right)^2}{(1-\rho^2)\int_u^t \sigma^2(s)ds}, \quad C(y) := \frac{\left(\frac{y^{1-\beta}}{1-\beta}\right)^2}{(1-\rho^2)\int_u^t \sigma^2(s)ds}.$$

4.4 Moment based random numbers generator

We start by showing how to compute efficiently the moments of $\Psi(u,t)$. Then, we consider the problem of generating random numbers given moments and, finally, we show how to include this moment based random number generator into a scheme for the simulation of stochastic volatility models.

4.4.1 Computation of moments

For the models considered in this chapter, the Laplace transform $\mathcal{L}(a) = \mathrm{E}(e^{-a\Psi(u,t)})$ exists in some closed form as shown in the appendix. Traditionally, the moments of $\Psi(u,t)$ are obtained from

$$\mathrm{E}\left[\Psi(u,t)^n\right] = (-1)^n \left.\frac{\partial^n}{\partial a^n}\mathcal{L}(a)\right|_{a=0}. \tag{4.14}$$

However, computing the moments from (4.14) might not be practicable as the Laplace transform might be given by special functions, which is, in fact, the case with the stochastic volatility models in this chapter. For example, consider the relevant Laplace transform (B.1) in the case of the Heston model. Evaluating the first three moments of $\Psi(u,t)$ from (4.14), using, e.g., the symbolic toolbox of Mathematica®, requires 97 evaluations of the modified Bessel function of the first kind, which is highly computationally intensive and endangers numerical errors.

In this chapter, we bypass this problem by numerical inversion of an adaptively modified moment generating function introduced by Choudhury and Lucantoni (1996). To this end, let μ_n be the n-th moment which is given by

$$\mu_n \approx \frac{n!}{2nlr_n^n\alpha_n^n}\left\{\mathcal{L}(\alpha_n r_n) + (-1)^n\mathcal{L}(-\alpha_n r_n) + 2\sum_{j=1}^{nl-1}\Re(\mathcal{L}(\alpha_n r_n e^{\pi ij/nl})e^{-\pi ij/l})\right\}, \quad (4.15)$$

where $i := \sqrt{-1}$ and $\Re(z)$ denotes the real part of z. We adopt the choice $r_n = 10^{-\gamma/(2nl)}$ to achieve accuracy of the order of $10^{-\gamma}$. Algorithm 1 summarizes the procedure for computing the first N moments as well as the parameter l and the adaptive α_n.

Algorithm 1 Numerical inversion of adaptively modified moment generating function

Input: N, γ, $\mathcal{L}(\cdot)$
Output: $\{\mu_n\}_{n=1}^N$

1: Set $l = \alpha_1 = 1$ and compute μ_1 from (4.15)
2: Compute $\alpha_2 = 1/\mu_1$ and μ_2
3: Set $l = 1 \vee 2$ and $\alpha_1 = \alpha_2 = 2\mu_1/\mu_2$ and compute new values for μ_1 and μ_2 (from 4.15)
4: Set $n = 3$
5: **while** $n \leq N$ **do**
6: $\quad l = 1 \vee 2$, compute $\alpha_n = (n-1)\mu_{n-2}/\mu_{n-1}$
7: $\quad$ Compute μ_n from (4.15)
8: $\quad n = n + 1$
9: **end**

The proposed method has several merits. First, for a known Laplace transform, we do not require recovery of the distribution function of the conditional integrated variance by transform inversion which has been standard in the literature since Broadie and Kaya (2006). Due to this, it is, second, fast: for the first three moments, the Laplace transform is evaluated 9 times, hence, for example, for (B.1), the modified Bessel function of the first kind is evaluated just 18 times which is a considerable reduction. Third, it is very accurate: using $\gamma = 11$ as per the suggestion of Choudhury and Lucantoni (1996), the error appears, consistently with them, only in the eleventh to thirteenth significant place. Finally, the Laplace transform can be evaluated at multiple points concurrently, which

is favourable for our applications requiring multiple moment computations for different random realizations of (4.7).

4.4.2 Random numbers given moments

The next step is to find an efficient way to draw random numbers from an unknown distribution given its moments sequence. As part of this research, we explore several ways of generating random numbers from the distribution of the conditional integrated variance $\Psi(u,t)$ given knowledge of its first four integer moments $\mu_1, \mu_2, \mu_3, \mu_4$. In particular, we have explored algorithms based on scale mixtures, series expansion and moment matching.

Algorithms based on scale mixtures are analyzed in Hörmann *et al.* (2004, pag. 325) and consist in generating random numbers from a mixture[1] of two Bernoulli random variables with the given first four integer moments. Secondly, we have explored a series expansion technique: given the moments is possible to implement a Cornish-Fisher expansion (see Abramowitz and Stegun, 1968, pg. 935) to approximate the inverse cumulative distribution function of the unknown distribution and, subsequently, draw random numbers using the inverse transform method (see, for example, Robert and Casella, 2010). Finally, as suggested in Devroye (1986), we consider moment matching. More specifically, we implement approximations based on the Johnson's and Pearson's system of distributions (see Section 1.2.1) and draw random numbers from the moment matched distribution belonging to the family. Among all these methods internal (unreported) numerical tests have shown superior performances of the Pearson's system. Indeed, though very fast, algorithms related to scale mixtures and series expansion have presented poor performances in terms of accuracy, with biases significantly larger than algorithms based on moment matching. Johnson's and Pearson's system of distributions have presented similar performances in terms of accuracy but the Pearson's system resulted to be much faster. This is mainly due to the fact that the procedure for family selection and parameter estimation given moments is faster for the Pearson's system than for the Johnson's one. Note indeed (see Section 1.2.1) that the set of rules for family selection in the Pearson's system is very simple, while for the Johnson's is more complicated, involving the Hill's algorithm. This algorithm must be ran for every random realization of (4.7) and may happen that, for certain parameter settings, it is very slow to converge (moreover, failure to convergence is also possible, see Simonato, 2011).

For these reasons, given the moments $\mu_1, \mu_2, \mu_3, \mu_4$ computed according to Algorithm 1, we implement moment matching through the Pearson's system of distributions and draw random numbers from the selected distribution of the family. Note that, for six out of seven distributions belonging to the system (these are summarized in Section 1.2.1),

[1] Several ways exist to create the mixture, we explore the usage of the uniform and normal distributions, see Hörmann *et al.* (2004, pag. 325) for more details.

random numbers generation is straightforward with routines readily available in most of the statistical softwares. Hence, from a computational point of view, the only remaining problem is to draw random numbers from the Type IV distribution of the Pearson's system. Amos and Daniel (1971) and Bouver and Bargmann (1974) provide extensive tables of quantiles, which can be used for random numbers generation through inverse transform sampling. We consider a different approach throughout this work, i.e. the one based on the exponential rejection method for log-concave densities developed in Devroye (1986, Section 7.2) which is adapted to the case of the Pearson Type IV distribution by Heinrich (2004).

The whole procedure for random numbers generation from Pearson's system of distributions given the first four integer moments is briefly summarized in Algorithm 2.

Algorithm 2 Moment matching: Pearson's family

Input: μ_1, μ_2, μ_3, μ_4

Output: random sample $\Psi(u,t)$

1: Compute skewness $= \frac{\mu_3 - 3\mu_1(\mu_2-\mu_1^2)-\mu^3}{(\mu_2-\mu_1^2)^{1.5}}$ and kurtosis $= \frac{\mu_4-4\mu_1\mu_3+6\mu^2\mu_2-3\mu_1^4}{(\mu_2-\mu_1^2)^2}$

2: Set $\beta_1 = \text{skewness}^2$, $\beta_2 = \text{kurtosis}$

3: Set c_0, a, c_1 and c_2 as in (1.7), (1.8) and (1.9)

4: Set $k = \frac{\beta_1(\beta_2+3)^2}{4(4\beta_2-3\beta_1)(2\beta_2-3\beta_1-6)}$

5: Select family type according to selection rules given at the end of Section 1.2.1

6: Draw random numbers Y from the selected distribution

7: Set $\Psi(u,t) = Y \cdot \sqrt{\mu_2 - \mu_1^2} + \mu$

8: **return** $\Psi(u,t)$

In principle, due to the efficiency of Algorithm 1, we could consider also higher order moments to generate random realizations from $\Psi(u,t)$. But, unfortunately, these are not computationally efficient as in the case of four. Indeed, algorithms based on scale mixtures are specifically designed to math four moments (hence not applicable for higher orders), Cornish-Fisher expansion may diverge when including many term (note indeed that Cornish Fisher approximation is the Legendre inversion of the Edgeworth expansion of a distribution, which typically diverges when including many moments, see, for example, Fusai and Tagliani, 2002). Moreover, despite some methods exist in order to make the Pearson's system to match more than four moments, this rely on numerical methods (see Rose and Smith, 2002, Chapter 5). Another possibility would be to resort to the Fleishman's family of distributions (see Devroye, 1986, pag. 694), but, also in this case, numerical methods are required to match more than four moments. We stress that addition of, for example, numerical solution of an integral in the simulation procedure would be an unacceptable cost since, as moments depend on the realization of (4.7), it

should be repeated for any simulation, causing, possibly, a procedure which is slower than exact simulation schemes with a benefit in terms of accuracy not commensurate with the extra labor involved. Finally, we will study in Section 4.6 how far are the higher order moments of 4-moments matched Pearson distribution to the true ones in the context of the Heston model, and will show that in practise the difference is very small also under challenging model parametrizations.

4.4.3 Stochastic volatility models simulation using moments

Typically, exact simulation schemes are too slow to be applied for the simulation of the whole price trajectory, implying that their most common application concerns pricing path independent derivative instruments for which the Laplace transform of $\Psi(u,t)$ is numerically inverted only once. As will be shown in the course of Section 4.6, the proposed method allows to reduce drastically the computing time, opening doors to the simulation of the stock price process on a set of discrete observation dates. We summarize the methodology in Algorithm 3.

Algorithm 3 Conditional moments-matched sampling scheme

Input: Parameters of the model specified in (4.1) and (4.2), (4.3) and (4.4) or (4.5) and (4.6), T (maturity), N (N^o of monitoring dates)
Output: $S(t)$ for $t = \{0, \Delta, 2\Delta, 3\Delta, ..., T\}$ (path of the underlying's price)

1: Set $\Delta = \frac{T}{N}$
2: **for** $t = 0 : \Delta : T - \Delta$ **do**
3: Given $\sigma(t)$ generate $\sigma(t+\Delta)$ or $\left(\sigma(t+\Delta), \int_t^{t+\Delta} \sigma(s)ds\right)$ using (4.7)
4: Define Laplace transform of $\Psi(t, t+\Delta)$ (see Eq. 4.8)
5: Compute moments of $\Psi(t, t+\Delta)$ using Algorithm 1
6: Sample from $\Psi(t, t+\Delta)$ given moments using Algorithm 2
7: Sample $S(t+\Delta)$ using (4.9), (4.10), (4.11), (4.12) or (4.13)
8: **end for**
9: **return** $S(t)$ for $t = \{0, \Delta, 2\Delta, 3\Delta, ..., T\}$.

This algorithm allows to obtain the stock price trajectory at some discrete dates with many possible applications in different areas of finance. Note that, if one is interested only in the distribution at the final date T of the stock price (as in the case, for example, of path independent derivative instruments pricing), is sufficient to pose $N = 1$. In this work, we apply Algorithm 3 to the problem of pricing derivative instruments and we will show in Section 4.6 that is fits very well this purpose. Despite that, we must also point out that the discounted stock price trajectory built according to Algorithm 3 does not constitute a true martingale due to the fact that the random realization from $\Psi(u,t)$ comes from an approximation (even if very accurate). For this reason, following Andersen

(2008), we also show that is possible to apply a martingale correction. From definition of martingale we need that:

$$\mathrm{E}[S(t)|S(u)] = e^{r(t-u)}S(u), \quad \forall u \leq t \tag{4.16}$$

using the law of iterated expectations we get:

$$\mathrm{E}[S(t)|S(u)] = \mathrm{E}\left[\mathrm{E}\left[S(t)\middle|\sigma(t), \sigma(u), \int_u^t \sigma^2(u)\right]\middle|S(u)\right] \tag{4.17}$$

where inner expectations are known from (4.9), (4.10), (4.11), (4.12) and (4.13). Our procedure follows now from Andersen (2008, Proposition 7); we consider, for illustrative purposes, the Heston model, solving inner expectation in (4.17) we get

$$\mathrm{E}[S(t)|S(u)] = S(u)e^{r(t-u)-\frac{\rho}{v}(k\theta(t-u))}\mathrm{E}\left[e^{\left(\frac{\rho k}{v}-\frac{1}{2}\right)\int_u^t \sigma^2(s)ds+\frac{\rho}{v}(\sigma^2(t)-\sigma^2(u))+\sqrt{(1-\rho^2)\int_u^t \sigma^2(s)ds}Z}\right] \tag{4.18}$$

where $Z \sim \mathcal{N}(0,1)$ (see also Broadie and Kaya, 2006, pag. 222). Defining $K^\star := -\frac{\rho}{v}(k\theta(t-u))$, in order to (4.16) hold true we need:

$$K^\star = \ln\left(-\mathrm{E}\left[e^{\left(\frac{\rho k}{v}-\frac{1}{2}\right)\int_u^t \sigma^2(s)ds+\frac{\rho}{v}(\sigma^2(t)-\sigma^2(u))+\sqrt{(1-\rho^2)\int_u^t \sigma^2(s)ds}Z}\right]\right), \tag{4.19}$$

where the key quantities involved in the expectation have been already simulated and, consequently, the expected value can be computed simply taking the average. Hence, substituting the quantity $-\frac{\rho}{v}(k\theta(t-u))$ with $K^\star$ computed as in (4.19) into (4.9) is possible to apply a martingale correction with the result that Algorithm 3 will produce a martingale process for the discounted stock price.

4.5 Advancing conditional Monte Carlo methods

In this section, we present conditional Monte Carlo methods to improve the efficiency of the simulation estimators for the prices of both path-independent, such as European plain vanilla, and path-dependent options with payoffs dependent on the maximum (or minimum) of the trajectory of an underlying asset's price, such as barrier and lookback options.

4.5.1 European path-independent options

Aiming to improve the efficiency of the simulation estimators under stochastic volatility models, Willard (1997) proposed a conditional Monte Carlo approach. Let $\Pi(\cdot)$ be a generic payoff function which depends on the price of the underlying asset at some ter-

minal time $t > u$, $S(u)$. Conditional on a path of the volatility process, the derivative's price at time u is given by

$$\mathrm{E}[e^{-r(t-u)}\Pi(S(t))] = \mathrm{E}[e^{-r(t-u)}\mathrm{E}[\Pi(S(t))|\mathcal{F}_t^\sigma]].$$

Thereby, the volatility can be treated as a deterministic quantity and the conditional derivative's price then boils down to that in the simplified model framework. For example, Willard (1997) presents the case of the conditional Heston model which is a lognormal model. Inspired by this, we remove the remaining block to a universal application that comprises different stochastic volatility models, such as SABR ($\beta = 1$) and OU-SV, but also path-dependent contracts.

Heston, SABR ($\beta = 1$) and OU-SV models

In what follows, let $\mathrm{BS}(S(u), \hat{\sigma})$ be the Black–Scholes price of a European plain vanilla call option written on some asset with initial price $S(u)$ and constant volatility $\hat{\sigma}$. The strike price is K, the maturity time T and the continuously compounded risk-free interest rate r. Then,

$$\begin{aligned} & \mathrm{E}\left[e^{-r(t-u)}(S(t)-K)^+ \middle| \mathcal{F}_t^\sigma\right] \\ = \; & e^{-r(t-u)}\left\{e^{m+\frac{1}{2}s^2}\Phi\left(\frac{m+s^2-\ln K}{s}\right) - K\Phi\left(\frac{m-\ln K}{s}\right)\right\} \\ = \; & \mathrm{BS}\left(S(u)\psi, \sqrt{\frac{1-\rho^2}{(t-u)}\int_u^t \sigma^2(s)ds}\right), \end{aligned} \tag{4.20}$$

where $x^+ := \max(x, 0)$, Φ is the standard normal cumulative distribution function, and

$$m := \mathrm{E}\left[\ln S(t) \middle| \mathcal{F}_t^\sigma\right] \text{ and } s^2 := \mathrm{Var}\left[\ln S(t) \middle| \mathcal{F}_t^\sigma\right] \tag{4.21}$$

are given by (4.9)–(4.11) for the Heston, OU-SV and SABR ($\beta = 1$) models. In addition,

$$\psi := \begin{cases} \exp\left\{-\frac{\rho^2}{2}\int_u^t \sigma^2(s)ds + \right. & \\ \left. +\frac{\rho}{v}\left(\sigma^2(t) - \sigma^2(u) - k\theta(t-u) + k\int_u^t \sigma^2(s)ds\right)\right\}, & \text{Heston} \\ \exp\left\{-\frac{\rho^2}{2}\int_u^t \sigma^2(s)ds + \frac{\rho}{v}(\sigma(t)-\sigma(u))\right\}, & \text{SABR } (\beta=1) \\ \exp\left\{-\frac{\rho v}{2}(t-u) + \frac{\rho}{2v}(\sigma^2(t)-\sigma^2(u)) - \frac{\rho}{v}k\theta\int_u^t \sigma(s)ds \right. & \\ \left. +\frac{\rho k}{v}\int_u^t \sigma^2(s)ds - \frac{\rho^2}{2}\int_u^t \sigma^2(s)ds\right\}, & \text{OU-SV} \end{cases}.$$

SABR model ($\beta \neq 1$)

In this case, we consider conditioning arguments and results from Cai *et al.* (2017, Theorem 5.1). Assuming that $\{S(t)\}$ have an absorbing boundary at 0 and $\beta \neq 1$, we get

$$\begin{aligned}
&\mathrm{E}\left[(S(t)-K)^+ \middle| \mathcal{F}_t^\sigma\right] \\
&\begin{cases}
= C_0(1)^{-\frac{1}{2(1-\beta)}} A_0^{(1+\gamma_0)/2}(1 - Q_{\chi'^2}(C_0(K); 3+\gamma_0, A_0)) - KQ_{\chi'^2}(A_0; 1+\gamma_0, C_0(K)) & \rho = 0 \\
\approx C(1)^{-\frac{1}{2(1-\beta)}} A^{(1+\gamma)/2}\Xi(-\frac{\rho^2\gamma}{2}, C(K), 3+\gamma, A) - KQ_{\chi'^2}(A; 1+\gamma, C(K)) & \rho \neq 0
\end{cases}
\end{aligned} \tag{4.22}$$

where

$$\begin{aligned}
\gamma_0 &:= \frac{\beta}{1-\beta} \\
\gamma &:= \frac{\beta}{(1-\beta)(1-\rho^2)}, \\
\Xi(p,k,\delta,\alpha) &:= 2^p \sum_{n=0}^{\infty} e^{-\frac{\alpha}{2}} \left(\frac{\alpha}{2}\right)^n \frac{\Gamma(\delta/2+p+n, k/2)}{n!\Gamma(\delta/2+n)}
\end{aligned}$$

and A_0, $C_0(\cdot)$ are as in (4.12), A and $C(\cdot)$ are as in (4.13).

4.5.2 Option payoffs dependent on maximum or minimum

Next, we present conditional Monte Carlo methods for path-dependent options with payoffs dependent on the maximum or minimum of the underlying asset price process during the life of the contract.

Heston and SABR ($\beta = 1$) models

Although the following exposition is expansible to lookback options, for the sake of exemplification, we focus here on the case of an up-and-out barrier call option with terminal payoff

$$\Pi(S(t)) := (S(t)-K)^+ \mathbf{1}_{\left\{\max_{u \leq t \leq T} S(t) \leq M\right\}},$$

where M is the fixed barrier level. Conditional on the information of the volatility path generated up until time T, the derivative's (forward) price is given by

$$\mathrm{E}[\Pi(S(t))|\mathcal{F}_t^\sigma].$$

This way, we gain access to the conditional joint distribution of the (log) price of the underlying asset and its maximum (or minimum) in the Heston model and we get from

De Gennaro Aquino and Bernard (forthcoming)

$$\mathrm{E}[\Pi(S(t))|\mathcal{F}_t^\sigma] = \int_0^{\ln\frac{M}{S(u)}} \int_{\ln\frac{K}{S(u)}}^{x} (S(u)e^x - K)\frac{2(2x-y)}{\sqrt{2\pi}s^3} e^{-\frac{(2x-y)^2-2my+m^2}{2s^2}} dydx, \quad (4.23)$$

where m and s^2 are as defined in (4.21). An analytical solution to (4.23) can be obtained with the aid of a symbolic toolbox such as Mathematica®.

Remark 4.1. *The pricing expression (4.23) refers to a continuously monitored barrier option. In addition, this can be indirectly extended to the case of a discretely monitored option using correction such as in Broadie* et al. *(1999).*

SABR ($\beta \neq 1, \rho = 0$) model

By conditioning with respect to the variance path, the SABR model with $\rho = 0$ reduces to a CEV diffusion, therefore conditional Monte Carlo methods for lookback and barrier options are still feasible. For illustration, we consider a lookback put option with terminal payoff

$$\Pi(S(t)) = \left(K - \min_{0\leq t\leq T} S(t)\right)^+.$$

Then, by conditional CEV diffusion, we recall from Davydov and Linetsky (2001, Lemma 1, Propositions 4–5) that

$$\mathrm{E}[\Pi(S(t))|\mathcal{F}_t^\sigma] = \begin{cases} \int_0^K F(y; S(u), t)dy, & S(u) \geq K \\ K - S(u) + \int_u^{S(u)} F(y; S(u), t)dy, & S(u) < K \end{cases}, \quad (4.24)$$

where $F(\cdot;\cdot,\cdot)$ satisfies

$$\int_0^\infty e^{-at} F(y; x, t)dt = \frac{1}{a}\sqrt{\frac{x}{y}} \frac{K_v\left(\frac{\sqrt{2a}x^{-(\beta-1)}}{\sigma(T)(\beta-1)}\right)}{K_v\left(\frac{\sqrt{2a}y^{-(\beta-1)}}{\sigma(T)(\beta-1)}\right)}, \quad 0 < y \leq x, \quad (4.25)$$

$K_v(\cdot)$ is the modified Bessel function of the second kind with v degrees of freedom and $a := 1/(2(\beta-1))$. Relevant results for barrier options are available in Davydov and Linetsky (2001, Proposition 3). It is worth highlighting that the pricing expression above depends only on $\sigma(T)$ (see Eq. 4.7) resulting in a perceptible speed-up of the simulation as the use of the Laplace transform (B.6) for the purpose of simulating the integrated variance is entirely sidestepped. Finally, $F(\cdot;\cdot,\cdot)$ is computed by numerical inversion of (4.25).

Table 4.1: Parameter settings for the Heston and OU-SV models

	H 1	H 2	H 3	H 4	H 5	H 6	OU-SV 1	OU-SV 2	OU-SV 3
$S(0)$	100	100	100	100	100	100	100	100	100
k	6.21	2	0.5	0.3	1	6.2	4	4	4
θ	0.019	0.09	0.04	0.04	0.09	0.02	0.02	0.02	0.02
v	0.61	1	1	0.9	1	0.6	0.1	0.1	0.1
$\sigma^2(0)$	0.010201	0.09	0.04	0.04	0.09	0.02	0.04	0.04	0.04
ρ	-0.7	-0.3	-0.9	-0.5	-0.3	-0.7	-0.7	-0.7	-0.7
r	3.19%	5%	3%	3%	3%	3%	9.531%	9.531%	9.531%
T	1	5	1	1	1	1	1	3	5

Legend: Notation as in formulae (4.1), (4.2), (4.5) and (4.6). H 1 and H 2 are taken from Broadie and Kaya (2006), H 3-6 are taken from Glasserman and Kim (2011), OU-SV 1-3 from Li and Wu (2019).

Table 4.2: Parameter settings for the SABR model

	SABR 1	SABR 2	SABR 3	SABR 4	SABR 5	SABR 6
$S(0)$	0.05	0.05	0.05	0.05	1.1	100
β	0.3	0.3	0.3	0.55	0.7	0.6
v	0.6	0.6	0.6	0.03	0.1	0.2
$\sigma(0)$	0.4	0.4	0.4	0.2	0.2	0.3
ρ	0.0	0.0	0.0	0.0	0.0	0.0
r	0	0	0	0	0	0
T	1.0	3.0	5.0	1.0	1.0	1.0

Legend: Notation as in formulae (4.3) and (4.4). Parameters in SABR 1, SABR 2 and SABR 3 are taken from Cai *et al.* (2017, Table 4), in SABR 4, SABR 5 and SABR 6 are taken from Cai *et al.* (2017, Table 1).

4.6 Numerical study

4.6.1 Parameter settings

We start by identifying the parameters used for numerical experiments. We select the same used by Broadie and Kaya (2006), Glasserman and Kim (2011), Cai *et al.* (2017) and Li and Wu (2019) in the original papers where exact simulation schemes are proposed. This choice allows for a direct comparison between our proposed method and the exact ones, whose measures of performances, i.e. root mean squared errors (RMSEs), are reported in original papers. Parameter settings for Heston and OU-SV models are reported in Table 4.1, for SABR in Table 4.2.

Note that for SABR model, we don't consider the case where $\rho \neq 0$, where exact simulation schemes does not exist (see Section 4.5 or, equivalently, Cai *et al.*, 2017, Proposition 2.1). Despite that, we stress that the proposed method can still be used in that case since approximations are required in simulating the forward price process and

Figure 4.1: Computing time (in seconds) for the first integer moments of conditional integrated variance in the Heston model

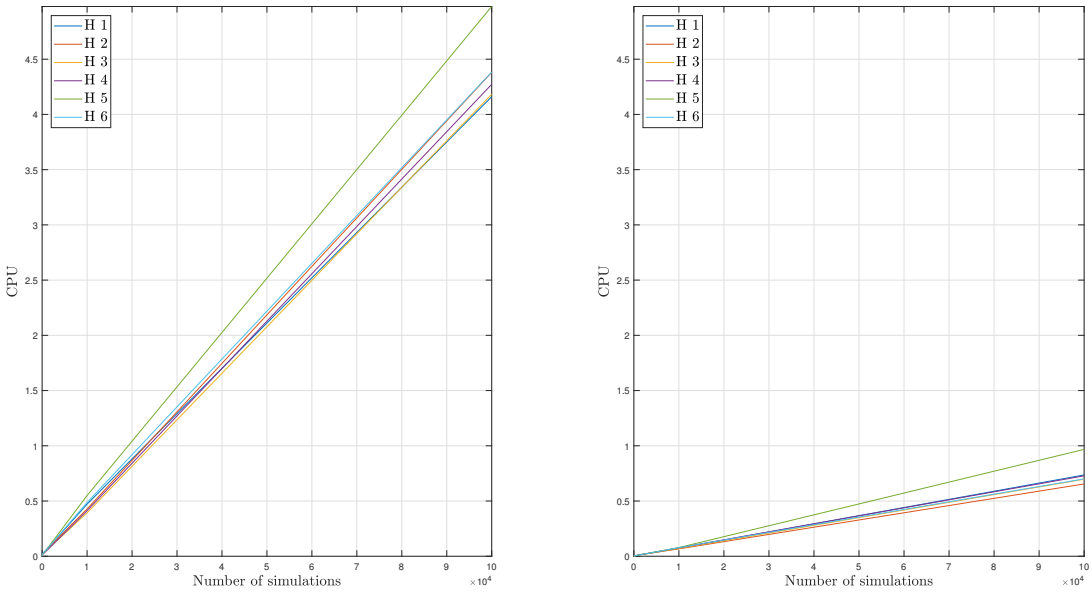

Legend: performances of analytical derivation are presented in left subplot, performances of Algorithm 1 in the right subplot.

not the conditional integrated variance.

4.6.2 Moments computation

We show here numerical performances of Algorithm 1 in computing moments of the conditional integrated variance. We consider here the Heston model since it is the most complicated from a computational point of view as Laplace transform in (B.1) depends on the modified Bessel function of the first kind. In Figure 4.1 we report the CPU time in seconds required for computing the first four integer moments of the conditional integrated variance for different numbers of simulations (i.e. for different numbers of realizations of the terminal variance), through analytical derivation (i.e. Eq. 4.14) of the Laplace transform in (B.1) and Algorithm 1. Results show that computing moments through Algorithm 1 allows for a significant computational saving with CPU time reduced by a factor of 6. This is due to the fact that the modified Bessel function of the first kind is evaluated a smaller amount of times.

Next, we investigate the following problem: we are matching the first four integer moments through the Pearson's system but what about higher order moments? How far are they from the true ones? In order to answer this question we implement the following numerical experiment: simulate 10^4 different random realizations for the terminal vari-

Figure 4.2: Actual vs supposed higher order moments

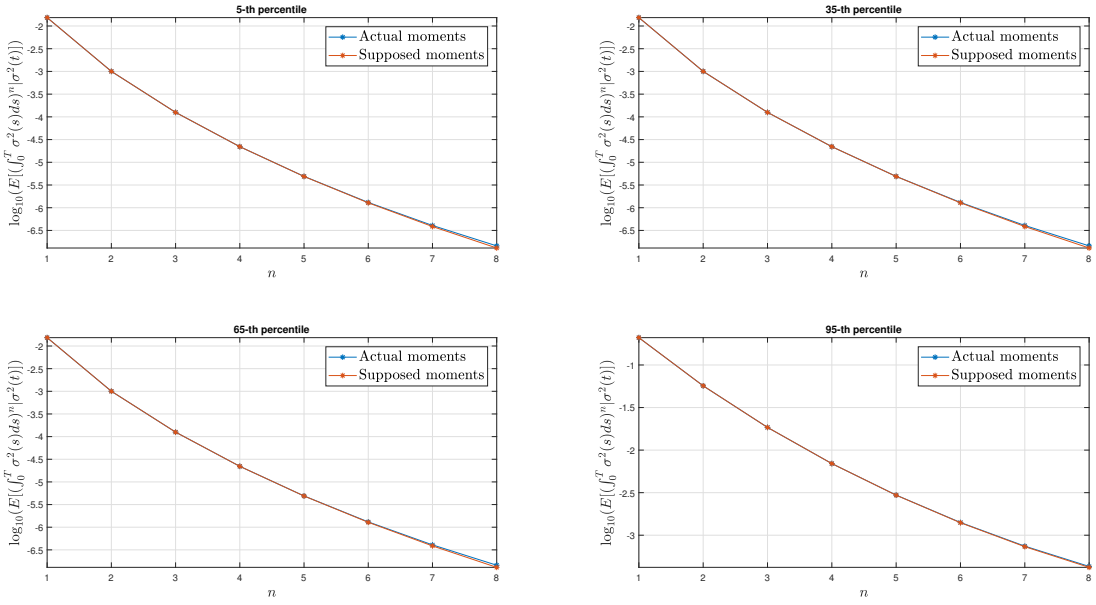

Legend: parameter setting H 4.

ance, consider only four of them (we choose to select them according to the percentile), compute the first eight integer moments through Algorithm 1 and compare with higher order moments of the moment matched distribution belonging to the Pearson's system. For numerical experiment, we consider the parameter setting H 4 since is the one where the proposed method presents the largest bias (this evidence will be presented, later, in Table 4.3). Results are reported in Figure 4.2 and show that the supposed higher order moments are extremely close to the true ones. Despite we are presenting here results related only to H 4, similar (or even better) results have been obtained also for the other parameter settings[2].

4.6.3 Pricing European options

We evaluate accuracy of the proposed method by a direct comparison with exact simulation methods proposed by Broadie and Kaya (2006), Cai *et al.* (2017) and Li and Wu (2019). For the Heston model we also consider as benchmark the Gamma Expansion method proposed by Glasserman and Kim (2011). Root mean squared error (RMSE) is used to compare performances: if $\hat{P}$ is the simulation estimator used for the derivative price and P is the true price, then the bias and the variance of the estimator are given

[2]We don't report here, for brevity, additional figures related to different parameter settings of percentiles.

Table 4.3: Estimated biases and standard errors of the proposed method.

	H 1	H 2	H 3	H 4	H 5	H 6
Option price	6.8061	34.9998	6.7304	7.0972	11.3743	7.0737
bias	-0.0002	-0.0058	-0.0007	0.0073	-0.0005	0.0023
standard error ($\times 10^3$)	0.3946	0.7959	0.2378	0.2117	0.2593	0.4565

Legend: option contract parameters: $S(0) = K = 100$, Number of simulations $= 10^8$, parameter settings as in Table 4.1.

by

$$\text{bias} = \mathrm{E}[\hat{P}] - P, \quad \text{variance} = \mathrm{E}[(\hat{P} - \mathrm{E}[\hat{P}])^2], \tag{4.26}$$

RMSE is then defined as

$$\text{RMSE} = (\text{bias}^2 + \text{variance})^{\frac{1}{2}}. \tag{4.27}$$

For each model and parameter setting, bias is estimated using 10^8 simulation trials with derivative prices computed by using conditional Monte Carlo methods, i.e. through (4.20) and (4.22), in order to reduce the standard error.

Let's start by considering the Heston model. We first evaluate the bias resulting from the proposed simulation method. Table 4.3 reports the estimated biases and standard errors for at-the-money options for the parameter settings in Table 4.1 together with exact option prices and confirms that biases are very small.

Next, we compare results with the exact simulation and the Gamma Expansion schemes. Numerical results are shown in Table 4.4. RMSE is taken from the original papers, e.g. Broadie and Kaya (2006, Tables 1 and 2) and Glasserman and Kim (2011, Table 7), while computing time is obtained by implementation of the Gamma Expansion method with infinite summations truncated at the tenth element. Figure 4.3 illustrates the speed-accuracy trade-off of the various methodologies. Each figure plots the RMSE against computing time on a log-log scale for each method and parameter setting. Finally, we compute the convergence rate by estimating the slopes of the lines in Figure 4.3 through a simple linear regression where the logarithm on base 10 of time in seconds is the regressor and the logarithm on base 10 of the RMSE is the dependent variable. As evident from Figure 4.3, estimated coefficients are very close to the optimum $-\frac{1}{2}$.

Let's consider now SABR and OU SV models. We apply moment matching and compare RMSEs with exact methods proposed by Cai *et al.* (2017) and Li and Wu (2019). Numerical results are reported in Table 4.5.

Table 4.4: Speed and accuracy of the proposed method compared with exact and gamma expansion simulation schemes

	Exact		Moment matching		Exact		Moment matching	
No. sims	RMSE	CPU	RMSE	CPU	RMSE	CPU	RMSE	CPU
	H 1				H 2			
10^4	0.0750	0.2092	0.0746	0.0802	0.6125	0.1195	0.6364	0.0857
$4 \cdot 10^4$	0.0373	0.7796	0.0372	0.2922	0.2904	0.4783	0.2879	0.3014
$16 \cdot 10^4$	0.0186	3.2520	0.0185	1.1783	0.1464	1.9149	0.1470	1.2207
$64 \cdot 10^4$	0.0093	12.7837	0.0093	4.8006	0.0726	7.6479	0.0723	4.8880
$256 \cdot 10^4$	0.0046	51.0394	0.0046	18.7324	0.0362	30.3411	0.0367	19.5991

	Gamma expansion		Moment matching		Gamma expansion		Moment matching	
No. sims	RMSE	CPU	RMSE	CPU	RMSE	CPU	RMSE	CPU
	H 3				H 4			
10^4	0.0489	0.1820	0.0489	0.0843	0.1050	0.2149	0.1087	0.0904
$4 \cdot 10^4$	0.0246	0.7418	0.0247	0.3125	0.0507	0.8463	0.0526	0.3271
$16 \cdot 10^4$	0.0123	3.1070	0.0123	1.2354	0.0257	3.3845	0.0273	1.2689
$64 \cdot 10^4$	0.0061	12.3070	0.0062	4.9161	0.0132	14.5513	0.0152	5.0985
$256 \cdot 10^4$	0.0031	49.4725	0.0031	19.4959	0.0068	55.9411	0.0099	20.0944

	Gamma expansion		Moment matching		Gamma expansion		Moment matching	
No. sims	RMSE	CPU	RMSE	CPU	RMSE	CPU	RMSE	CPU
	H 5				H 6			
10^4	0.1889	0.3568	0.2164	0.0907	0.0784	0.3226	0.0822	0.0730
$4 \cdot 10^4$	0.0973	1.2743	0.0987	0.3245	0.0394	1.1840	0.0414	0.2862
$16 \cdot 10^4$	0.0489	5.4148	0.0502	1.2724	0.0198	5.1863	0.0205	1.1032
$64 \cdot 10^4$	0.0248	22.4245	0.0245	5.1089	0.0099	21.8374	0.0105	4.5873
$256 \cdot 10^4$	0.0124	90.2900	0.0123	20.2172	0.0050	89.5185	0.0056	18.0950

Legend: $K = 100$, other parameters as in Table 4.1.

Figure 4.3: Speed and accuracy comparisons between exact simulation and gamma expansion schemes and the proposed moment based one

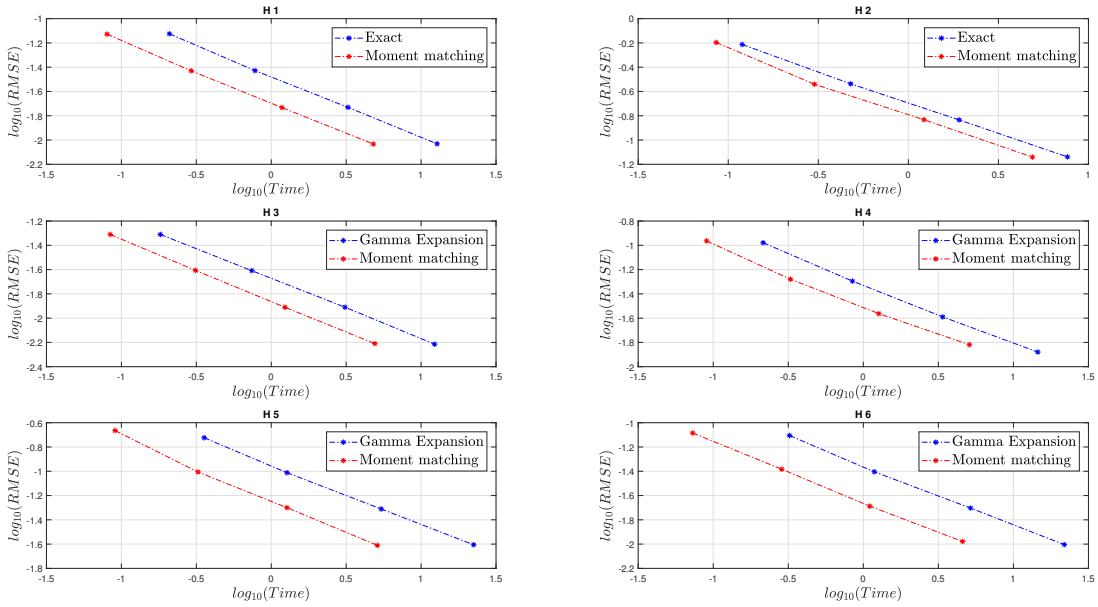

Legend: parameters as in Table 4.1.

Table 4.5: Speed and accuracy comparison for SABR and OU-SV models

	Exact		Moment matching		Exact		Moment matching	
No. sims	RMSE	CPU	RMSE	CPU	RMSE	CPU	RMSE $\cdot 10^4$	CPU
	SABR 1				SABR 2			
10^4	0.4080	0.6898	0.4095	0.0694	0.3950	0.7025	0.4018	0.0614
$4 \cdot 10^4$	0.2040	2.6759	0.2106	0.2540	0.1980	2.6832	0.2035	0.2282
$16 \cdot 10^4$	0.1030	10.8399	0.1126	1.3278	0.0996	11.0898	0.1082	1.2360
$64 \cdot 10^4$	0.0514	41.5034	0.0689	5.3678	0.0499	43.2027	0.0643	5.0225

	Exact		Moment matching		Exact		Moment matching	
No. sims	RMSE	CPU	RMSE	CPU	RMSE	CPU	RMSE	CPU
	SABR 3				OU-SV 1			
10^4	0.3860	0.6914	0.3866	0.0610	0.1529	7.8694	0.1495	0.0293
$4 \cdot 10^4$	0.1930	2.7214	0.1960	0.2295	0.0764	32.2796	0.0752	0.0684
$16 \cdot 10^4$	0.0976	10.5206	0.0975	1.1631	0.0382	127.7071	0.0378	0.5590
$64 \cdot 10^4$	0.0489	43.6587	0.0490	4.8123	0.0192	466.6427	0.0192	2.2737

	Exact		Moment matching		Exact		Moment matching	
No. sims	RMSE	CPU	RMSE	CPU	RMSE	CPU	RMSE	CPU
	OU-SV 2				OU-SV 3			
10^4	0.4703	10.0329	0.4283	0.0272	0.7648	9.4976	0.6752	0.0249
$4 \cdot 10^4$	0.2345	37.6895	0.2162	0.0640	0.3774	38.0485	0.3322	0.0617
$16 \cdot 10^4$	0.1176	148.8763	0.1068	0.5052	0.1891	154.1310	0.1681	0.5094
$64 \cdot 10^4$	0.0591	458.1360	0.0537	2.2862	0.0951	579.0554	0.0841	2.3021

4.6.4 Path dependent derivative instruments

We evaluate the performances of our conditional moment based Monte Carlo approach in pricing path dependent derivative instruments.

Continuous monitoring

We start by considering the more complicated case of a continuous monitoring setting. In this context we apply pricing formulas developed in Section 4.5.2 and show the prices of continuously monitored up and out call barrier and lookback put on minimum options under the Heston model and lookback put on minimum under the SABR ($\rho = 0$) model. In this case pricing formulas which can be used for computation of a true option price are not available, hence, computation of bias and RMSE is precluded. In order to evaluate correctness of the proposed method, we still report some benchmark results. For the Heston model we use the pricing method proposed by De Gennaro Aquino and Bernard (forthcoming). This is based on the numerical inversion of the joint characteristic function of the variance and its integral. We employ, as suggested by the authors, 2D COS method (see Ruijter and Oosterlee, 2012) to obtain the joint probability density function and then compute option prices through numerical integration. Results are reported in Table 4.6. We note some discrepancies between the prices computed through Monte Carlo simulation and 2D COS method. The most evident are in the parameter settings H 4 and H 5. In order to understand which of the two pricing procedures fail to produce the correct price we proceed with the following experiment: consider H 4, compute the corresponding European call option price and compare with the true one computed through standard (1D) COS method. The result is that the true price is 11.3743 (see also Table 4.3) against 11.4193 produced by 2D COS and 11.3694 obtained through our Monte Carlo simulation scheme (with 10^4 simulations). Hence, 2D COS results inaccurate under certain parameter settings.

Secondly, we compute prices of lookback put on minimum options both in Heston and SABR ($\rho = 0$) models. The choice of this instrument depends on the fact that it turns out to be less computationally demanding than other options written on maximum (or minimum) in the case of the SABR model. Note indeed that formula (4.24) only involves definite integrals and the only special function involved is the modified Bessel function of the second kind. Pricing alternative written on maximum (or minimum) options would be more computationally intensive due to the presence of improper integrals and other special functions, such as Whittaker function (we refer to Davydov and Linetsky, 2001 for more details and explicit formulas). Finally, we specify that, in order to implement formula (4.24), we compute the integral numerically using the global adaptive quadrature method and use the Euler inversion algorithm of Abate and Whitt (1995) to invert the Laplace transform in (4.25). As benchmarks we consider in this case the 2D COS for

Table 4.6: Barrier option prices in the Heston model

	H 1	H 2	H 3	H 4	H 5	H 6
2D COS	4.5577	0.4239	6.2011	3.9100	1.9543	3.9439
	Conditional Monte Carlo with moment matching, 10^5 simulations					
Price	4.5588	0.4217	6.2399	4.1281	1.8182	3.9364
s.e.	0.0084	0.0007	0.0087	0.0069	0.0051	0.0071
CPU	0.8073	0.8386	0.8008	0.8767	0.8492	0.7584
	Conditional Monte Carlo with moment matching, 10^6 simulations					
Price	4.5549	0.4214	6.2239	4.1247	1.8216	3.9519
s.e.	0.0027	0.0002	0.0028	0.0022	0.0016	0.0022
CPU	9.0835	9.0827	9.7867	9.3907	9.2173	8.3119
	Conditional Monte Carlo with moment matching, 10^7 simulations					
Price	4.5547	0.4211	6.2234	4.1259	1.8221	3.9505
s.e.	0.0008	0.0001	0.0009	0.0007	0.0005	0.0007
CPU	86.9056	88.9092	90.8531	90.4657	92.4597	83.2074

Legend: $K = 100$, barrier level = 120, other parameters as in Table 4.1.

the case of the Heston model and the sampling scheme developed by Chen *et al.* (2012) for the SABR. Results for Heston model are reported in Table 4.7. Similarly to the case of the up and out call barrier option, we note discrepancies between the prices. This is particularly evident in parameter setting H 5 (for which the numerical inversion of the joint characteristic function appears very complicated). Proceeding as described above, we note that true price of the European option is 11.3743, while the one computed through 2D COS is 11.4193 and through Monte Carlo simulation (with 10^4 simulations) is 11.3729. Thanks to these results, we also state superiority of our proposed method in pricing continuously monitored written on maximum (or minimum) options under the Heston model with respect to 2D COS adopted by De Gennaro Aquino and Bernard (forthcoming).

Finally, we report prices of lookback put on minimum options under SABR ($\rho = 0$) in Table 4.8. Also in this case, we note a big difference between prices in the case of SABR 6. This discrepancy is due to the fact that we are computing the price of continuously monitored option using a discretization grid. Morever, we stress that the benchmark is not an "exact" simulation scheme: it is based on approximations, hence, is not expected exact coincidence between the prices.

Discrete monitoring

In order to test accuracy of Algorithm 3, we consider the problem of pricing a discretely monitored (with 12 monitoring dates) arithmetic average Asian option in the Heston model (see Eq. 2.2 for its payoff specification). The algorithm works for any stochastic volatility model considered throughout this work but we choose the Heston model because

Table 4.7: Prices of put on minimum lookback options in the Heston model

	H 1	H 2	H 3	H 4	H 5	H 6
2D COS	1.9179	8.9025	2.4293	3.6693	8.0595	2.1962
	Conditional Monte Carlo with moment matching, 10^5 simulations					
Price	1.9211	8.8792	2.8467	3.7207	8.8516	2.2001
s.e.	0.0123	0.0344	0.0311	0.0279	0.0335	0.0125
CPU	0.9418	0.8045	0.8163	0.8951	0.8938	0.7524
	Conditional Monte Carlo with moment matching, 10^6 simulations					
Price	1.9154	8.9221	2.8235	3.7389	8.7708	2.1920
s.e.	0.0039	0.0109	0.0097	0.0088	0.0105	0.0039
CPU	9.4718	9.6611	9.7001	9.6342	9.8464	8.3108
	Conditional Monte Carlo with moment matching, 10^7 simulations					
Price	1.9225	8.9224	2.8320	3.7343	8.7849	2.1963
s.e.	0.0012	0.0035	0.0031	0.0028	0.0033	0.0012
CPU	90.1315	91.7200	90.9875	92.7497	94.1687	83.8275

Legend: $K = 90$, other parameters as in Table 4.1.

Table 4.8: Prices of put on minimum lookback options in the SABR ($\rho = 0$) model

	10^4 simulations			10^5 simulations		
Method	Price	s.e.	CPU	Price	s.e.	CPU
			SABR 4			
Chen *et al.* (2012)	0.0256	0.0001	28.3843	0.0255	0.0000	258.9329
Formula (4.24)	0.0256	0.0000	23.2103	0.0256	0.0000	214.1672
			SABR 5			
Chen *et al.* (2012)	0.1589	0.0011	26.5118	0.1611	0.0004	242.8413
Formula (4.24)	0.1633	0.0002	18.8153	0.1630	0.0000	172.6288
			SABR 6			
Chen *et al.* (2012)	3.6917	0.0282	27.8818	3.7396	0.0090	256.7871
Formula (4.24)	3.3143	0.0157	16.8790	3.3129	0.0050	164.2185

Legend: $K = S(0)$, other parameters as in Table 4.2.

Table 4.9: Estimated biases for pricing a discretely monitored (12 monitoring dates per year) arithmetic average Asian option in the Heston model through Algorithm 3

	H 1	H 2	H 3	H 4	H 5	H 6
Option price	3.5665	18.1581	4.1062	4.3219	6.6506	3.8591
bias	0.0005	-0.0013	0.0001	0.0007	0.0002	-0.0001

Legend: option contract parameters: $S(0) = K = 100$, Number of simulations $= 10^8$.

of the fact that a very accurate pricing procedure for discretely monitored arithmetic average Asian option exists. More specifically, we employ the very sharp lower bound pricing approximations developed by Fusai and Kyriakou (2016) for the option price as control variate within a Monte Carlo simulation. The resulting option prices are provided in Table 4.9 and are supposed to be extremely accurate. Then, we simulate price trajectories through Algorithm 3 and compute the price of discretely monitored arithmetic average Asian option, biases for parameter settings in Table 4.1 are reported in Table 4.9.

Next, we compute RMSE of the proposed method and compare with results of the Quadratic Exponential scheme (QE) proposed by Andersen (2008) which is used as benchmark. In order to compare the performances of the proposed method and the benchmark we select 150 time discretization steps per year for implementation of the QE scheme, with this choice we obtain similar CPU times for both methods and can compare accuracy simply looking at the RMSEs. These are reported, together with the computing times, in Table 4.10 and Figure 4.4.

4.6.5 Comments on numerical results

We comment here the performances of Algorithm 3 in pricing both path dependent and independent derivative instruments.

For what concerns the path independent case, we point out the impressive performances of our proposed method. First, it is faster than exact simulation schemes (and Gamma Expansion) used as benchmarks. The reason is evident: no numerical methods are required at any stage, with the obvious consequence that the whole simulation procedure results extremely fast. Moreover, as shown in Figure 4.1 the usage of Algorithm 1 instead of analytical derivation for moments computation allows to speed up the code perceptively, especially in the Heston model, where the Laplace transform depend on the modified Bessel function of the first kind. Contrarily, exact simulation schemes crucially depend on numerical methods, such as numerical integration and root finding algorithms, the consequence is that a speed-accuracy trade-off is intrinsically established: on one hand, increasing the desired accuracy of numerical methods allows to eliminate simulation bias but increases the computing time, on the other hand, diminishing the

Table 4.10: Speed and accuracy comparison for Asian option pricing for Heston model

	QE		Moment matching		QE		Moment matching	
No. sims	RMSE	CPU	RMSE	CPU	RMSE	CPU	RMSE $\cdot 10^4$	CPU
	H 1				H 2			
10^4	0.0424	1.3520	0.0381	1.2321	0.3230	7.3106	0.2606	6.9714
$4 \cdot 10^4$	0.0260	4.3703	0.0192	4.3874	0.2209	23.8769	0.1387	26.6618
$16 \cdot 10^4$	0.0201	17.4439	0.0096	19.3048	0.1855	96.0225	0.0684	114.7599
$64 \cdot 10^4$	0.0179	88.1052	0.0025	76.9831	0.1731	501.6341	0.0171	480.7504
	QE		Moment matching		QE		Moment matching	
No. sims	RMSE	CPU	RMSE	CPU	RMSE	CPU	RMSE	CPU
	H 3				H 4			
10^4	0.0363	1.0525	0.0310	1.1284	0.0607	1.1162	0.0581	1.1039
$4 \cdot 10^4$	0.0238	3.3223	0.0155	4.5351	0.0342	3.4724	0.0287	4.3373
$16 \cdot 10^4$	0.0195	13.2218	0.0078	18.6096	0.0231	13.6736	0.0145	18.4828
$64 \cdot 10^4$	0.0180	55.0731	0.0020	77.7490	0.0184	61.2445	0.0037	78.7453
	QE		Moment matching		QE		Moment matching	
No. sims	RMSE	CPU	RMSE	CPU	RMSE	CPU	RMSE	CPU
	H 5				H 6			
10^4	0.1084	1.3928	0.1068	1.2773	0.0471	1.4900	0.0447	1.2398
$4 \cdot 10^4$	0.0600	4.6011	0.0525	5.2758	0.0284	5.1578	0.0221	5.1414
$16 \cdot 10^4$	0.0387	18.7495	0.0262	22.1779	0.0211	20.4507	0.0111	21.9403
$64 \cdot 10^4$	0.0292	83.7759	0.0065	91.8810	0.0182	100.7752	0.0028	89.4101

Figure 4.4: Speed and accuracy comparisons between the QE scheme and the proposed moment based one

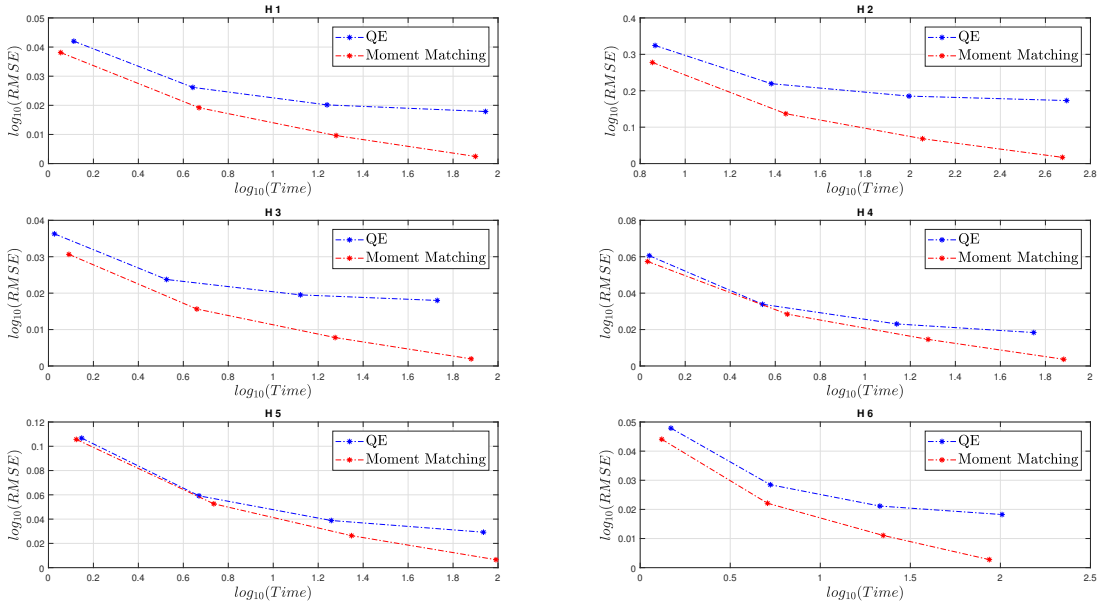

Legend: parameters as in Table 4.1.

accuracy may help reducing the computational burden but would introduce some bias[3]. Second, it is accurate, as reported in Table 4.3, the bias is extremely small, appearing only in the third-fourth decimal place. This evidence allows us to state that in the path independent case the proposed simulation scheme is almost unbiased as confirmed also by RMSEs reported in Tables 4.4, 4.5 and Figure 4.3, where is possible to see how close are the RMSEs to the ones obtained in the original papers where the exact simulation schemes are proposed (resulting, in some cases, even smaller). Hence, we also ask ourselves which factors explain such good performances of the method, not only in terms of computing time, but also in terms accuracy. First, note that, due to existence of its Laplace transform, the moment problem for the random variable $\Psi(u,t)$ is determinate (see Criterion 1), thus is reasonable to approximate $\Psi(u,t)$ through its moments. Second, as shown in Figure 4.2, also higher order moments are implicitly matched. Third, the Pearson's system is explictly designed for moment matching (see Devroye, 1986) and is very flexible covering a variety of shapes ensuring a very good fitting to the true but unknown distribution of $\Psi(u,t)$. These facts provide the theoretical basis which ensure that the proposed method is highly accurate.

The recent result of De Gennaro Aquino and Bernard (forthcoming) regarding the joint distribution of time changed Brownian motion and its maximum (see Section 4.5) allows to extend the results obtained in the case of path independent derivative instruments to the path dependent. This implies that in order to price these kind of options is sufficient to simulate (only one time) $\Psi(u,t)$ and then apply pricing formulas such as (4.23) to price options extending the good results outlined above to the case of continuously monitored written on maximum (or minimum) options. Since in this case, to the best of our knowledge, exact pricing formulas does not exist for the models considered, we simply report the prices of up and out call barrier and lookback put on minimum options and compare with the 2D COS method originally proposed by De Gennaro Aquino and Bernard (forthcoming) in Tables 4.6 and 4.7. Results show that the proposed method is much more accurate (and also faster) than 2D COS, which fails under some parameter settings to produce correct option prices. Same methodology applies also to the OU-SV model. Regarding the SABR ($\rho = 0$) we propose a conditional Monte Carlo approach to price continuously monitored written on maximum (or minimum) options and apply to the case of put on minimum lookbacks. This approach does not depend on the key quantity $\Psi(u,t)$, hence moment based approximations are not necessary. Numerical results are given in Table 4.8 and show that the proposed method outperforms the benchmark which is represented by the time discretization based simulation scheme proposed by Chen *et al.* (2012) (which is implemented over a very thin time discretization grid in

[3]The same happens also in the case of the Gamma Expansion method of Glasserman and Kim (2011), where the choice of the term where truncating the infinite summations impacts both on the accuracy and the speed of the methodology.

order to produce, as much possible, continuous monitoring), resulting more accurate and faster.

Finally, we discuss numerical results of the proposed Algorithm 3 in pricing path dependent derivatives instrument with finite number of monitoring dates. Despite the algorithm can be used to simulate each of the models considered throughout this work, we restrict our attention to the Heston model, for which accurate pricing methodologies for discretely sampled path dependent options (such as Asian options) exist, allowing us to compute properly biases (reported in Table 4.9) and RMSEs. In particular, we test the ability of Algorithm 3 to produce correct price estimates for discrete Asian options and compare with a benchmark represented by the Andersen (2008) quadratic exponential scheme. Numerical results show that the proposed method is, for a similar level of CPU time, much more accurate than the benchmark (see Table 4.10 and Figure 4.4).

4.7 Extensions and further research

In this section we consider some other possible applications of the proposed method. First, we explore the possibility to extend the Conditional Monte Carlo approach outlined in Section 4.5 to the pricing of American put options. Second, we investigate the possibility to adapt (with few modifications) Algorithm 3 in order to simulate more sophisticated models, such as the Double Heston and the 4/2 stochastic volatility models.

4.7.1 American put options

In the cases of the Heston, SABR ($\beta = 1$) and OU-SV models the conditional distribution of the log-stock price is normal with known mean and variance. Consequently, the European call option can be computed according to (4.20). Barone-Adesi and Whaley (1987) propose a simple methodology to find the price of the American put option given European put option price under the Black-Scholes model. Exploiting this useful fact and that the European put option prices can be computed by applying the Black-Scholes formula (see Eq. 4.20) we state that is possible to compute American put option prices through our method. Unfortunately, two problems arise: first, the method connecting European and American put option prices is not exact, but only approximated, secondly, it involves the usage of numerical methods, which must be employed in any simulation. The result is that the whole procedure may result slow and, possibly, also inaccurate. Hence, it necessitates of further investigations. In order to show some preliminary result we compute American put option prices under the Heston model through this method and compare with the prices reported in Fang and Oosterlee (2011, Table 4). For at the money option, we obtain an estimated price of 0.5207, which is quite similar to the one reported by the authors (i.e. 0.520030).

4.7.2 Simulation of the Double Heston model

Christoffersen *et al.* (2009) propose a model where the stock price evolves according to the following triple of SDEs:

$$dS(t) = rS(t)dt + \sigma_1(t)S(t)\left(\rho_1 dW_3(t) + \sqrt{1-\rho_1^2}dW_1(t)\right) + \sigma_2(t)S(t)\left(\rho_2 dW_4(t) + \sqrt{1-\rho_2^2}dW_2(t)\right)$$
$$d\sigma_1^2(t) = k_1(\theta_1 - \sigma_1^2(t))dt + v_1\sigma_1(t)dW_3(t)$$
$$d\sigma_2^2(t) = k_2(\theta_2 - \sigma_2^2(t))dt + v_2\sigma_2(t)dW_4(t)$$

where Brownian motions are mutually independent. We note that, since $dW_3(t)$ and $dW_4(t)$ are uncorrelated, the couples $\left(\sigma_1^2(t), \int_u^t \sigma_1^2(s)ds \middle| \sigma_1^2(u)\right)$ and $\left(\sigma_2^2(t), \int_u^t \sigma_2^2(s)ds \middle| \sigma_2^2(u)\right)$ can be simulated separately through the exact simulation method of Broadie and Kaya (2006) or our method proposed in Section 4.2. Then, we get:

$$\ln S(t) \sim \mathcal{N}(m, s^2)$$

where

$$m = \ln S(u) + r(t-u) + \sum_{j=1}^{2}\rho_j \int_u^t \sigma_j(s)dW_{j+2}(s) - \frac{1}{2}\int_u^t \sigma_j^2(s)ds,$$
$$s = \sum_{j=1}^{2}(1-\rho_j^2)\int_u^t \sigma_j^2(s)ds$$

and $\int_u^t \sigma_j(s)dW_{j+2}(s) = \frac{1}{v_j}\left(\sigma_j^2(t) - \sigma_j^2(u) - k_j\theta_j(t-u) + k_j\int_u^t \sigma_j^2(s)ds\right)$. The proposed method can thus be extended to the Double Heston model.

4.7.3 Simulation of the 4/2 stochastic volatility model

Grasselli (2017) propose the following stochastic volatility model to describe the stock price process:

$$dS(t) = rS(t)dt + S(t)\left(\alpha\sigma(t) + \frac{\beta}{\sigma(t)}\right)(\rho dW_2(t) + \sqrt{1-\rho^2}dW_1(t))$$
$$d\sigma^2(t) = k(\theta - \sigma^2(t))dt + v\sigma(t)dW_2(t)$$

Let's start noting that the variance dynamics coincides with (4.2), thus $\sigma^2(t)|\sigma^2(u)$ can be simulated exactly through (4.7). Then, the conditional moment generating function of $Y(t)|\sigma^2(t)$, where $Y(t) := \ln S(t)$, is known analytically (cfr. Grasselli, 2017, Proposition

4.1):

$$\begin{aligned}\mathrm{E}[e^{aY(t)}|\sigma^2(t),\sigma^u,Y(u)] = \exp\Bigg(aY(u) + a\left(r - \alpha\beta - \frac{\alpha\rho k\theta}{v} + \frac{\beta\rho k}{v}\right)(t-u) + \\ + a^2(1-\rho^2)\alpha\beta(t-u)\Bigg)\exp\left(\frac{a\alpha\rho}{v}(\sigma^2(t)-\sigma^2(u)) + \frac{a\beta\rho}{v}\ln\frac{\sigma^2(t)}{\sigma^2(u)}\right)\times \\ \times\frac{\sqrt{A(a)}\sinh\left(\frac{k(t-u)}{2}\right)}{k\sinh\left(\frac{\sqrt{A(a)}(t-u)}{2}\right)}e^{\frac{\sigma^2(t)+\sigma^2(u)}{v^2}\left(k\coth\left(\frac{k(t-u)}{2}\right)-\sqrt{A(a)}\coth\left(\frac{\sqrt{A(a)}(t-u)}{2}\right)\right)}\times \\ \times\frac{I_{\frac{2}{v^2}\sqrt{\left(k\theta-\frac{v^2}{2}\right)^2+2v^2B(a)}}\left(\frac{2\sqrt{A(a)\sigma^2(u)\sigma^2(t)}}{v^2\sinh\left(\frac{\sqrt{A(a)}(t-u)}{2}\right)}\right)}{I_{\frac{2k\theta}{v^2}-1}\left(\frac{2k\sqrt{\sigma^2(u)\sigma^2(t)}}{v^2\sinh\left(\frac{k(t-u)}{2}\right)}\right)} \qquad (4.28)\end{aligned}$$

with

$$\begin{aligned}A(a) &= k^2 - 2v^2\left(a\left(\frac{\alpha\rho k}{v} - \frac{1}{2}\alpha^2\right) + \frac{1}{2}a^2(1-\rho^2)\alpha^2\right),\\ B(a) &= a\left(\frac{\beta\rho}{v}\left(\frac{v^2}{2} - k\theta\right) - \frac{\beta^2}{2}\right) + \frac{1}{2}a^2(1-\rho^2)\beta^2.\end{aligned}$$

Hence, conditional $Y(t)$ can be simulated exactly by inverting numerically (4.28) and applying inverse transform sampling. The whole procedure is similar to one proposed by Broadie and Kaya (2006) with the obvious exception that $\int_u^t \sigma^2(s)ds|\sigma^2(t),\sigma^2(u)$ is not involved in the simulation procedure. In order to speed up the code, one can consider the approach proposed throughout this work, i.e. compute the conditional moments of $Y(t)$ through Algorithm 1 and generate random numbers from $Y(t)|\sigma^2(t),\sigma^2(u),Y(u)$ through Algorithm 2. This procedure is expected to be fast, enabling the simulation of the stock price trajectory at discrete times and, consequently, pricing path dependent derivative instruments, which, to the best of our knowledge, is an unexplored topic for this model.

4.8 Conclusions

In this chapter we propose a new methodology for simulating stochastic volatility models. We start from exact simulation schemes and show how to circumvent the most time consuming step of that methods by computing the moments of the unknown distribution of the integral of the variance process conditional on the terminal variance. Then, we show how to create a moment based random numbers generator which is very efficient, as not requiring any numerical method at any stage. The speed of the procedure allows, contrarily to exact simulation schemes, to generate whole price trajectories in a reason-

able amount of time, enabling pricing of path dependent derivative instruments whose price is observed on a discrete time grid. We apply the method to the Heston, SABR and OU-SV stochastic volatility models, but, with few modifications, is also possible to extend the methodology to other, more complicated, models. This is left as future research. Subsequently, we consider the problem of pricing derivative instruments and show that proposed method can be successfully embedded into a conditional Monte Carlo framework, allowing to price efficiently a large class of path independent and path dependent derivative instruments, such as barriers and lookback. The same methodology can be possibly extended to the pricing of American put options, leaving some other space to future research. We present extensive numerical results. We start by highlighting the good performances of the proposed algorithm in computing the moments of the unknown distribution with respect to more traditional competitors. Then, we test its accuracy by computing European option prices and performing an extensive comparison with exact methods. It turns out that, for a similar accuracy, our proposed method is much faster. In the context of pricing path dependent derivative instrument, we compare the proposed algorithm with alternative methods proposed in literature based on time discretization. For similar computing time, our method results more accurate than benchmark competitors.

Chapter 5

Asian options pricing in Hawkes-type jump-diffusion models

In this chapter we propose a method for pricing Asian options in market models with the risky asset dynamics driven by a Hawkes process with exponential kernels. For these processes the couple $(\lambda(t), X(t))$ is affine, this property allows to extend the general methodology introduced by Hubalek *et al.* (2017) for geometric Asian option pricing to jump-diffusion models with stochastic jumps intensity. Although the system of ordinary differential equations providing the characteristic function of the related affine process cannot be solved in closed form, a COS-type algorithm allows to obtain the relevant quantities needed for options valuation. We describe, by means of graphical illustrations, the dependence of Asian options prices by the main parameters of the driving Hawkes process, finally, by using geometric Asian options values as control variates, we show that arithmetic Asian options prices can be computed in a fast and efficient way by standard Monte Carlo methods.

5.1 Introduction

Several different kind of models have been proposed during the last 40 years in order to improve the forecasting performances of the Black-Scholes model, which is based on a geometric Brownian motion description of the risky asset dynamics. In particular, models with jumps (see Cont and Tankov, 2004) are able to provide smiles for the implied volatility, although not very realistic for long maturities. Models introducing a stochastic dynamics for the diffusion coefficient of the Brownian motion, named stochastic volatility models, can provide smiles realistic only for long maturities. More sophisticated models introduce both stochastic volatility and jumps in order to provide realistic smiles for all maturities. The model proposed by Bates (1996a) combines the features of the jump-diffusion model proposed by Merton (1976) with those of the stochastic volatility

model proposed by Heston (1993). Barndorff-Nielsen and Shephard (2001) and Barndorff-Nielsen *et al.* (2002) introduced a model in which the volatility dynamics is described by an Ornstein-Uhlenbeck process driven by a subordinator. Another reasonable attempt to improve the asset price dynamics description has been done by Carr *et al.* (2003) and Carr and Wu (2004), which propose the so-called Time-Changed Lévy models. We mention also the model introduced by Bates (2000), in which an affine (deterministic) dependence is included between the stochastic volatility and the jumps intensity.

All the above mentioned pricing models in which stochastic volatility features have been combined with jumps belong to the large family of the so-called affine models, according to the definition provided by Duffie *et al.* (2003). This class includes almost all the most popular pricing models existing in the literature related to many different type of underlying assets: fixed income securities, credit risk models, equities and commodities. Many relevant features of these models can be described in a unified way by the very general framework provided by the affine process approach. For an extensive treatment of the general properties of affine models and some related technical issues we refer to Keller-Ressel (2008).

In the paper by Hubalek *et al.* (2017) a general methodology for geometric Asian option pricing is introduced, and for several specific models of affine type closed-form solutions are obtained for the Riccati equations providing the affine characteristics for the joint dynamics of log-returns, volatility and their average processes, and their joint moment generating functions. This approach allows to compute the geometric Asian options price by a simple inversion of a Laplace transform, which represents the only numerical step in the pricing procedure and for which several fast and accurate algorithms are available.

Recently, new models have been proposed in order to describe risky assets price dynamics, including jumps with self-exciting features. Evidence has been provided that jumps appear in clusters, this phenomenon is investigated in the paper by Filimonov *et al.* (2014), where a large amount of price sudden movements is shown to be of endogenous type, i.e. they are produced by previous sudden movements. The most popular way to introduce self-excited jumps in the asset price dynamics is by using Hawkes processes. In the paper by Bacry *et al.* (2013) a limit order book modelling approach is presented, offering a micro-structure foundation for Hawkes-type models. Ait-Sahalia *et al.* (2015) adopt a Hawkes vector framework in order to describe mutually exciting jumps in the market and Fulop *et al.* (2015) propose a Bayesian learning approach to jumps cluster detection and provide evidence of jumps clustering since the 1987 market crash, which appeared even more pronounced after the 2008 global financial crisis. Rambaldi *et al.* (2015) propose a model based on Hawkes processes in order to describe the foreign exchange markets and Kiesel and Paraschiv (2017) introduce a Hawkes-type model in order to describe the power price dynamics in energy markets.

Marked Hawkes processes are compound Poisson processes with stochastic intensity; when the kernel characterizing the self-exciting dynamics is of exponential type, the couple $(\lambda(t), X(t))$, where $\lambda(t)$ is the jump intensity and $X(t)$ is the log-asset price, is an affine process. This allows to apply the general framework introduced in Hubalek *et al.* (2017) in order to evaluate geometric Asian options.

The purpose of the present chapter is to propose a fast and efficient pricing method for Asian options in a Hawkes modelling setting. As a reference model we shall adopt the jump-diffusion model proposed by Hainaut and Moraux (2018), but our approach could be easily adapted to other models based on Hawkes processes with exponential kernel. The Riccati equations describing the joint dynamics of log-returns and their arithmetic average, unfortunately, cannot be solved in closed form, but the well-known COS method proposed by Fang and Oosterlee (2008) can be used to get option prices with a reasonable amount of characteristic function evaluations. To our knowledge, this is the first attempt to solve the valuation problem for Asian options in a Hawkes-type modelling framework.

It is well known that, the usage of the geometric Asian options values as control variates in a Monte Carlo simulation for arithmetic Asian options pricing allows to reduce dramatically the variance of the simulation step. We shall use this property in order to compute the arithmetic Asian options price as well and illustrate how the simulation method can be made fast and efficient once the geometric Asian options values are obtained through the proposed method.

The plan of the work is the following: in Section 5.2 we introduce our self-exciting jump-diffusion model by following the proposal by Hainaut and Moraux (2018) and we illustrate their affine features. Then we formulate the basic results for geometric Asian options pricing for jump-diffusion models with stochastic intensity by introducing the required modifications in the approach proposed in Hubalek *et al.* (2017) for affine stochastic volatility models. In Section 5.3 we derive the closed form solution for the geometric Asian option prices and illustrate the simulation approach adopted for arithmetic Asian options valuation, in which geometric Asian options values are in use as a control variate. In Section 5.4 we show and discuss numerical results, Section 5.5 concludes.

5.2 Model setup

We model the log-returns of the underlying under the risk neutral measure Q through the following couple of SDEs:

$$dX(t) = \left(r - \frac{\sigma^2}{2} - \mathrm{E}[e^J - 1]\lambda(t)\right) dt + \sigma dW(t) + d\left(\sum_{i=1}^{N(t)} J_i\right) \tag{5.1}$$

$$d\lambda(t) = \alpha(\theta - \lambda(t))dt + \eta dL(t) \tag{5.2}$$

where $X(t) := \ln S(t)$, $S(t)$ denotes the price of the underlying at time t, r is the risk-less rate, σ is the diffusion coefficient, J_i is the size of the i-th jump, $N(t) \sim \text{Poisson}(\lambda(t))$ and $L(t)$ is a jump process defined as:

$$L(t) = \sum_{i=1}^{N(t)} |J_i|$$

with $J_i \sim \mathcal{DE}(p, \rho^+, \rho^-)$, where $\mathcal{DE}(p, \rho^+, \rho^-)$ is the double exponential distribution, with probability of positive jumps denoted with p, average sizes of positive and negative shocks given, respectively, by $\frac{1}{\rho^+}$ and $\frac{1}{\rho^-}$. In agreement with the present notation $X(0) = \ln S(0)$.

Remark 5.1. *We model directly the asset dynamics under the risk-neutral measure* Q*. A measure change preserving the model structure and the relations between parameters under the historical measure* P *and the risk-neutral measure* Q *is proposed in Hainaut and Moraux (2018), together with an estimation method and a hedging strategy based on European options trading.*

Proposition 5.1. *Hainaut and Moraux (2018)*

Given the model specified by equations (5.1) and (5.2), consider $t \in [0, T]$ the joint characteristic function of $(X(T),\lambda(T))$ is given by:

$$\mathrm{E}^0[e^{u_1 X(T)+u_2\lambda(T)}|X(0), \lambda(0)] = \exp\left(A(0,T) + \lambda(0)B(0,T) + u_1 X(0)\right), \tag{5.3}$$

for all $(u_1, u_2) \in i\mathbb{R}^2$ where $A(t,T)$ and $B(t,T)$ are given by the solution of the following ODEs system:

$$\begin{cases} \frac{\partial A}{\partial t} = F(u_1, B), & B(T,T) = u_2 \\ \frac{\partial B}{\partial t} = R(u_1, B), & A(T,T) = 0 \end{cases} \tag{5.4}$$

where $\mathrm{E}^0[\cdot]$ indicates that the expectation is taken with respect to the risk neutral measure, $F(u_1, B) = -\alpha\theta B - \left(r - \frac{\sigma^2}{2}\right) u_1 - \frac{\sigma^2}{2}u_1^2$, $R(u_1, B) = -\alpha B + k u_1 - (\psi(B\eta, u_1) - 1)$, $k = \mathrm{E}^0[e^J - 1]$ and $\psi(z_1, z_2) = p\frac{\rho^+}{\rho^+ - (z_1+z_2)} + (1-p)\frac{\rho^-}{\rho^- - (z_1 - z_2)}$ is the joint moment generating function of the distribution of the jumps size and their absolute value.

Errais *et al.* (2010) show that (X, λ) is an affine process, we aim to exploit this result extending the validity of Proposition 5.1 to the following quantities:

$$Y(T) := \int_0^T X(s)ds, \quad \Lambda(T) := \int_0^T \lambda(s)ds. \tag{5.5}$$

We get the following theoretical result:

Proposition 5.2. *If (X, λ) is an affine model with functional characteristics (F, R), then the joint characteristic function of $(X(T), \lambda(T), Y(T), \Lambda(T))$ is given by:*

$$\mathrm{E}^0[e^{u_1 X(T)+u_2\lambda(T)+u_3 Y(T)+u_4\Lambda(T)}|X(0),\lambda(0)] = \exp\Big(A(0,T)+(u_1+u_3T)X(0)+B(0,T)\lambda(0)\Big), \tag{5.6}$$

for all $(u_1, u_2, u_3, u_4) \in i\mathbb{R}^4$ where A and B are given by the solution of the following ODEs system:

$$\begin{cases} \frac{\partial A}{\partial t} = F(u_1+u_3t, B), \quad A(T,T) = 0 \\ \frac{\partial B}{\partial t} = R(u_1+u_3t, B) - u_4, \quad B(T,T) = u_2 \end{cases} \tag{5.7}$$

and $F(\cdot,\cdot)$ and $R(\cdot,\cdot)$ are as in Proposition 5.1.

Proof. Since (X, λ) is an affine process, the proof follows from Hubalek *et al.* (2017, Proposition 3) ■

This result enables the pricing of European and fixed strike geometric Asian options through simple changes of arguments, we are going to detail this in next section. As far as the Average Strike options are concerned, we need to extend to the present case the results on the change of numéraire obtained in Hubalek *et al.* (2017, Section 4). If we denote by Q^0 and Q^1 respectively the risk-neutral probabilities with the money market account and the risky asset as numéraires, the results can be reformulated as follows:

Lemma 5.1. *If (X, λ) is affine under Q^0 with functional characteristics F^0 and R^0, then it is affine under Q^1 with functional characteristics F^1 and R^1 given by*

$$F^1(u_1,u_2) = F^0(u_1+1,u_2), \quad R^1(u_1,u_2) = R^0(u_1+1,u_2). \tag{5.8}$$

Lemma 5.2. *If (X, λ) is an affine model, then the joint law of $(X_t, Y_t = \int_0^t X_s ds)$ under Q^1 is described by*

$$E^1[e^{u_1X(t)+u_2Y(t)}|X(0),\lambda(0)] = \exp\left(C(t,u_1,u_2)+X(0)(u_1+u_2t)+\lambda(0)D(t,u_1,u_2)\right) \tag{5.9}$$

for all $(u_1, u_2) \in i\mathbb{R}^2$, where

$$\partial_t C(t,u_1,u_2) = F^0(u_1+1+u_2t, D(t,u_1,u_2)) \qquad C(0,u_1,u_2) = 0 \tag{5.10}$$

$$\partial_t D(t,u_1,u_2) = R^0(u_1+1+u_2t, D(t,u_1,u_2)) \qquad D(0,u_1,u_2) = u_2. \tag{5.11}$$

Moreover, the Riccati equations can be extended to all parameters values in the effective domain (for the definition of the effective domain we refer to Hubalek et al.*, 2017).*

Proof. The proof of the two previous statements follows step by step the proof provided

in Hubalek *et al.* (2017), by assuming the stochastic intensity λ as a state variable instead of the variance. ■

In next section we are going to illustrate how the general results presented in this section can be applied in order to get geometric Asian options prices.

Remark 5.2. *In the following, in agreement with Hainaut and Moraux (2018), we always assume the relevant characteristic/moment generating functions and cumulants to exist finite for the parameters values considered. Conditions on the affine characteristics granting moments and cumulants existence can be found in Keller-Ressel (2011).*

5.3 Option pricing

In this section we show how to price European and Asian (fixed and floating strike) options for the model specified in (5.1) and (5.2). We start by identifying the characteristic functions which will be used to get the price of the various derivative instruments, this will be inverted numerically through the COS method (see Appendix A) to get the price of European and geometric Asian options. In this context, we also show how to compute a proper truncation range for an efficient implementation of the COS method. Finally, we discuss arithmetic Asian options pricing.

5.3.1 Option pricing given the characteristic function

Let's start recalling that $S(T) := e^{X(T)}$ and defining the geometric average of the price process at maturity as $G(T) := e^{\frac{Y(T)}{T}}$. The price of European and fixed and average strike geometric Asian options is given, respectively, by:

$$p_E = e^{-rT}\mathrm{E}^0[(S(T)-K)^+] = e^{-rT}\int_{-\infty}^{\infty}(e^x-K)^+ f_X(x)dx \tag{5.12}$$

$$p_{GFS} = e^{-rT}\mathrm{E}^0[(G(T)-K)^+] = e^{-rT}\int_{-\infty}^{\infty}(e^{\frac{y}{T}}-K)^+ f_Y(y)dx \tag{5.13}$$

$$p_{GAS} = e^{-rT}\mathrm{E}^1[(1-e^{Z(T)})^+] = e^{-rT}\int_{-\infty}^{\infty}(1-e^z)^+ f_Z(z)dz, \tag{5.14}$$

where r is the risk-less rate, T is the option maturity, K is the strike price, $S(0)$ is the starting price, $Z(T) := \frac{Y(T)}{T} - X(T)$ and $f_\cdot(\cdot)$ is the probability density function (henceforth pdf). Proposition 5.2 and Lemmas 5.1 and 5.2 can be used to derive the characteristic function of $X(T)$, $Y(T)$, $Z(T)$ through simple changes of arguments. Let's start considering the case of European and fixed strike geometric Asian options: in the case where $u_2 = u_3 = u_4 = 0$ (respectively, $u_1 = u_2 = u_4 = 0$) Proposition 5.2 allows to identify the characteristic function of the log-returns (integrated log-returns) which can

be inverted numerically to obtain the price of the European (geometric Asian) option. Similarly, consider replacing $u_1 = -1$ and $u_2 = \frac{u}{T}$ into (5.9), Lemma 5.2 identifies the characteristic function under Q^1 of $Z(T)$.

These results open the doors to options pricing through standard inversion algorithms, such as FFT and COS methods. Hainaut and Moraux (2018) propose pricing formulas for European calls and puts based on FFT, but the COS method is usually preferable because of its exponential convergence to the true solution (while its computational complexity is linear), see Fang and Oosterlee (2008). The most obvious consequence is that option price can be estimated through a smaller number of evaluations of the characteristic functions, this is particularly important when it is given by time consuming numerical techniques such as, for example, solution of an ODEs system as in the present case. Main features of the COS method are summarized in Appendix A.

In what follows, we show how to compute explicitly the cumulants of the probability density functions involved in (5.12), (5.13) and (5.14). This is important since, as pointed out by Fang and Oosterlee (2008, pag. 840), if $L = 10$ then formula (A.5) gives a truncation error around 10^{-12}, enlarging the interval $[a, b]$ would require larger N to reach the same level of accuracy.

Remark 5.3. *The choice of N impacts on the efficiency of the method as the characteristic function of log-returns must be evaluated $N-1$ times. This aspect is crucial when the characteristic function must be computed through time consuming numerical techniques such as, for example, by solving an ODEs system.*

Hence, given the characteristic function of log-returns, the pdf can be recovered from formula (A.3). Given the pdf, the price of the option can be computed from equations (5.12), (5.13) and (5.14) by computing the integral numerically.

5.3.2 Truncation range computation

In this section we show how to compute the moments of log-returns in the model specified in (5.1) and (5.2) given the characteristic function in (5.3). These will be then used for computing a proper truncation range for implementation of COS method for European options pricing. For sake of brevity and clarity, we restrict our attention to the cumulants of log-returns, but the same argument applies also to $Y(T)$ and $Z(T)$. Taking the logarithm of (5.3) one gets the cumulant generating function:

$$\psi(u_1, u_2, u_3, u_4) = A(0,T) + (u_1 + u_3 T)X(0) + B(0,T)\lambda(0). \tag{5.15}$$

By setting $u_1 = u$, $u_2 = u_3 = u_4 = 0$, we get the cumulants of log-returns[1] according to:

$$k_n = \frac{\partial^n \psi(u)}{\partial u^n}\bigg|_{u=0} = \frac{\partial^n A(0,T)}{\partial u^n}\bigg|_{u=0} + \frac{\partial^n u}{\partial u^n}\bigg|_{u=0} \cdot X(0) + \frac{\partial^n B(0,T)}{\partial u^n}\bigg|_{u=0} \cdot \lambda(0), \quad (5.16)$$

with $\frac{\partial^n u}{\partial u^n}\big|_{u=0} \cdot X(0) = \begin{cases} X(0) & \text{if} \quad n = 1 \\ 0 & \text{if} \quad n \geq 2 \end{cases}$ and

$$\begin{cases} \frac{\partial}{\partial t}\left(\frac{\partial^n A(t,T)}{\partial u^n}\Big|_{u=0}\right) & = \frac{\partial^n F(u,B)}{\partial u^n}\Big|_{u=0}, \quad A(T,T) = 0 \\ \frac{\partial}{\partial t}\left(\frac{\partial^n B(t,T)}{\partial u^n}\Big|_{u=0}\right) & = \frac{\partial^n R(u,B)}{\partial u^n}\Big|_{u=0}, \quad B(T,T) = 0 \end{cases}. \quad (5.17)$$

Tedious maths show that this system can be solved analytically for each $n \in \mathbb{N}^+$ (we don't report here analytical solution, Mathematica® codes are given in Appendix C.2). Finally, we stress that, taking the logarithm of (5.9) one gets the cumulant generating function of $Z(T)$, which can be used for the case of Average Strike. Given cumulants, moments can be computed analytically using Faá di Bruno's formula for high derivatives of composite functions:

$$\mathrm{E}[X^n] = \sum_{i=1}^{n} \mathrm{B}_{n,i}(k_1, ..., k_{n-i+1}),$$

where $\mathrm{B}_{n,i}$ are the incomplete Bell polynomials. A first application of this result concerns the calculation of the proper truncation range for implementation of the COS method. We note that moments of $\ln\left(\frac{S(T)}{K}\right)$ can be expressed as function of the moments of X:

$$z_n := \mathrm{E}\left[\left(\ln\left(\frac{S(T)}{K}\right)\right)^n\right] = \mathrm{E}\left[\left(\ln\left(\frac{S(0)}{K}\right) + X\right)^n\right]. \quad (5.18)$$

By solving equation (5.18) for $n = \{1, 2, 3, 4\}$ one can compute the cumulants in (A.5) according to:

$$c_1 = z_1, \quad c_2 = z_2 - z_1^2, \quad c_3 = z_3 - 3z_2z_1 + 2z_1^3, \quad c_4 = z_4 - 4z_3z_1 - 3z_2^2 + 12z_2z_1^2 - 6z_1^4. \quad (5.19)$$

By substituting these into (A.5) one gets the truncation range.

[1] Similarly, posing $u_3 = u$, $u_1 = u_2 = u_4 = 0$ one gets the cumulants of $Y(T)$.

5.3.3 Pricing arithmetic Asian options

Since the distribution of the arithmetic average is unknown even under very simple model assumptions for the underlying's price (e.g. geometric Brownian motion), simple exact closed form solutions does not exist for the price of arithmetic average Asian options. Several techniques based on moments, lower and upper bounds and Monte Carlo simulation have been proposed in literature to approximate their value under different dynamics for the price process (see, for example, Section 1.5 for the case of Black-Scholes model, or Fusai and Kyriakou, 2016 for alternative models). In this chapter, since we are dealing with a very involved dynamics for the log-returns, we consider Monte Carlo methods. The simulation of a Hawkes process is not a trivial task, Ogata (1981) and Dassios and Zhao (2013) present exact schemes, with the latter outperforming the former in terms of runtime speed. Despite that, such method is still very time consuming, as a result, we choose to simulate the SDE in (5.2) using the Euler scheme[2]. This choice reduces drastically the computing time, but introduces a large discretization error. Consequently, crude Monte Carlo simulation is not a convenient choice and can be only used as benchmark (a very fine discretization grid and a large number of simulations is needed to achieve a good accuracy). Runtime-accuracy performances can be highly improved by using control variates methods, which are easily implementable in our context thanks to the availability of a semi-closed form solution for the price of geometric (fixed and floating) strike Asian option (see Kemna and Vorst, 1990 and Fu *et al.*, 1999).

More specifically, let's denote with $A(T) := \frac{1}{T}\int_0^T S(t)dt$ the arithmetic average of the price process, the value of fixed and average strike arithmetic Asian option can be computed, respectively, as:

$$p_{AFS} = e^{-rT}\mathrm{E}^0\left[(A(T)-K)^+ + \zeta_1\left((G(T)-K)^+ - p_{GFS}\right)\right], \tag{5.20}$$

$$p_{AAS} = e^{-rT}\mathrm{E}^0\left[(S(T)-A(T))^+ + \zeta_2\left((S(T)-G(T))^+ - p_{GAS}\right)\right] \tag{5.21}$$

where p_{GFS} and p_{GAS} are computed as in (5.13) and (5.14), the control variates coefficients $\zeta_{1,2}$ are estimated, following Glasserman (2004) and Cont and Tankov (2004), running pilot simulations[3].

5.4 Numerical results

Numerical results are provided in this section. We start by identifying some parameter settings taken from literature for the model specified by equations (5.1) and (5.2). By using the *peaks over treshold* method, Hainaut and Moraux (2018) calibrate the model specified by equations (5.1) and (5.2) on the S&P 500 index, we consider three different

[2]The author acknowledges Luca Gonzato for helpful discussions on the simulation of Hawkes processes.
[3]In particular we are using here 10^2 pilot simulations.

Table 5.1: Parameter settings in literature for the model in (5.1) and (5.2).

	r	σ	α	θ	η	p	ρ^+	ρ^-
A	0.05	0.12	14.71	4.68	244.82	0.36	42.74	-46.17
B	0.05	0.12	14.71	5.57	291.36	0.37	35.58	-39.01
C	0.05	0.12	14.71	6.44	337.08	0.37	30.47	-33.90

Figure 5.1: Probability density functions of $X(T)$ (left subplot) and $\frac{Y(T)}{T}$ (right subplot)

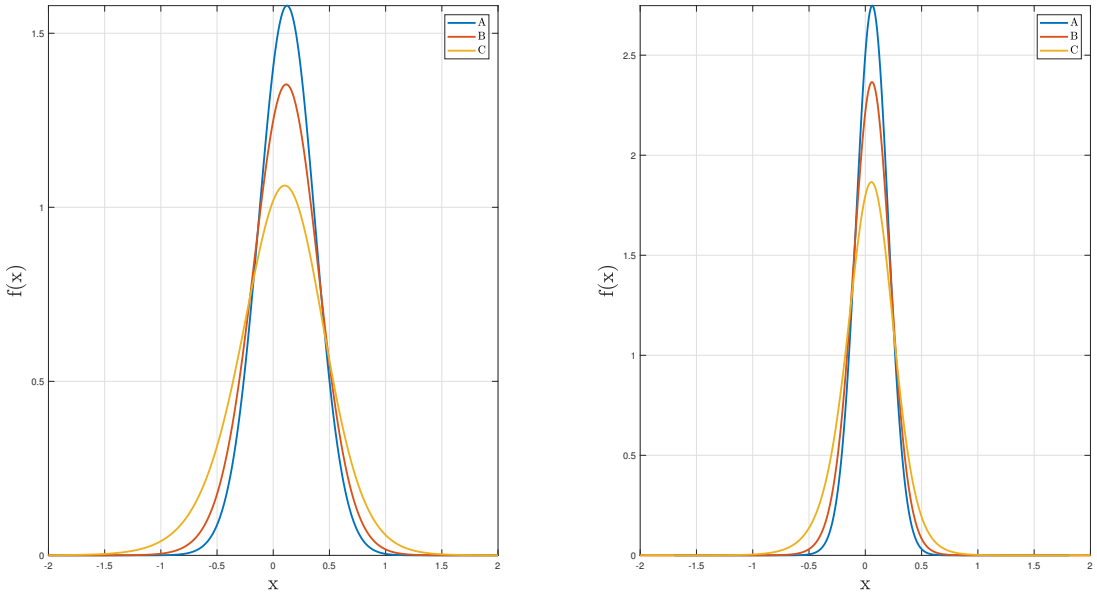

Legend: parameter settings as in Table 5.1, final date $T = 3$ years.

parameter settings taken from their results (these are summarized in Table 5.1). We note immediately that jumps are very frequent (parameter η is very high) and that since positive jumps are rarer than negative, the resulting distribution of the log-returns (and, as a consequence, of the average returns) presents elevated kurtosis and heavy left tail. The resulting probability density function for the parameter settings in Table 5.1 is shown in Figure 5.1.

Secondly, we implement the following numerical exercise: compute the price of European and geometric Asian (fixed and floating strike) call options through Monte Carlo (which is used as benchmark) and COS method. Following Hubalek and Sgarra (2011) we consider five different strikes $K = \{80, 90, 100, 110, 120\}$ and three different maturities $T = \{1, 2, 3\}$ years. Prices are computed using the COS method with characteristic functions as in Proposition 5.2 and Lemma 5.2, and ODEs systems characterizing the characteristic functions are solved numerically using an explicit Runge-Kutta (4,5) formula[4]. Absolute and relative tolerances are set equal to, respectively, 10^{-9} and 10^{-10}.

The truncation range is computed as in formula (A.5) and infinite summations are

[4]We use the built-in Matlab® function `ode45`.

Table 5.2: Price and confidence interval of European call options for different strikes and maturities calculated through Monte Carlo simulation and the COS method

	$T=1$		$T=2$		$T=3$	
	95% C.I.	COS	95% C.I.	COS	95% C.I.	COS
			A			
$K=80$	(24.0513,24.1074)	24.0884	(28.0686,28.1478)	28.1007	(31.7868,31.8841)	31.8421
$K=90$	(15.3780,15.4297)	15.4152	(20.1502,20.2240)	20.1798	(24.3599,24.4520)	24.4117
$K=100$	(8.3931,8.4356)	8.4297	(13.4922,13.5574)	13.5210	(17.9296,18.0138)	17.9752
$K=110$	(3.8473,3.8778)	3.8785	(8.4248,8.4791)	8.4509	(12.6910,12.7653)	12.7309
$K=120$	(1.5052,1.5246)	1.5241	(4.9345,4.9773)	4.9547	(8.6674,8.7310)	8.7028
CPU	115.1754	1.0911	212.1326	1.0728	368.1458	1.0472
			B			
$K=80$	(24.2826,24.3473)	24.3422	(28.5492,28.6411)	28.6035	(32.4618,32.5757)	32.5067
$K=90$	(15.9370,15.9961)	15.9928	(21.0221,21.1077)	21.0759	(25.4458,25.5534)	25.4915
$K=100$	(9.2439,9.2935)	9.2918	(14.7122,14.7887)	14.7649	(19.3928,19.4919)	19.4373
$K=110$	(4.7346,4.7724)	4.7742	(9.8167,9.8824)	9.8657	(14.4075,14.4968)	14.4480
$K=120$	(2.1988,2.2257)	2.2275	(6.2912,6.3457)	6.3318	(10.4701,10.5489)	10.5071
CPU	115.0458	1.1361	213.0240	1.0222	384.1418	1.0120
			C			
$K=80$	(24.9868,25.0674)	25.0330	(29.8733,29.9914)	29.9447	(34.2306,34.3800)	34.2774
$K=90$	(17.1450,17.2189)	17.1854	(22.9766,23.0872)	23.0442	(27.8994,28.0414)	27.9413
$K=100$	(10.8308,10.8950)	10.8673	(17.1704,17.2717)	17.2340	(22.4243,22.5576)	22.4591
$K=110$	(6.3776,6.4307)	6.4083	(12.5303,12.6212)	12.5877	(17.8197,17.9434)	17.8490
$K=120$	(3.6082,3.6509)	3.6318	(8.9902,9.0706)	9.0398	(14.0420,14.1558)	14.0666
CPU	114.5119	1.0286	228.2773	1.0843	354.4452	1.0414

Legend: Parameter setting as in Table 5.1 and initial price is $S(0)=100$. Monte Carlo simulation is implemented using 10^6 simulations and discretizing the time grid with $1000 \cdot T$ equally spaced points. COS is implemented truncating infinite summations at 2^7, CPU time is expressed in seconds.

truncated at $N=2^7$. In Table 5.2 we show the price of the European call option computed through Monte Carlo simulation and the COS method. We note that both procedures are very accurate with the COS price always falling into the confidence interval provided by Monte Carlo. In Table 5.3 we show the same results regarding the geometric (fixed and floating strike) Asian call option. We note that Monte Carlo is less accurate in this situation (this is particularly evident looking at the price of the floating strike Asian options) and the bias is certainly due to time discretization.

We also investigate the sensitivity of the price of the fixed strike Geometric Asian call options on the Hawkes process parameters (α, θ and η), see Figure 5.2. We note that the parameter α (which indicates the speed of mean reversion of the Hawkes process) impacts negatively the call option price, indeed, the higher α, the lower the expected number of jumps (and, consequently, the variance of the distribution at maturity of the average of log-returns). A similar argument holds for the long run mean jump intensity θ and the parameter η (which controls the magnitude of jumps in the marked Hawkes process).

Finally, we exploit availability of geometric Asian call options values in order to price arithmetic Asian call options through the control variates method (see formulas (5.20)

Table 5.3: Price and confidence interval of geometric (fixed and floating strike) Asian call options for different strikes and maturities calculated through Monte Carlo simulation and the COS method

	$T = 1$		$T = 2$		$T = 3$	
	95% C.I.	COS	95% C.I.	COS	95% C.I.	COS
			A			
$K = 80$	(21.2443,21.2761)	21.2705	(22.4207,22.4646)	22.4542	(23.5066,23.5588)	23.5395
$K = 90$	(11.9546,11.9848)	11.9971	(13.8471,13.8881)	13.8929	(15.5058,15.5547)	15.5501
$K = 100$	(4.4014,4.4236)	4.4702	(6.8445,6.8775)	6.9026	(8.8503,8.8915)	8.9056
$K = 110$	(0.8707,0.8812)	0.9187	(2.5748,2.5963)	2.6254	(4.2865,4.3170)	4.3392
$K = 120$	(0.1031,0.1068)	0.1169	(0.7450,0.7567)	0.7743	(1.7697,1.7896)	1.8084
AS	(4.7818,4.8068)	4.7545	(7.6911,7.7301)	7.6840	(10.2945,10.3458)	10.2930
CPU - FS	115.0179	1.5225	212.1204	1.4365	368.0770	1.3121
CPU - AS	114.9270	1.0027	212.0176	1.4562	367.9541	1.6107
			B			
$K = 80$	(21.2016,21.2380)	21.2537	(22.3959,22.4464)	22.4557	(23.5062,23.5666)	23.5551
$K = 90$	(12.0750,12.1089)	12.1853	(14.0917,14.1382)	14.1983	(15.8227,15.8784)	15.9092
$K = 100$	(4.7785,4.8039)	4.9527	(7.3992,7.4370)	7.5511	(9.5109,9.5584)	9.6314
$K = 110$	(1.1896,1.2035)	1.3214	(3.1763,3.2028)	3.3244	(5.0800,5.1168)	5.2063
$K = 120$	(0.2266,0.2332)	0.2828	(1.1533,1.1699)	1.2556	(2.4438,2.4702)	2.5489
AS	(5.3466,5.3766)	5.2231	(8.5373,8.5840)	8.4416	(11.3337,11.3952)	11.2552
CPU - FS	115.0533	2.0634	213.0202	1.7715	384.0936	1.6361
CPU - AS	114.9365	1.0327	212.9111	1.3264	383.9907	1.6529
			C			
$K = 80$	(21.1833,21.2270)	21.3327	(22.4272,22.4893)	22.6529	(23.5980,23.6731)	23.8174
$K = 90$	(12.3513,12.3911)	12.6791	(14.6083,14.6647)	14.9734	(16.4880,16.5568)	16.8109
$K = 100$	(5.3968,5.4277)	5.8742	(8.3759,8.4230)	8.8429	(10.7006,10.7606)	11.0980
$K = 110$	(1.7385,1.7583)	2.1507	(4.2506,4.2869)	4.7130	(6.4915,6.5411)	6.9008
$K = 120$	(0.5110,0.5229)	0.7561	(1.9950,2.0215)	2.3645	(3.7471,3.7867)	4.1116
AS	(6.4647,6.5055)	6.0223	(10.2901,10.3548)	9.8779	(13.5475,13.6340)	13.1777
CPU - FS	114.5002	2.2244	228.2661	2.2353	354.3970	1.7965
CPU - AS	114.3982	1.0126	228.1672	1.3011	354.2999	1.6413

Legend: "FS" denotes "Fixed Strike", "AS" denotes "Average Strike". Further notes: refer to Table 5.2.

Figure 5.2: Price of fixed strike Geometric Asian options for different α, θ and η

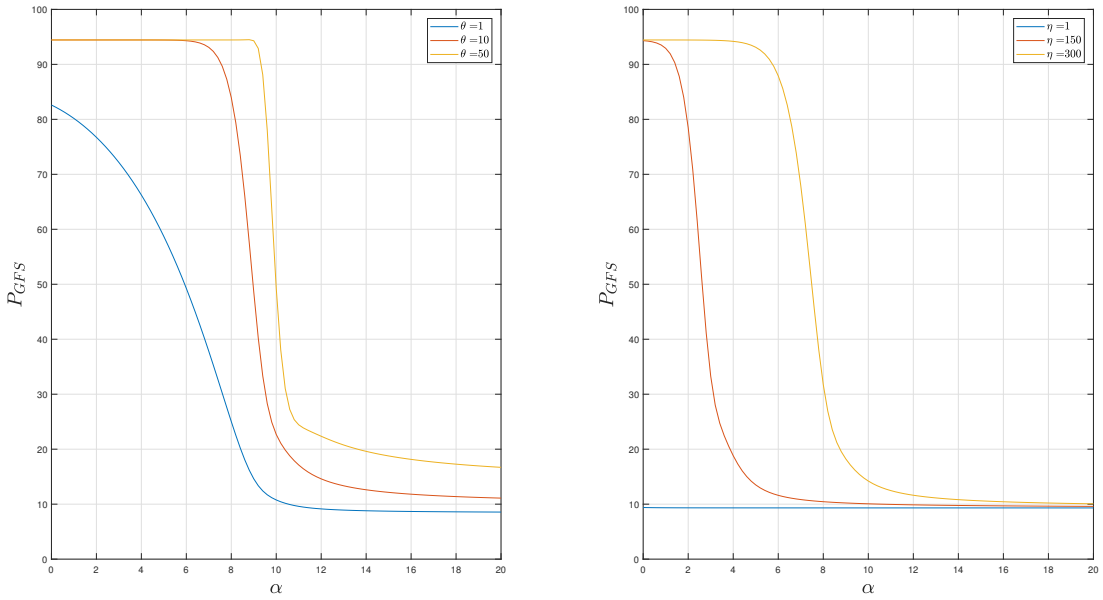

Legend: other parameters are as in parameter setting "C" (see Table 5.1) with maturity $T = 3$ years.

and (5.21)). The numerical results are reported in Table 5.4. The usage of control variates method allows to reduce significantly the number of simulations required to get a good estimate of the price (indeed we use 10^5 simulations instead of 10^6 as in Tables 5.2 and 5.3) and to reduce the time discretization bias.

5.5 Conclusions

With the aim of taking into account the jump clustering phenomena widely observed in financial markets, we model the log-returns dynamics of the underlying asset through a self-exciting jump diffusion model of Hawkes-type and, by exploiting the affine features of the model considered, we derive the characteristic function of the arithmetic average of log-returns in the form of the solution of an ODEs system. By starting with this general result as a building block, we derive semi-closed form solutions for geometric (fixed and floating strike) Asian options under this model by applying the COS method. We evaluate accuracy and efficiency of such approach through an extensive numerical study based on the usage of Monte Carlo simulation as a benchmark. Numerical results show that the proposed pricing method is fast and accurate. Finally, we show that this closed form solutions can be easily incorporated into a Monte Carlo simulation as control variables, allowing for an efficient pricing of arithmetic Asian options as well.

Table 5.4: Price and confidence interval of arithmetic (fixed and floating strike) Asian call options for different strikes and maturities calculated through Monte Carlo simulation with geometric average counterpart used as control variable

	$T=1$			$T=2$			$T=3$		
	Price	SE $\cdot 10^5$	95% C.I.	Price	SE $\cdot 10^5$	95% C.I.	Price	SE $\cdot 10^5$	95% C.I.
					A				
$K=80$	21.3591	0.2717	(21.3575,21.3608)	22.7841	0.6134	(22.7803,22.7879)	24.0815	0.9161	(24.0758,24.0872)
$K=90$	12.0743	0.3353	(12.0722,12.0763)	14.1945	0.6795	(14.1903,14.1987)	16.0526	1.0277	(16.0463,16.0590)
$K=100$	4.5373	0.4301	(4.5346,4.5399)	7.1622	0.8264	(7.1571,7.1673)	9.3531	1.1462	(9.3460,9.3602)
$K=110$	0.9676	0.3950	(0.9651,0.9700)	2.8228	0.9250	(2.8171,2.8286)	4.7074	1.2150	(4.6999,4.7150)
$K=120$	0.1315	0.3394	(0.1294,0.1336)	0.8875	0.8663	(0.8821,0.8928)	2.0706	1.1831	(2.0633,2.0779)
AS	4.6855	0.3852	(4.6831,4.6879)	7.4333	0.7735	(7.4285,7.4381)	9.8557	1.2261	(9.8481,9.8633)
CPU - FS		13.2173			26.5489			59.0626	
CPU - AS		12.4671			25.0717			37.6292	
					B				
$K=80$	21.4056	0.3696	(21.4033,21.4078)	22.9016	0.7821	(22.8967,22.9064)	24.2635	1.3712	(24.2550,24.2720)
$K=90$	12.3136	0.4271	(12.3110,12.3163)	14.5958	0.8681	(14.5905,14.6012)	16.5550	1.4746	(16.5458,16.5641)
$K=100$	5.0572	0.5528	(5.0537,5.0606)	7.8899	0.9723	(7.8838,7.8959)	10.2040	1.5753	(10.1942,10.2138)
$K=110$	1.3925	0.6387	(1.3885,1.3965)	3.5906	1.0223	(3.5842,3.5969)	5.6863	1.6242	(5.6762,5.6964)
$K=120$	0.3030	0.7985	(0.2981,0.3080)	1.4321	0.8834	(1.4266,1.4375)	2.9134	1.5680	(2.9037,2.9231)
AS	5.1130	0.5356	(5.1096,5.1163)	8.1028	0.9736	(8.0967,8.1088)	10.6837	1.6420	(10.6736,10.6939)
CPU-FS		13.1373			24.7512			38.7536	
CPU-AS		12.5227			23.0554			37.1071	
					C				
$K=80$	21.6181	0.6944	(21.6138,21.6224)	23.3743	1.4701	(23.3652,23.3835)	24.9273	3.2365	(24.9073,24.9474)
$K=90$	12.9109	0.8226	(12.9058,12.9160)	15.6038	1.6275	(15.5937,15.6139)	17.8027	3.3642	(17.7819,17.8236)
$K=100$	6.0463	0.9975	(6.0401,6.0525)	9.3784	1.7325	(9.3677,9.3892)	11.9704	3.4279	(11.9491,11.9916)
$K=110$	2.2626	1.0850	(2.2558,2.2693)	5.1484	1.7614	(5.1375,5.1594)	7.6505	3.4157	(7.6293,7.6716)
$K=120$	0.8031	1.1175	(0.7962,0.8100)	2.6882	1.7041	(2.6776,2.6987)	4.7280	3.2948	(4.7075,4.7484)
AS	5.8049	1.0628	(5.7983,5.8115)	9.3295	2.0474	(9.3168,9.3422)	12.2271	4.8515	(12.1970,12.2571)
CPU - FS		15.7604			23.0520			41.6911	
CPU - AS		13.5132			22.7089			37.5917	

Legend: Prices computed according to (5.20) and (5.21). Further notes: refer to Tables 5.2 and 5.3.

Appendix

A The COS method

Consider a model where the underlying's price at time T is given by $S(T) = S(0)e^{X(T)}$, where $X(T)$ is the distribution of log-returns at maturity. The COS method allows to price efficiently European-style options given only the knowledge of the characteristic function of $X(T)$. Suppose to have an European option, whose price can be computed according to

$$p = e^{-rT}\mathrm{E}[(S(T) - K)^+] = e^{-rT}\int_0^\infty (S(0)e^x - K)^+ f_X(x)dx \tag{A.1}$$

Given a characteristic function (denoted with $\phi(\cdot)$), the probability density function (pdf in the following) can be computed as follows:

$$f(x) = \frac{1}{2\pi}\int_{\mathbb{R}} e^{-iux}\phi(u)du. \tag{A.2}$$

Several algorithms can be used to solve the integral in (A.2), we refer to Fang and Oosterlee (2008) for a review. Among them, the best performances are obtained through the COS method, where the inverse Fourier integral in (A.2) is computed via cosine expansion and the pdf is approximated as follows:

$$f(x) = \sum_{k=1}^{\infty} F_k \cos\left(k\pi\frac{x-a}{b-a}\right) + \frac{1}{b-a} \approx \sum_{k=1}^{N-1} F_k \cos\left(k\pi\frac{x-a}{b-a}\right) + \frac{1}{b-a}, \tag{A.3}$$

where $F_k = \frac{2}{b-a}\mathrm{Real}\left(\phi\left(\frac{k\pi}{b-a}\right)\cdot\exp\left(-i\frac{ka\pi}{b-a}\right)\right)$ and $[a,b] \in \mathbb{R}$ is chosen such that:

$$\int_a^b e^{iux} f(x)ds \approx \int_{\mathbb{R}} e^{iux} f(x)dx. \tag{A.4}$$

In other words, in order to implement the COS method is necessary to truncate the domain of the pdf through a suitable choice of a and b. In order to do that, Fang and

Oosterlee (2008) propose the following formulas:

$$a = c_1 - L\sqrt{c_2 + \sqrt{c_4}}, \quad b = c_1 + L\sqrt{c_2 + \sqrt{c_4}} \tag{A.5}$$

where L can be chosen arbitrary large and c_i denotes the $i-th$ cumulant of $\ln\left(\frac{S(T)}{K}\right)$. Since cumulants can be expressed as functions of moments, the choice of the truncation range is related to the moments of log-returns. Hence, given the characteristic function of log-returns, the pdf can be recovered from formula (A.3). Given the pdf, the price of the option can be computed from equation (A.1) by computing the integral numerically, for example using the trapezoidal method.

B Laplace transforms

In this appendix, we provide explicit expressions for the Laplace transforms of the time-integral of the variance (its reciprocal for the SABR model) conditional on the level of volatility at the endpoints of the time interval $[u, t]$ (and the integrated volatility in the case of the OU-SV model).

B.1 Heston model

The Laplace transform of the conditional integrated variance is

$$\begin{aligned}\mathcal{L}(a) &= \mathrm{E}\left[\exp\left(-a\int_u^t \sigma^2(s)ds\right)\middle|\,\sigma(u),\sigma(t)\right] = \frac{\gamma(a)e^{-(\gamma(a)-k)(t-u)/2}(1-e^{-k(t-u)})}{k(1-e^{-\gamma(a)(t-u)})}\times \\ &\exp\left\{\frac{\sigma^2(u)+\sigma^2(t)}{v^2}\left(\frac{k(1+e^{-k(t-u)})}{1-e^{-k(t-u)}} - \frac{\gamma(a)(1+e^{-\gamma(a)(t-u)})}{1-e^{-\gamma(a)(t-u)}}\right)\right\}\times \\ &\frac{I_{d/2-1}\left(\sigma(u)\sigma(t)\frac{4\gamma(a)e^{-\gamma(a)(t-u)/2}}{v^2(1-e^{-\gamma(a)(t-u)})}\right)}{I_{d/2-1}\left(\sigma(u)\sigma(t)\frac{4ke^{-k(t-u)/2}}{v^2(1-e^{-k(t-u)})}\right)},\end{aligned} \tag{B.1}$$

where $\gamma(a) := \sqrt{k^2 + 2v^2 a}$ and $I_\nu(\cdot)$ denotes the modified Bessel function of the first kind.

Aiming to speed up random sampling from the conditional distribution of the integrated variance, as we explain later, Glasserman and Kim (2011) provide an alternative characterization for it:

$$\left(\int_u^t \sigma^2(s)ds\middle|\,\sigma(u),\sigma(t)\right) \overset{\mathcal{D}}{=} X_1 + X_2 + \sum_{j=1}^{\eta} Z_j, \tag{B.2}$$

where $X_1, X_2, \eta, Z_1, Z_2, ...$ are mutually independent random variables, Z_j are independent

copies of a random variable Z, and η is a Bessel random variable with parameters

$$\nu := \frac{d}{2} - 1, \quad z := \frac{2k}{v^2 \sinh\left(\frac{k(t-u)}{2}\right)} \sigma(u)\sigma(t).$$

X_1, X_2 and Z have the representations:

$$X_1 \stackrel{\mathcal{D}}{=} \sum_{n=1}^{\infty} \frac{1}{\gamma_n} \sum_{j=1}^{N_n} \mathrm{Exp}_j(1), \quad X_2 \stackrel{\mathcal{D}}{=} \sum_{n=1}^{\infty} \frac{\Gamma_n(\frac{d}{2}, 1)}{\gamma_n}, \quad Z \stackrel{\mathcal{D}}{=} \sum_{n=1}^{\infty} \frac{\Gamma_n(2, 1)}{\gamma_n},$$

where $\gamma_n := (k^2(t-u)^2 + 4\pi^2 n^2)/(2v^2(t-u)^2)$, N_n are independent Poisson random variables with mean $16\pi^2 n^2(\sigma^2(u) + \sigma^2(t))/(v^2(t-u)(k^2(t-u)^2 + 4\pi^2 n^2))$, $\mathrm{Exp}_j(1)$ are independent exponential random variables with mean 1, and $\Gamma_n(a, b)$ are independent gamma random variables with shape parameter a and scale parameter b. Moreover, the Laplace transforms of X_1, X_2 and Z are given by

$$\mathcal{L}_{X_1}(a) = \exp\left\{ \frac{\sigma^2(u) + \sigma^2(t)}{v^2} \left(k \coth \frac{k(t-u)}{2} - L(a) \coth \frac{L(a)(t-u)}{2} \right) \right\}, \tag{B.3}$$

$$\mathcal{L}_{X_2}(a) = \left(\frac{L(a) \sinh \frac{k(t-u)}{2}}{k \sinh \frac{L(a)(t-u)}{2}} \right)^{\frac{d}{2}}, \tag{B.4}$$

$$\mathcal{L}_{Z}(a) = \left(\frac{L(a) \sinh \frac{k(t-u)}{2}}{k \sinh \frac{L(a)(t-u)}{2}} \right)^{2}, \tag{B.5}$$

where $L(a) := \sqrt{2v^2 a + k^2}$. The proposed decomposition (B.2) by Glasserman and Kim (2011) enjoys a speed-up gain compared to the original Broadie and Kaya (2006) as, from (B.4)–(B.5), the Laplace transforms of X_2 and Z do not depend on the level of the variance at the endpoints of the time interval $[u, t]$, therefore they are numerically inverted once and stored in the initialization of the Monte Carlo simulation. Also, generating samples $(X_1 | \sigma(u), \sigma(t))$ based on inversion of (B.3) is faster as it does not involve evaluation of a special function.

B.2 SABR model

The Laplace transform of the conditional reciprocal of the integrated variance is

simulation

$$\begin{aligned} \mathcal{L}(a) &= \mathrm{E}\left[\exp\left\{ -a \left(\int_u^t \sigma^2(s) ds \right)^{-1} \right\} \middle| \sigma(u), \sigma(t) \right] \\ &= \exp\left\{ -\frac{g\left(\ln \frac{\sigma(t)}{\sigma(u)}, \frac{av^2}{\sigma(u)^2} \right)^2 - \ln\left(\frac{\sigma(t)}{\sigma(u)} \right)^2}{2v^2(t-u)} \right\}, \end{aligned} \tag{B.6}$$

where $g(x,\lambda) := \operatorname{arcosh}(\lambda e^{-x} + \cosh(x))$.

B.3 OU-SV model

The Laplace transform of the conditional integrated variance is

$$\mathcal{L}(a) = \mathrm{E}\left[\exp\left(-a\int_u^t \sigma^2(s)ds\right)\middle|\, \sigma(u), \sigma(t), \int_u^t \sigma(s)ds\right] = \frac{f(\sqrt{k^2+2av^2})}{f(k)}, \qquad \text{(B.7)}$$

where

$$f(x) := \frac{x^2}{2\pi\sqrt{\eta(x)}}\exp\left\{-\frac{1}{2\eta(x)v^2}\left[2x^2\left((\sigma(t)+\sigma(u))\int_u^t \sigma(s)ds - \sigma(u)\sigma(t)(t-u)\right)+\right.\right.$$
$$x^2\left((\sigma^2(t)+\sigma^2(u))(t-u) - 2(\sigma(t)+\sigma(u))\int_u^t \sigma(s)ds\right)\cosh(x(t-u))+$$
$$\left.\left. x\left(x^2\left(\int_u^t \sigma(s)ds\right)^2 - (\sigma(t)-\sigma(u))^2\right)\sinh(x(t-u))\right]\right\}$$

and

$$\eta(x) := 2 - 2\cosh(x(t-u)) + x(t-u)\sinh(x(t-u)).$$

C Mathematica® codes

C.1 Proposition 2.1

The following is the code for implementing formula (2.10) in the case where the BDLP is the Brownian motion, i.e. $\psi(u) := \frac{u^2\sigma^2}{2}$. Alternative $\psi(\cdot)$ can be found in Table 2.1.

```
(*Define the function f(t,s) *)
f[t_, s_] := Exp[-a*(t - s)];
(*Define the logarithm of the moment generating function psi(u) *)
psi[u_] := u^2*sg^2/2;
(* set variable n*)
n = 12;
(* implement formula 3.10 *)
Exp[Sum[((Integrate[
      psi[(Sum[gam[k]*f[t[i], s], {k, j, n}])], {s,t[j-1],t[j]}]]
```

C.2 Cumulants in formula (5.16)

The following is the code for computing the first $M-1$ cumulants in (5.16). We assume here, without loss of generality, that $X(0) = 0$.

```
(* M denotes the number of desired cumulants - 1*)
M=5
(* Define joint moment generating function, see Proposition 3.6*)
psi[z1_,z2_]:=p*rp/(rp-(z1+z2)) + (1-p)*rm/(rm-(z1 - z2))
(* Define functional characteristic, see Proposition 3.6*)
F[u_,tau_]:= -(-a*th*B[u,tau]-(r-sg^2/2)*u - sg^2/2*u^2);
R[u_,tau_]:=-(a*B[u,tau]+k*u-(psi[u,B[u,tau]*eta]-1));
(* Compute cumulants *)
For[i=1,i<M,i++,
Print[i];
(* Compute derivative of R with respect to u*)
Rprime = D[R[u,tau],{u,i}]/.{D[B[u,tau],{u,i}]->y[t],D[B[u,tau],{u,n_}]
->Part[fvect,n]}/.u->0/.B[0,tau]->0;
(* Solve the first order linear ODE*)
sol =DSolve[{y'[t]==Rprime, y[0]==0},y[t],t];
f[t_]:=y[t]/.sol[[1]];
(* Save the value of f[t] in a list for later usage in the for cycle*)
If[i>1,fvect = Append[fvect,f[t]],fvect=List[f[t]]];
Print[DB[i]];
Print[Simplify[f[t]]];
(* Compute derivative of F with respect to u*)
Fprime = D[F[u,tau],{u,i}]/.D[B[u,tau],{u,i}]->f[t]/.u->0/.B[0,tau]->0;
(* Solve ODE by passing to the integral *)
func[C_]:=Integrate[Fprime,t ]+C/.t->0;
sol2 = Solve[func[C]== 0,C];
Cstar =C/.sol2[[1]];
Print[DA[i]];
Print[Simplify[Simplify[Integrate[Fprime,t]+Cstar]]];
(* i-th cumulant is now given by DA[i] + theta*DB[i])*)
]
```

Bibliography

Abate, J. and Whitt, W. (1995) Numerical inversion of Laplace transforms of probability distributions. *ORSA Journal on Computing*, **7**, 36–43.

Abramowitz, M. and Stegun, I. A. (1968) *Handbook of Mathematical Functions with Formulas, Graphs, and Mathematical Tables*. Dover Books on Mathematics, Dover, New York, 2 edn.

Ait-Sahalia, Y., Chaco-Diaz, S. and Laeven, R. (2015) Modelling financial contagion using mutually exciting jump processes. *Journal of Financial Economics*, **117**, 585–606.

Akhiezer, N. I. (1965) *The Classical Moment Problem: And Some Related Questions in Analysis*. University mathematical monographs. Oliver & Boyd.

Albrecher, H. and Predota, M. (2004) On Asian option pricing for NIG Lévy processes. *Journal of Computational and Applied Mathematics*, **172**, 153–168.

Amos, D. E. and Daniel, S. L. (1971) Tables of percentage points of standardized Pearson distributions. *Record Report SC-RR-710348, Sandia Laboratories, Albuquerque, New Mexico*.

Andersen, L. (2008) Simple and efficient simulation of the Heston stochastic volatility model. *Journal of Computational Finance*, **11**, 1–42.

Andersen, T., Fusari, N. and Todorov, V. (2015) The risk premia embedded in index options. *Journal of Financial Economics*, **117**, 558–584.

B. C. of Banking Supervision, B. I. (2011) A global regulatory framework for more resilient banks and banking system. *Bank for International Settlements, Techincal Report*, **28**.

Bacry, E., Delattre, S., Hoffman, M. and Muzy, J. (2013) Modelling microstructure noise by mutually exciting point processes. *Quantitative Finance*, **13**, 65–77.

Bakshi, G., Cao, C. and Chen, Z. (1997) Empirical performance of alternative option pricing models. *The Journal of Finance*, **52**, 2003–2049.

Bakshi, G., Kapadia, N. and Madan, D. (2003) Stock return characteristics, skew laws and the differential pricing of individual equity options. *Review of Financial Studies*, **16**, 101–143.

Bakshi, G. and Madan, D. (2000) Spanning and derivative security valuation. *Journal of Financial Economics*, **55**, 205–238.

Ballotta, L. (2010) Efficient pricing of ratchet equity-indexed annuities in a variance-gamma economy. *North American Actuarial Journal*, **14**, 355–368.

Ballotta, L., Fusai, G. and Marena, M. (2016) A gentle introduction to default risk and counterparty credit modelling. *Available at SSRN:* `http://dx.doi.org/10.2139/ssrn.2816355`.

Ballotta, L., Gerrard, R. and Kyriakou, I. (2017) Hedging of Asian options under exponential Lévy models: computation and performance. *The European Journal of Finance*, **23**, 297–323.

Ballotta, L. and Kyriakou, I. (2014) Monte Carlo simulation of the CGMY process and option pricing. *Journal of Futures Markets*, **34**, 1095–1121.

Barndorff-Nielsen, O., Nicolato, E. and Shephard, N. (2002) Some recent developments in stochastic volatility modelling. *Quantitative Finance*, **2**, 11–23. Special issue on volatility modelling.

Barndorff-Nielsen, O. and Shephard, N. (2001) Non-Gaussian Ornstein-Uhlenbeck-based models and some of their uses in financial economics. *Journal of the Royal Statistical Society. Series B. Statistical Methodology*, **63**, 167–241.

Barone-Adesi, G. and Whaley, R. (1987) Efficient analytic approximation of American option values. *Journal of Finance*, **42**, 301–320.

Basu, S., Gil, M. and Auddy, S. (2015) The MLP distribution: a modified lognormal power-law model for the stellar initial mass function. *Monthly Notices of the Royal Astronomical Society*, **449**, 2413–2420.

Bates, D. (1996a) Jumps and stochastic volatility: The exchange rate processes implicit in Deutsche Mark options. *Review of Financial Studies*, **9**, 69–107.

Bates, D. (2000) Post-'87 crash fears in the S&P 500 futures option market. *Journal of Econometrics*, **94**, 181–238.

Bates, D. S. (1996b) Dollar jump fears, 1984-1992: Distributional abnormalities implicit in currency futures options. *Journal of International Money and Finance*, **15**, 65–93.

Benth, F. E., Di Persio, L. and Lavagnini, S. (2018) Stochastic modeling of wind derivatives in energy markets. *Risks*, **6**, article number 56.

Benth, F. E. and Šaltytė-Benth, J. (2004) The normal inverse Gaussian distribution and spot price modelling in energy markets. *International Journal of Theoretical and Applied Finance*, **7**, 177–192.

Benth, F. E. and Šaltytė-Benth, J. (2005) Stochastic modelling of temperature variations with a view towards weather derivatives. *Applied Mathematical Finance*, **12**, 53–85.

Bertsimas, D., Popescu, I. and Sethuraman, J. (2000) Moment problems and semidefinite programming. *Handbook on semidefinite programming: Theory, Algorithms, and Applications*, 469–509.

Bessembinder, H., Coughenour, J. F., Seguin, P. J. and Smoller, M. M. (1995) Mean reversion in equilibrium asset prices: Evidence from the futures term structure. *The Journal of Finance*, **50**, 361–375.

Bharucha-Reid, A. T. (1960) *Elements of the Theory of Markov Processes and Their Applications*. Dover Books on Mathematics. Mineola, New York: Dover Publications.

Börger, R., Cartea, Á., Kiesel, R. and Schindlmayr, G. (2009) Cross-commodity analysis and applications to risk management. *The Journal of Futures Markets*, **29**, 197–217.

Bouver, H. and Bargmann, R. E. (1974) Tables of the standardized percentage points of the Pearson system of curves in terms of β_1 and β_2. *Technical Report No. 107, University of Georgia*.

Brignone, R. and Sgarra, C. (Forthcoming) Asian options pricing in Hawkes-type jump-diffusion models. *Annals of Finance*.

Brigo, D. and Mercurio, F. (2006) *Interest Rate Models: Theory and Practice with Smile, Inflation and Credit*. 2nd ed. New York: Springer Verlag.

Brigo, D., Mercurio, F., Rapisarda, F. and Scotti, R. (2004) Approximated moment-matching for basket-options pricing. *Quantitative Finance*, **4**, 1–16.

Brigo, D., Morini, M. and Pallavicini, A. (2013) *Counterparty Credit Risk, Collateral and Funding*. Wiley, Chichester, U.K.

Broadie, M., Glasserman, P. and Kou, S. G. (1999) Connecting discrete and continuous path-dependent options. *Finance and Stochastics*, **3**, 55–82.

Broadie, M. and Kaya, O. (2006) Exact simulation of stochastic volatility and other affine jump diffusion processes. *Operations Research*, **54**, 217–231.

Cai, N. and Kou, S. G. (2011) Option pricing under a mixed-exponential jump diffusion model. *Management Science*, **57**, 2067–2081.

Cai, N., Li, C. and Shi, C. (2014) Closed-form expansions of discretely monitored Asian options in diffusion models. *Mathematics of Operations Research*, **39**, 789–822.

Cai, N., Song, T. and Chen, N. (2017) Exact simulation of the SABR model. *Operations Research*, **65**, 931–951.

Canabarro, E. and Duffie, D. (2003) *Measuring and marking counterparty risk, in Asset/Liability Management for Financial Institutions*. Institutional Investor Books.

Carr, P., Geman, H., Madan, D. and Yor, M. (2003) Stochastic volatility for Lévy processes. *Mathematical Finance*, **13**, 345–382.

Carr, P. and Madan, D. (1999) Option valuation using the fast Fourier transform. *Journal of Computational Finance*, **2**, 61–73.

Carr, P. and Wu, L. (2004) Time-changed Lévy processes and option pricing. *Journal of Financial Economics*, **71**, 113–141.

Carson, J. M., Doran, J. S. and Peterson, D. (2006) Market crash risk and implied volatility skewness: Evidence and implications for insurer investments. Working paper, Florida State University.

Černý, A. and Kyriakou, I. (2011) An improved convolution algorithm for discretely sampled Asian options. *Quantitative Finance*, **11**, 381–389.

Chang, C. C. and Tsao, C. (2011) Efficient and accurate quadratic approximation methods for pricing Asian strike options. *Quantitative Finance*, **11**, 729–748.

Chen, B., Oosterlee, C. W. and van der Heide, H. (2012) A low-bias simulation scheme for the SABR stochastic volatility model. *International Journal of Theoretical and Applied Finance*, **15**, 125–161.

Choudhury, G. L. and Lucantoni, D. M. (1996) Numerical computation of the moments of a probability distribution from its transform. *Operations Research*, **44**, 368–381.

Christoffersen, P., Heston, S. and Jacobs, K. (2009) The shape and term structure of the index option smirk: Why multifactor stochastic volatility models work so well. *Management Science*, **55**, 1914–1932.

Cont, R. and Tankov, P. (2004) *Financial Modelling With Jump Processes*. Financial Mathematics Series. Boca Raton: Chapman & Hall/CRC.

Corrado, C. J. and Su, T. (1996) Skewness and kurtosis in S&P 500 index returns implied by option prices. *Journal of Financial Research*, **19**, 175–192.

Cox, J., Ingersoll, J. and Ross, S. (1985) A theory of the term structure of interest rates. *Econometrica*, **53**, 385–407.

Creemers, S. (2018) Moments and distribution of the net present value of a serial project. *European Journal of Operational Research*, **267**, 835–848.

Crépey, S. (2015) Bilateral counterparty risk under funding constraints – part 2: CVA. *Mathematical Finance*, **25**, 23–50.

Cummins, J. D. and Geman, H. (1993) An Asian option approach to the valuation of insurance futures contracts. Working Paper, Financial Institutions Center, The Wharton School, University of Pennsylvania.

D'Amico, M., Fusai, G. and Tagliani, A. (2003) Valuation of exotic options using moments. *Operational Research*, **2**, 157–186.

Dassios, A. and Zhao, H. (2013) Exact simulation of Hawkes process with exponentially decaying intensity. *Electronic Communications in Probability*, **18**, 1–13.

Davydov, D. and Linetsky, V. (2001) Pricing and hedging path-dependent options under the CEV process. *Management Science*, **47**, 949–965.

De Gennaro Aquino, L. and Bernard, C. (forthcoming) Closed-form prices for lookback and barrier options under the Heston model. *Decisions in Economics and Finance*.

DeMiguel, V., Plyakha, Y., Uppal, R. and Vilkov, G. (2011) Improving portfolio selection using option-implied volatility and skewness. Working paper, London Business School.

Deng, S. (1999) Stochastic models of energy commodity prices and their applications: Mean-reversion with jumps and spikes. In *Technical report, POWER*.

Devroye, L. (1986) *Non-Uniform Random Variate Generation*. Springer-Verlag, New York.

Diavatopoulos, D., Doran, J. S., Fodor, A. and Peterson, D. (2008) The information content of implied skewness and kurtosis changes prior to earnings announcements for stock and option returns. Working paper, Villanova University.

Doran, J. S., Peterson, D. and Tarrant, B. C. (2007) Is there information in the volatility skew? *Journal of Futures Markets*, **27**, 921–959.

Dothan, L. (1978) On the term structure of interest rates. *Journal of Financial Economics*, **6**, 59–69.

Driouchi, T., Bennett, D. and Battisti, G. (2006) Capacity planning under uncertainty: an Asian option approach. In *Proceedings of 10th Annual International Conference on Real Options*.

Duffie, D., Filipović, D. and Schachermayer, W. (2003) Affine processes and applications in finance. *The Annals of Applied Probability*, **13**, 984–1053.

Dufresne, D. (2000) Laguerre series for Asian and other options. *Mathematical Finance*, **10**, 407–428.

Eberlein, E. and Prause, K. (2002) The generalized hyperbolic model: financial derivatives and risk measures. *In H. Geman, D. Madan, S. Pliska, and T. Vorst (Eds.), Mathematical Finance, Bachelier Congress 2000, Springer*, 245–267.

Eberlein, E. and Raible, S. (1999) Term structure models driven by general Lévy processes. *Mathematical Finance*, **9**, 31–53.

Errais, E., Giesecke, K. and Goldberg, L. (2010) Affine point processes and portfolio credit risk. *SIAM Journal on Financial Mathematics*, **1**, 642–665.

Eydeland, A. and Wolyniec, K. (2003) *Energy and Power Risk Management: New Developments in Modeling, Pricing, and Hedging*. Wiley Finance. Hoboken, New Jersey: John Wiley & Sons, Inc.

Fang, F. and Oosterlee, C. (2008) A novel pricing method for European options based on Fourier-cosine series expansions. *SIAM Journal on Scientific Computing*, **31**, 826–848.

Fang, F. and Oosterlee, C. (2011) A Fourier-based valuation method for Bermudan and barrier options under Heston's model. *SIAM J. Financial Math.*, **2**, 439–463.

Feunou, B. and Okou, C. (2018) Risk-neutral moment-based estimation of affine option pricing models. *Journal of Applied Econometrics*, **33**, 1007–1025.

Filimonov, V., Bicchetti, D., Maystre, N. and Sornette, D. (2014) Quantification of the high level of endogeneity and of structural regime shifts in commodity markets. *Journal of International Money and Finance*, **42**, 174–192.

Filipović, D., Mayerhofer, E. and Schneider, P. (2013) Density approximations for multivariate affine jump-diffusion processes. *Journal of Econometrics*, **176**, 93–111.

Fu, M. C., Madan, D. B. and Wang, T. (1999) Pricing continuous Asian options: a comparison of Monte Carlo and Laplace transform inversion methods. *Journal of Computational Finance*, **2**, 49–74.

Fulop, A., Li, J. and Yu, J. (2015) Self-exciting jumps, learning, and asset pricing implications. *The Review of Financial Studies*, **28**, 876–912.

Fusai, G. and Kyriakou, I. (2016) General optimized lower and upper bounds for discrete and continuous arithmetic Asian options. *Mathematics of Operations Research*, **41**, 531–559.

Fusai, G., Marena, M. and Roncoroni, A. (2008) Analytical pricing of discretely monitored Asian-style options: Theory and application to commodity markets. *Journal of Banking and Finance*, **32**, 2033–2045.

Fusai, G. and Tagliani, A. (2002) An accurate valuation of Asian options using moments. *International Journal of Theoretical and Applied Finance*, **5**, 147–169.

Gatheral, J. (2006) *The volatility surface: A practitioner's guide*. Wiley Finance. John Wiley & Sons.

Geman, H. (2005) *Commodities and Commodity Derivatives: Modeling and Pricing for Agriculturals, Metals and Energy*. Wiley Finance. John Wiley & Sons, Inc.

Geman, H. (2008) *Risk Management in Commodity Markets: From Shipping to Agriculturals and Energy*. Wiley Finance. John Wiley & Sons, Inc.

Geman, H. and Roncoroni, A. (2006) Understanding the fine structure of electricity prices. *The Journal of Business*, **79**, 1225–1261.

Geman, H. and Yor, M. (1993) Bessel processes, Asian options and perpetuities. *Mathematical Finance*, **3**, 349–375.

Ghamami, S. and Goldberg, L. R. (2014) Stochastic intensity models of wrong way risk: Wrong way CVA need not exceed independent CVA. *The Journal of Derivatives*, **21**, 24–35.

Glasserman, P. (2004) *Monte Carlo Methods in Financial Engineering*. Stochastic Modelling and Applied Probability. New York: Springer.

Glasserman, P. and Kim, K. K. (2011) Gamma expansion of the Heston stochastic volatility model. *Finance and Stochastics*, **15**, 267–296.

Glasserman, P. and Yang, L. (2016) Bounding wrong-way risk in measuring counterparty risk. *Mathematical Finance*, **28**, 268–305.

Godwin, H. J. (1964) *Inequalities on Distribution Functions*. Charles Griffin, London.

Golan, A., Judge, G. and Miller, D. (1996) *Maximum Entropy Econometrics: Robust Estimation with Limited Data*. J. Wiley & Sons.

Gotoh, J. and Konno, H. (2002) Bounding option prices by semidefinite programming: A cutting plane algorithm. *Management Science*, **48**, 665–678.

Grasselli, M. (2017) The 4/2 stochastic volatility model: A unified approach for the Heston and the 3/2 model. *Mathematical Finance*, **27**, 1013–1034.

Gregory, J. (2012) *Counterparty Credit Risk and Credit Value Adjustment: A Continuing Challenge for Global Financial Markets*. Wiley, Chichester, U.K.

Grønborg, N. S. and Lunde, A. (2016) Analyzing oil futures with a dynamic Nelson-Siegel model. *The Journal of Futures Markets*, **36**, 153–173.

Guillaume, F. and Schoutens, W. (2013) A moment matching market implied calibration. *Quantitative Finance*, **13**, 1359–1373.

Guillaume, F. and Schoutens, W. (2014) A bootstrapping market implied moment matching calibration for models with time-dependent parameters. *Journal of Computational and Applied Mathematics*, **271**, 100–116.

Hagan, P. S., Kumar, D., Lesniewski, A. S. and Woodward, D. E. (2002) Managing smile risk. *Wilmott Magazine*, 84–108.

Hainaut, D. and Moraux, F. (2018) Hedging of options in the presence of jump clustering. *Journal of Computational Finance*, **22**, 1–35.

Harvey, C., Liechty, J. C., Liechty, M. W. and Müller, P. (2010) Portfolio selection with higher moments. *Quantitative Finance*, **10**, 469–485.

Heinrich, J. (2004) A guide to the Pearson Type IV distribution. Available on-line at `http://www-cdf.fnal.gov/publications/cdf6820_pearson4.pdf`.

Heston, S. (1993) A closed-form solution for options with stochastic volatility with applications to bond and currency options. *Review of Financial Studies*, **6**, 327–343.

Heston, S. L. and Rossi, A. G. (2017) A spanning series approach to options. *The Review of Asset Pricing Studies*, **7**, 2–42.

Hill, I. D., Hill, R. and Holder, R. L. (1976) Algorithm as 99: Fitting Johnson curves by moments. *Journal of the Royal Statistical Society*, **Series C (Applied Statistics)**, 180–189.

Hilliard, J. E. and Reis, J. A. (1999) Jump processes in commodity futures prices and options pricing. *American Journal of Agricultural Economics*, **81**, 273–286.

Hörmann, W., Leydold, J. and Derflinger, G. (2004) *Automatic Nonuniform Random Variate Generation*. Springer-Verlag Berlin Heidelberg.

Hubalek, F., Keller-Ressel, M. and Sgarra, C. (2017) Geometric Asian option pricing in general affine stochastic volatility models with jumps. *Quantitative Finance*, **17**, 873–888.

Hubalek, F. and Sgarra, C. (2011) On the explicit evaluation of the geometric Asian options in stochastic volatility models with jumps. *Journal of Computational and Applied Mathematics*, **235**, 3355–3365.

Hull, J. and White, A. (1987) The pricing of options on assets with stochastic volatilities. *The Journal of Finance*, **42**, 281–300.

Hull, J. and White, A. (1990) Pricing interest-rate derivative securities. *The Review of Financial Studies*, **3**, 573–592.

Hull, J. C. and White, A. (2012) CVA and wrong-way risk. *Financial Analysts Journal*, **68**, 59–69.

Islah, O. (2009) Solving SABR in exact form and unifying it with LIBOR market model. Working paper.

Jaimungal, S., de Souza, M. O. and Zubelli, J. P. (2013) Real option pricing with mean-reverting investment and project value. *The European Journal of Finance*, **19**, 625–644.

Jarrow, R. and Rudd, A. (1982) Approximate option valuation for arbitrary stochastic processes. *Journal of Financial Economics*, **10**, 347–349.

Jaynes, E. T. (1978) *Where do we stand on maximum entropy.* R. D. Levine and M. Tribus eds., The Maximum Entropy Formalism, MIT press.

Johnson, N. (1949) Systems of frequency curves generated by methods of translation. *Biometrika*, **36**, 149–176.

Johnson, N., Kotz, S. and Balakrishnan, N. (1994a) *Continuous Univariate Distributions*, vol. 1. Wiley-Interscience, 2 edn.

Johnson, N., Kotz, S. and Balakrishnan, N. (1994b) *Continuous Univariate Distributions*, vol. 2. Wiley-Interscience, 2 edn.

Jones, D. L. (2014) Johnson curve toolbox for Matlab: analysis of non-normal data using the Johnson family of distributions. *College of Marine Science, University of South Florida, St. Petersburg, Florida, USA.*

Keller-Ressel, M. (2008) *Affine processes — Theory and applications in finance.* Dissertation, Vienna University of Technology.

Keller-Ressel, M. (2011) Moment explosions and long-term behavior of affine stochastic volatility models. *Mathematical Finance*, **21**, 73–98.

Kemna, A. and Vorst, A. (1990) A pricing method for options based on average asset values. *Journal of Banking and Finance*, **14**, 113–129.

Kendall, M. and Stuart, A. (1977) *The Advanced Theory of Statistics, Vol. 1.* Macmillan, New York.

Kesavan, H. K. and Napur, J. N. (1992) *Entropy Optimization Principles with Applications.* Academic Press.

Kiesel, R. and Paraschiv, F. (2017) Econometric analysis of 15-minute intraday electricity prices. *Energy Economics*, **64**, 77–90.

Klebanov, L. and Mkrtchyan, S. (1985) Estimating the proximity of distributions in terms of coinciding moments. *Selected Translations in Mathematical Statistics and Probability*, **16**, 1–10.

Kyriakou, I., Pouliasis, P. K. and Papapostolou, N. C. (2016) Jumps and stochastic volatility in crude oil prices and advances in average option pricing. *Quantitative Finance*, **16**, 1859–1873.

Lasserre, J. B., Prieto-Rumeau, T. and Zervos, M. (2006) Pricing a class of exotic options via moments and SDP relaxations. *Mathematical Finance*, **16**, 469–494.

Levy, E. (1992) Pricing European average rate currency options. *Journal of International Money and Finance*, **11**, 474–491.

Li, C. and Wu, L. (2019) Exact simulation of the Ornstein–Uhlenbeck driven stochastic volatility model. *European Journal of Operational Research*, **275**, 768–779.

Li, M. and Mercurio, F. (2015) Jumping with default: Wrong-way risk modeling for CVA. *Risk*, **November**, 58–63.

Lin, G. D. (2017) Recent developments on the moment problem. *Journal of Statistical Distributions and Applications*, **4**.

Lindsay, B. G. and Basak, P. (2000) Moments determine the tail of a distribution (but not much else). *The American Statistician*, **54**, 248–251.

Lindsay, B. G. and Roeder, K. (1997) Moment-based oscillation properties of mixture models. *The Annals of Statistics*, **25**, 378–386.

Lo, C., Palmer, K. and Yu, M. (2014) Moment-matching approximations for Asian options. *The Journal of Derivatives*, **21**, 103–122.

Lukacs, E. (1970) *Characteristic Functions*. Charles Griffin, London.

Lütkebohmert, E. and Sester, J. (forthcoming) Tightening robust price bounds for exotic derivatives. *Quantitative Finance*.

Marena, M., Roncoroni, A. and Fusai, G. (2013) Asian options with jumps: A closed form formula. *Argo Newsletter: New Frontiers in Practical Risk Management*, **1**, 47–56.

Markowitz, H. (1952) Portfolio selection. *The Journal of Finance*, **7**, 77–91.

Merton, R. (1976) Option pricing when underlying stock returns are discontinuous. *The Journal of Financial Economics*, **3**, 125–144.

Milevsky, M. A. and Posner, S. E. (1998) Asian options, the sum of lognormals and the reciprocal gamma distribution. *Journal of Financial and Quantitative Analysis*, **33**, 409–422.

Navatte, P. and Villa, C. (2000) The information content of implied volatility, skewness and kurtosis: Empirical evidence from long-term CAC 40 options. *European Financial Management*, **6**, 41–56.

Ogata, Y. (1981) On Lewis simulation method for point processes. *IEEE Transactions on Information Theory*, **27**, 23–31.

Pearson, E. S. and Hartley, H. O. (1972) *Biometrika Tables for Statisticians*. Cambridge University Press.

Pearson, K. (1895) Contributions to the mathematical theory of evolution, II: Skew variation in homogeneous material. *Philosophical Transactions of the Royal Society*, **186**, 343–414.

Pellegrino, T. and Sabino, P. (2014) On the use of the moment-matching technique for pricing and hedging multi-asset spread options. *Energy Economics*, **45**, 172–185.

Poirot, J. and Tankov, P. (2006) Monte Carlo option pricing for tempered stable (CGMY) processes. *Asia-Pacific Financial Markets*, **13**, 327–344.

Prayoga, A. and Privault, N. (2017) Pricing CIR yield options by conditional moment matching. *Asia-Pacific Financial Markets*, **24**, 19–38.

Press, W. H., Teukolsky, S. A., Vetterling, W. T. and Flannery, B. P. (1992) *Numerical Recipes in Fortran 77: The Art of Scientific Computing*. Cambridge University Press.

Privault, N. and Yu, J. (2016) Stratified approximations for the pricing of options on average. *Journal of Computational Finance*, **19**, 95–113.

Provost, S. (2005) Moment-based density approximants. *The Mathematica Journal*, **9**, 727–756.

Rambaldi, Q., Pennesi, X. and Lillo, F. (2015) Modeling foreign exchange market activity around macroeconomic news: Hawkes process approach. *Phys. Rev. E*, **91**, 012819.

Ritchken, P., Sankarasubramanian, L. and Vijh, A. (1990) The valuation of path-dependent contracts on the average. *Management Science*, **39**, 1202–1213.

Robert, C. and Casella, G. (2010) *Introducing Monte Carlo Methods with R.* Springer-Verlag New York.

Rogers, L. C. G. and Shi, Z. (1992) The value of an Asian option. *Journal of Applied Probability*, **32**, 1077–1088.

Roncoroni, A., Fusai, G. and Cummins, M. (2015) *Handbook of multi-commodity markets and products: Structuring, trading and risk management.* The Wiley Finance Series. Chichester, West Sussex: John Wiley & Sons.

Rose, C. and Smith, M. (2002) *Mathematical Statistics with Mathematica.* Springer-Verlag, New York.

Ruijter, M. and Oosterlee, C. (2012) Two-dimensional Fourier cosine series expansion method for pricing financial options. *SIAM Journal on Scientific Computing*, **34**, B642–B671.

Ruiz, I., Del Boca, P. and Pachón, R. (2015) Optimal right and wrong-way risk from a practitioner standpoint. *Financial Analysts Journal*, **71**.

Schöbel, R. and Zhu, J. (1999) Stochastic volatility with an Ornstein–Uhlenbeck process: An extension. *European Finance Review*, **3**, 23–46.

Schwartz, E. S. (1997) The stochastic behavior of commodity prices: Implications for valuation and hedging. *The Journal of Finance*, **52**, 923–973.

Scott, L. (1987) Option pricing when the variance changes randomly: Theory, estimation, and an application. *Journal of Financial Quantitative Analysis*, **22**, 419–438.

Sesana, D., Marazzina, D. and Fusai, G. (2014) Pricing exotic derivatives exploiting structure. *European Journal of Operational Research*, **236**, 369–381.

Shiraya, K. and Takahashi, A. (2011) Pricing average options on commodities. *The Journal of Futures Markets*, **31**, 407–439.

Shohat, J. A. and Tamarkin, J. D. (1943) *The problem of moments.* Mathematical Survey 1. American Mathematical Society, New York City.

Simonato, J. G. (2011) The performance of Johnson distributions for value at risk and expected shortfall computation. *Journal of Derivatives*, **19**, 7–24.

Stace, A. W. (2007) A moment matching approach to the valuation of a volume weighted average price option. *International Journal of Theoretical and Applied Finance*, **10**, 95–110.

Stein, E. and Stein, J. (1991) Stock price distributions with stochastic volatility: An analytic approach. *Review of Financial Studies*, **4**, 727–752.

Stoyanov, J. (1997) *Counterexamples in Probability (2nd edition)*. Wiley Series in Probability and Statistics.

Tanaka, K., Yamada, T. and Watanabe, T. (2010) Applications of Gram–Charlier expansion and bond moments for pricing of interest rates and credit risk. *Quantitative Finance*, **10**, 645–662.

Thompson, G. (1998) Fast narrow bounds on the value of Asian options. Working Paper, University of Cambridge.

Tuenter, H. (2001) An algorithm to determine the parameters of s_u curves in the Johnson system of probability distributions by moment matching. *Journal of Statistical Computation and Simulation*, **70**, 325–347.

Turnbull, S. and Wakeman, L. (1991) A quick algorithm for pricing European average options. *Journal of Financial and Quantitative Analysis*, **26**, 377–389.

Wheeler, R. (1980) Quantile estimators of Johnson curve parameters. *Biometrika*, **67**, 725–728.

Widder, D. V. (1941) *The Laplace Transform*. Princeton University Press, Princeton, N.J.

Willard, G. A. (1997) Calculating prices and sensitivities for path-independent derivative securities in multifactor models. *Journal of Derivatives*, **5**, 54–61.

Willems, S. (2019) Asian option pricing with orthogonal polynomials. *Quantitative Finance*, **19**, 605–618.

Yamazaki, A. (2014) Pricing average options under time-changed Lévy processes. *Review of Derivatives Research*, **17**, 79–111.

Zahra, S. and Reza, R. (2012) Asian real option: New approach to project economic valuation. In *2012 International Conference on Information Management, Innovation Management and Industrial Engineering*, vol. 2, 475–479.